

**COMPACTION AND SHEARING RESISTANCE OF COMPACTED
BENTONITE-GRANULAR MATERIALS MIXTURES FOR SALT
AND POTASH MINE BACKFILL**



**A Thesis Submitted in Partial Fulfillment of the Requirements for the
Degree of Master of Engineering in Geotechnology**

Suranaree University of Technology

Academic Year 2017

การבודัดและกำลั้งเื้อนของส่วนผสมเบนทอไนต์บุดอัดกับวัสดุเม็ด ลำหรับการ
ถมกลับเหมืองเกลือและเหมืองโพแทช



นางสาวกรรช พงษ์เพ็ง

วิทยานิพนธ์นี้เป็นส่วนหนึ่งของการศึกษาตามหลักสูตรปริญญาวิศวกรรมศาสตรมหาบัณฑิต
สาขาวิชาเทคโนโลยีธรณี
มหาวิทยาลัยเทคโนโลยีสุรนารี
ปีการศึกษา 2560

**COMPACTION AND SHEARING RESISTANCE OF COMPACTED
BENTONITE-GRANULAR MATERIALS MIXTURES FOR
SALT AND POTASH MINE BACKFILL**

Suranaree University of Technology has approved this thesis submitted in partial fulfillment of the requirements for a Master's Degree.

Thesis Examining Committee




(Asst. Prof. Dr. Akkhapun Wannakomol)

Chairperson



(Asst. Prof. Dr. Decho Phueakphum)

Member (Thesis Advisor)



(Asst. Prof. Dr. Helmut Durrast)

Member



(Prof. Dr. Santi Maensiri)

Vice Rector for Academic Affairs
and Internationalization



(Assoc. Prof. Ft. Lt. Dr. Kontorn Chamniprasart)

Dean of Institute of Engineering

กรกช พงษ์เพ็ง : การบดอัดและกำลังเฉือนของส่วนผสมเบนทอนไนต์บดอัดกับวัสดุเม็ด
สำหรับการถมกลับเหมืองเกลือและเหมืองโพแทช (COMPACTION AND SHEARING
RESISTANCE OF COMPACTED BENTONITE-GRANULAR MATERIALS
MIXTURES FOR SALT AND POTASH MINE BACKFILL) อาจารย์ที่ปรึกษา : ผู้ช่วย
ศาสตราจารย์ ดร. เดโช เพ็ชกรภูมิ, 85 หน้า

วัตถุประสงค์ของการศึกษานี้คือ เพื่อวัดค่าศักยภาพเชิงกลศาสตร์ของส่วนผสมดินเบนทอน
ไนต์ วัสดุเม็ดและน้ำเกลืออิ่มตัวที่ถูกบดอัด เพื่อใช้เป็นวัสดุถมกลับในช่องเหมืองเกลือและโพแทช
วัสดุเม็ดประกอบด้วย ดินตะกอนประปา ทราบ เกล็ดเกลือ กรวดเม็ดละเอียด และกรวดเม็ดหยาบ มี
ขนาดตั้งแต่ 0.425 ถึง 10 มิลลิเมตร อัตราส่วนผสมของแร่เบนทอนไนต์ต่อวัสดุเม็ดผันแปรจาก 30:70
ถึง 90:10 โดยน้ำหนัก ผลการทดสอบระบุว่าปริมาณความชื้นของน้ำเกลือที่เหมาะสมมีค่าตั้งแต่ 9.7
ถึง 19.7 เปอร์เซ็นต์โดยน้ำหนัก และมีความหนาแน่นแห้งสูงสุดตั้งแต่ 1.82 ถึง 2.03 กรัมต่อ
ลูกบาศก์เซนติเมตร การบดอัดของส่วนผสมที่มีขนาดเม็ดใหญ่ให้ค่าความเค้นเฉือนสูงกว่าส่วนผสม
ที่มีขนาดเม็ดเล็ก มุมเสียดทานมีค่าเพิ่มขึ้นเมื่อปริมาณของวัสดุเม็ดในส่วนผสมมากขึ้นซึ่งมีค่าตั้งแต่
19 ถึง 37 องศา ความเค้นยึดติดผันแปรจาก 0.14 ถึง 0.26 เมกะปาสกาล กำลังรับแรงอัดในแกนเดียว
และสัมประสิทธิ์ความยืดหยุ่นของส่วนผสมที่มีขนาดเม็ดใหญ่มีค่าต่ำกว่าส่วนผสมที่มีขนาดเม็ด
ละเอียด อัตราส่วนบิวของสัลดลงเมื่อปริมาณเบนทอนไนต์เพิ่มขึ้น ความสามารถในการบวมตัวและ
การดูดซับเพิ่มขึ้นเมื่อปริมาณน้ำเกลือเริ่มต้นลดลง โดยส่วนผสมเหล่านี้สามารถใช้เป็นค่าตัวแปร
เริ่มต้นในการติดตั้งเมื่อมีการถมกลับในช่องเหมืองเกลือและโพแทช

สาขาวิชา เทคโนโลยีธรณี
ปีการศึกษา 2560

ลายมือชื่อนักศึกษา กรกช
ลายมือชื่ออาจารย์ที่ปรึกษา D. Phueakphum


KORAKOCH PONGPENG : COMPACTION AND SHEARING
RESISTANCE OF COMPACTED BENTONITE-GRANULAR
MATERIALS MIXTURES FOR SALT AND POTASH MINE BACKFILL.
THESIS ADVISOR : ASST. PROF. DECHO PHUEKPHUM, Ph.D., 85 PP.

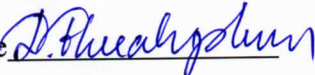
SHEAR STRENGTH/COMPRESSIVE STRENGTH/ELASTIC/BACKFILL

The objective of this study is to determine the mechanical performance of compacted bentonite-to-granular mixtures with saturated brine for use as backfill materials in salt and potash mine openings. The granular include sludge, sand, crushed salt, fine and coarse gravels. Their grain sizes range from 0.425 to 10 mm. The mixing ratios of the bentonite-to-granular mixtures are from 30:70 to 100:0 by weight percent. The test results indicate that the optimum brine content is ranged from 9.7% to 19.7% by weight with the corresponding maximum dry densities from 1.82 to 2.03 g/cc. The compacted mixtures with larger grains show greater shear strength than those of the smaller ones. The friction angles increase with increasing granular content, ranging from 19 to 37 degrees. The cohesions range from 0.14 to 0.26 MPa. The uniaxial compressive strengths and elastic moduli of the mixtures containing larger grains are lower than those with the finer grains. The Poisson's ratios also decrease with increasing the bentonite content. The swelling and absorption capacities increase with decreasing initial brine content. These mixtures can be used as initial installation parameters for the backfills in salt and potash mine openings.

School of Geotechnology

Academic Year 2017

Student's Signature 

Advisor's Signature 

ACKNOWLEDGMENTS

I wish to acknowledge the funding support from Suranaree University of Technology (SUT).

I would like to express my sincere thanks to Prof. Dr. Kittitep Fuenkajorn for his valuable guidance and efficient supervision. I appreciate his strong support, encouragement, suggestions and comments during the research period. I also would like to express my gratitude to Asst. Prof. Dr. Akkhapun Wannakomol, Asst. Prof. Dr. Decho Phueakphum and Asst. Prof. Dr. Helmut Durrast for their constructive advice, valuable suggestions and comments on my research works as thesis committee members. Grateful thanks are given to all staffs of Geomechanics Research Unit, Institute of Engineering who supported my work.

Finally, I would like to thank beloved parents for their love, support and encouragement.

Korakoch Pongpeng

TABLE OF CONTENTS

	Page
ABSTRACT (THAI)	I
ABSTRACT (ENGLISH).....	II
ACKNOWLEDGEMENTS	III
TABLE OF CONTENTS.....	IV
LIST OF TABLES	VIII
LIST OF FIGURES	IX
SYMBOLS AND ABBREVIATIONS.....	XIII
CHAPTER	
I INTRODUCTION	1
1.1 Background and rationale.....	1
1.2 Research objectives.....	1
1.3 Research methodology.....	2
1.3.1 Literature review	2
1.3.2 Sample collection and preparation.....	2
1.3.2.1 Samples.....	2
1.3.2.2 Sample preparation.....	4
1.3.3 Compaction test	4
1.3.4 Direct shear test	5

TABLE OF CONTENTS (Continued)

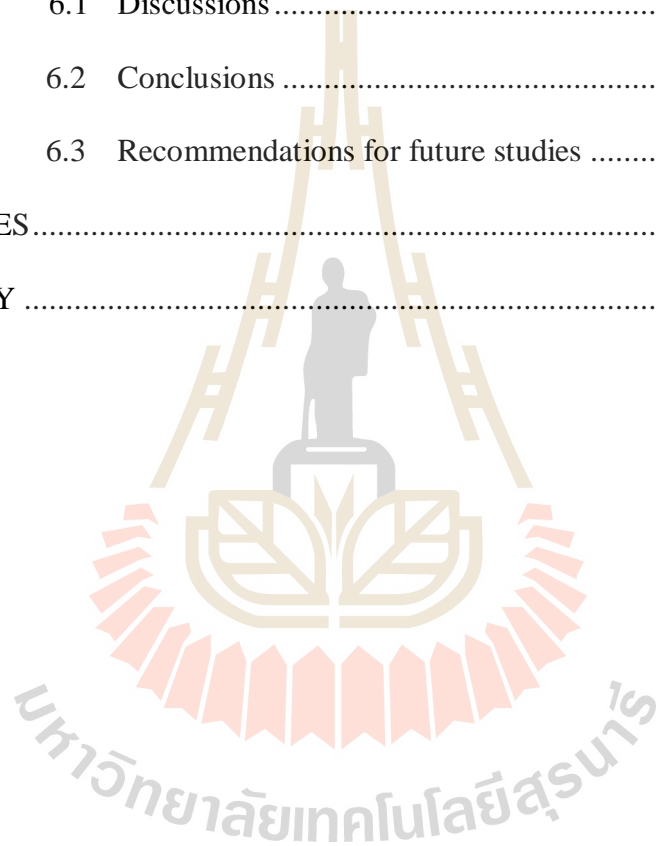
	Page
1.3.5 Uniaxial compressive strength tests	5
1.3.6 Swelling and absorption tests	5
1.3.7 Discussions and conclusion	6
1.3.8 Thesis writing	6
1.4 Scope and limitations	6
1.5 Thesis contents.....	7
II LITERATURE REVIEW	8
2.1 Introduction	8
2.2 Compaction test of backfill materials in salt and potash	
opening.....	8
2.3 Direct shear test of backfill materials in salt and potash	
opening.....	13
2.4 Uniaxial compressive strength tests.....	19
2.5 Swelling tests.....	21
2.6 Experimental researches on backfill materials	23
III SAMPLE PREPARATION	28
3.1 Introduction	28
3.2 Granular material preparation.....	28
3.2.1 Bentonite.....	28
3.2.2 Crushed salt	32

TABLE OF CONTENTS (Continued)

	Page
3.2.3 Gravel.....	32
3.2.4 Sand.....	32
3.2.5 Granular classifications	34
3.2.6 Saturated brine	36
3.2.7 Sludge.....	36
3.3 Mixing preparations	38
IV GEOTECHNICAL AND MECHANICAL TESTING	39
4.1 Introduction	39
4.2 Test methods.....	39
4.2.1 Compaction test	39
4.2.2 Direct shear test	40
4.2.3 Compression test.....	41
4.3 Test results.....	42
4.3.1 Compaction results	42
4.3.2 Direct shear results	50
4.3.3 Compression results	68
V SWELLING AND ABSORPTION TESTING	74
5.1 Introduction	74
5.2 Test methods.....	74
5.3 Test results.....	76

TABLE OF CONTENTS (Continued)

	Page
VI DISCUSSIONS AND CONCLUSIONS	82
6.1 Discussions.....	82
6.2 Conclusions.....	83
6.3 Recommendations for future studies.....	84
REFERENCES.....	86
BIOGRAPHY.....	93



LIST OF TABLES

Table	Page
3.1	Chemical compositions of tested bentonite and sludge.....30
3.2	Atterberg's limits and specific gravity of bentonite and sludge.....31
3.3	Particle shape classification of granular materials based on Power.....36
4.1	Compaction test results.....45
4.2	Compaction test results of three-ring and ASTM standard molds.....49
4.3	Direct shear results.....56
4.4	Direct shear test comparison result.....62
4.5	Compression test results.....73
5.1	Bentonite properties after compaction.....75
5.2	Pictures of specimens before swelling.....78
5.3	Pictures of specimens after swelling.....79
5.4	Results of swelling capacity of bentonite.....80
5.5	Results of absorption capacity.....81

LIST OF FIGURES

Figure	Page
1.1 Research methodology.....	3
2.1 Three-ring mold.....	9
2.2 Three-ring shear mold apparatus.....	9
2.3 Volumetric strain and brine flow as function of time.....	11
2.4 Compaction as a function of water content and particle size gradation.....	12
2.5 Shear stress as a function of displacement for GMZ07 bentonite saturated by NaCl solutions under different vertical stresses.....	14
2.6 Three-ring compaction and direct shear testing device.....	16
2.7 Diagram of direct shear test arrangement.....	17
2.8 Comparison of results for different shearing rates in large and small boxes..	18
2.9 Mohr-Coulomb criterion as a function of shear strengths and normal stresses.....	19
2.10 Effect of sand content on the unconfined compression strength of the bentonite-sand mixture.....	20
3.1 Bentonite from Thai Nippon Chemical Industry Co., LTD, Thailand.....	28
3.2 Particle size distribution of bentonite.....	29
3.3 Crystalline structure of sodium montmorillonite with interlamellar water layer.....	30

LIST OF FIGURES (Continued)

Figure	Page
3.3	Particle size distribution of crushed salt particle with sizes from 4-6 mm.....32
3.4	Particle size distribution of gravels with sizes of 6.35-9.53 and 4-6 mm.....33
3.5	Particle size distribution of sand with particle sizes of 1-2 mm.....33
3.6	Examples of sand particles.....34
3.7	Examples of crushed salt particles.....35
3.8	Examples of fine gravel (a) and coarse gravel (b) particles.....35
3.9	Sludge samples from Metropolitan Waterworks Authority.....37
3.10	Particle size distribution of sludge.....37
4.1	Uniaxial compression test equipment.....41
4.2	Maximum dry densities as a function of brine contents.....43
4.3	Maximum dry densities (a) and optimum brine contents (b) as a function of bentonite-to-granular weight ratios.....44
4.4	Dry density as a function of brine content of bentonite-to-crushed salt obtain from the three-ring mold and the ASTM standard mold.....46
4.5	Dry density as a function of brine content of bentonite-to-fine gravel obtain from the three-ring mold and the ASTM standard mold.....47
4.6	Maximum dry density as a function of weight ratios of bentonite obtain from the three-ring mold and the ASTM standard mold (a) and optimum brine content as a function of weight ratios of bentonite obtain from the three-ring mold and the ASTM standard mold (b).....48

LIST OF FIGURES (Continued)

Figure	Page
4.7	Shear strength as a function of displacement of bentonite-to-sludge.....51
4.8	Shear strength as a function of displacement of bentonite-to-sand.....52
4.9	Shear strength as a function of displacement of bentonite-to-crushed salt.....52
4.10	Shear strength as a function of displacement of bentonite-to-fine gravel.....53
4.11	Shear strength as a function of displacement of bentonite-to-coarse gravel...53
4.12	Shear strength as a function of normal stress of granular materials.....54
4.13	Cohesions (a) and friction angles (b) as a function of bentonite-to-granular weight ratios55
4.14	Shear strength as a function of displacement of bentonite-to-crushed salt for ASTM direct shear (a) and three-ring direct shear (b) apparatus.....57
4.15	Shear strength as a function of displacement of bentonite-to-fine gravel for ASTM direct shear (a) and three-ring direct shear (b) apparatus.....58
4.16	Shear strength as a function of normal stress obtain from the three-ring mold and the ASTM standard mold of bentonite-to-crushed salt.....59
4.17	Shear strength as a function of normal stress obtain from the three-ring mold and the ASTM standard mold of bentonite-to-fine gravel.....60
4.18	Cohesion(a) and friction angle (b) as a function of weight ratios of bentonite obtain from the three-ring mold and the ASTM standard mold61
4.19	Normal displacement as a function of displacement of bentonite-to-sludge...63
4.20	Normal displacement as a function of displacement of bentonite-to-sand.....63

LIST OF FIGURES (Continued)

Figure	Page
4.21 Normal displacement as a function of displacement of bentonite-to-crushed salt.....	64
4.22 Normal displacement as a function of displacement of bentonite-to-fine gravel.....	64
4.23 Normal displacement as a function of displacement of bentonite-to-coarse gravel.....	65
4.24 Dilation angles as a function of normal stress of granular materials.....	66
4.25 Dilation rate as a function of weight ratios of bentonite.....	67
4.26 Post-test specimens of granular materials after compression testing.....	69
4.27 Stress-strains curves.....	70
4.28 Compressive strengths as a function of bentonite-to-granular weight ratios.....	71
4.29 Elastic moduli (a) and Poisson's ratio (b) as a function of bentonite-to-granular weight ratios.....	72
5.1 Density of bentonite as a function of brine content.....	75
5.2 Swelling capacity of bentonite as a function of times.....	80
5.3 Absorption capacity of bentonite as a function of brine contents.....	81

SYMBOLS AND ABBREVIATIONS

ε	=	Strains
ϕ	=	Friction Angle
ν	=	Poisson's ratio
ρ_{Brine}	=	Density of saturated brine (measured with a hydrometer (kg/m ³))
ρ_{water}	=	Density of water equal 1,000 kg/m ³
σ_1	=	Stress
σ_c	=	Compressive strengths
σ_n	=	Normal Stress
τ	=	Shear Stress
Ψ	=	Dilation Angle
c	=	Cohesion
D	=	Swelling capacity
E	=	Elastic modulus
J	=	Compaction energy per unit volume
L	=	Height of drop of hammer

SYMBOLS AND ABBREVIATIONS (Continued)

N	=	Number of blows per layer
S _B	=	Solubility of salt in dissolved water
SG _{Brine}	=	Specific gravity of saturated brine
T	=	Number of layers
V	=	Volume of mold
W	=	Weight of hammer
W ₁	=	Weight wet soil and container (g)
W ₂	=	Weight dry soil and container (g)
W _B	=	Brine content (%)
W _{can}	=	Weight container (g)
W _i	=	Initial water content (%)

CHAPTER I

INTRODUCTION

1.1 Background of problems and significance of the study

The mechanical properties of soil are necessary for the design and analysis of earth structures and can be used to determine the initial installation parameters of the compacted granular and clayey backfill in salt and potash mine openings. Soil strength indicates the ability of the foundation in carrying applied load. The direct shear test (ASTM D3080-11) and uniaxial compressive strength test (ASTM D2938-95) are performed to obtain soil properties using as the design parameters of backfill in salt and potash mines. A disadvantage of the standard shear test method and equipment is however that the compacted soil samples need to be removed from the 100-mm diameter compaction mold, trimmed and installed into the smaller shear mold (60-mm diameter). The process could disturb the samples physical properties (Lamandé et al., 2007). The relatively small shear mold also limits the maximum particle size of the test samples (Bagherzadeh and Mirghasemi, 2009; Liu et al., 2009). The three-ring compaction and shear mold (Sonsakul and Fuenkajorn, 2013) have been using as an alternative method to determine the properties of the compacted mixtures without disturbing the specimens when they are installed in the direct shear mold.

1.2 Research objectives

The objective of this study is to determine the optimum brine content, maximum

dry density and mechanical properties of compacted soil samples. The mixtures of bentonite-to-sludge, bentonite-to-sand, bentonite-to-gravels and bentonite-to-crushed salt with saturated brine under ambient temperatures are used as testing materials for the compaction, direct shear and uniaxial compression tests to determine is the mechanical properties. Swelling and absorption tests are performed to determine the physical properties of backfill material for use in salt and potash mines.

1.3 Research methodology

The research methodology (Figure 1.1) comprises 8 steps, including literature review, sample collection and preparation, compaction test, direct shear test, uniaxial compression test, swelling and absorption tests, discussions and conclusions and thesis writing.

1.3.1 Literature Review

Literature review is carried out to study the determination of soil strength parameters and the relevant theories of compaction test, direct shear test, uniaxial compressive strength and swelling test. The sources of information are from text books, journals, technical reports and conference papers. A summary of the literature review has been given in the thesis.

1.3.2 Sample Collection and Preparation

1.3.2.1) Samples

Construction grade bentonite (B) used in this study in from Thai Nippon Chemical Industry Co., LTD, Thailand is selected for the verification test of the three-ring mold. This is primarily because it is highly uniform, low permeability and consistent in engineering properties. The maximum dry density, optimum water

content, and shear strengths are determined. Bentonite is prepared for the compaction, direct shear, compression, and swelling and absorption tests, (ASTM D 1557-12; D 3080-11; D2938-95 and D5890-11).

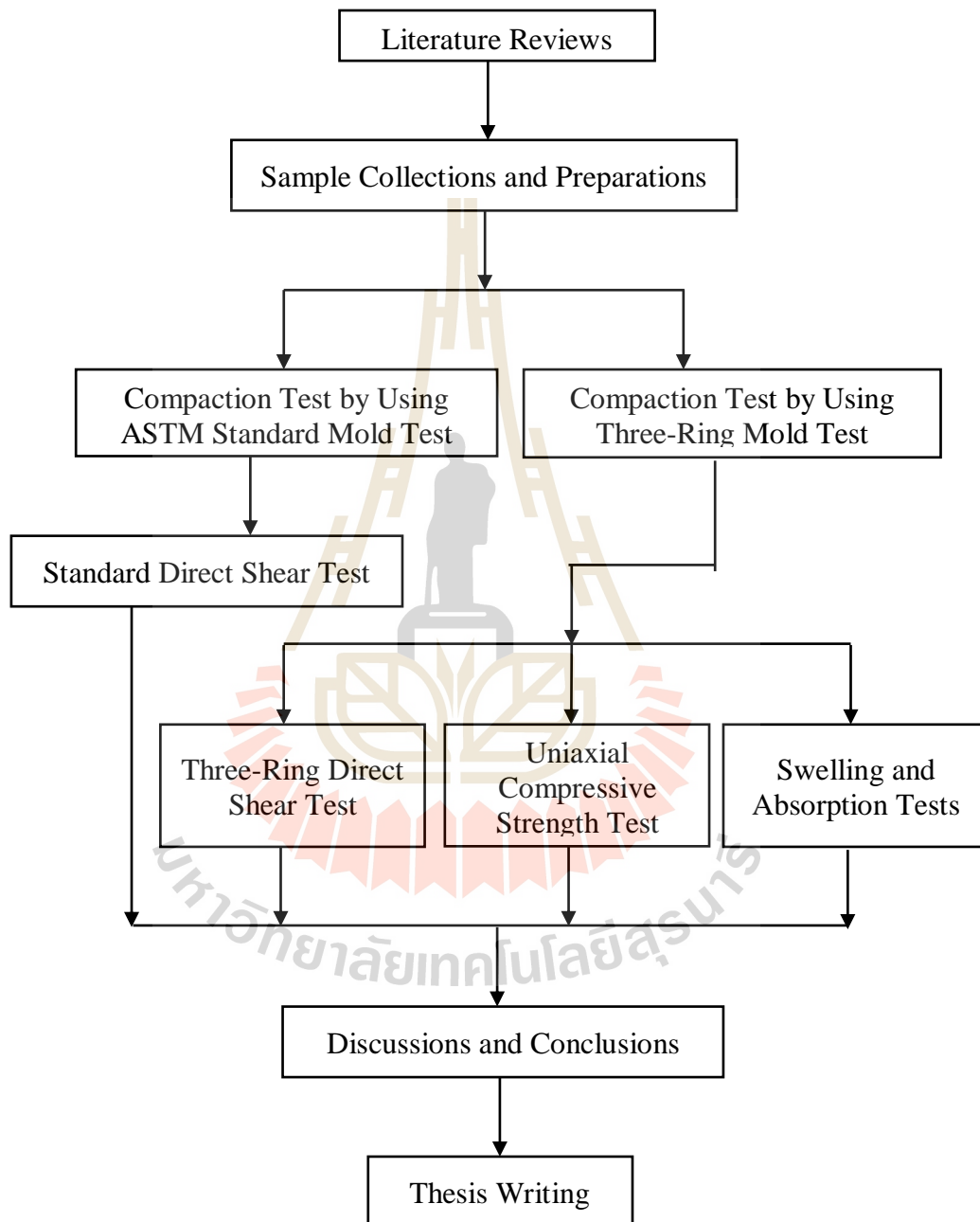


Figure 1.1 Research Methodology.

Crushed salt (CS) used in this study is prepared from the middle members of the Maha Sarakham formation, northeast Thailand.

Gravel is collected from Khok Kruat sub-district used in the study is divided into 2 size ranges: 4-6 mm (FG) for performance assessment comparison and 6.35-9.53 mm (CG) for backfill analyzing in salt and potash mine openings.

Sand (SA) is collected from Khok Kruat sub-district having particle sizes of 1-2 mm.

Saturated brine is prepared by mixing pure salt (NaCl) with distilled water in plastic tank. It is stirred continuously for 20 minutes. The proportion of salt to water is about 39.1% by weight.

Sludge (SL) samples have been donated by the Metropolitan Waterworks Authority are collected from the sludge dewatering plant of Bang Khen Water Treatment Plant located in Bangkok Metropolis.

1.3.2.2) Sample preparation

The bentonite-to-sludge (B:SL), bentonite-to-sand (B:SA), bentonite-to-crushed salt (B:CS), bentonite-to-fine gravel (B:FG) and bentonite-to-coarse gravel (B:CG) mixing ratios of 90:10, 70:30, 50:50 and 30:70 by weight ratio of bentonite. The mixtures are prepared in plastic tray by 2,700 kilograms of total weight. The brine is added by spaying on the mixture, using a plastic spatula. The mixtures are compacted in the three-ring mold.

1.3.3 Compaction Test

The compacted materials are dynamic compaction with a release of weight steel hammer 10 pounds in mold of 27 times per layer in six layers of three-ring compaction test. The standard compaction materials are dynamic compaction with a release of weight steel hammer 10 pounds in mold of 25 times per layer in five layers. The maximum dry density and optimum brine content obtained from the compaction

test by using three-ring mold (Sonsakul and Fuenkajorn, 2013) of bentonite-to-crushed salt (B:CS) and bentonite-to-gravel (B:FG) mixtures has been verified with the ASTM standard mold.

The maximum dry density and optimum brine content from using three-ring mold of bentonite-to-sludge (B:SL), bentonite-to-sand (B:SA), bentonite-to-crushed salt (B:CS), bentonite-to-gravel (B:FG) and bentonite-to-gravel (B:CG) mixtures is used to determine direct shear and uniaxial compressive strength tests.

1.3.4 Direct Shear Test

The shear strengths obtained from the direct shear test by used three-ring direct shear of compacted bentonite-to-crushed salt (B:CS) and bentonite-to-gravel (B:FG) mixtures have been verified with the ASTM standard mold. Compacted bentonite-to-sludge (B:SL), bentonite-to-sand (B:SA), bentonite-to-crushed salt (B:CS), bentonite-to-gravel (B:FG) and bentonite-to-gravel (B:CG) mixtures is analyzed of backfill materials in salt and potash mine openings. The normal force is applied by the vertical hydraulic load cell ranging from 0.2, 0.4, 0.6, 0.8 to 1 MPa.

1.3.5 Uniaxial compressive strength tests

The uniaxial compressive strength test follows the ASTM (D2938-95). A total of compacted at the optimum brine content specimens are tested. The results are used to determine the elastic moduli and Poisson's ratio. The elastic moduli (E) and Poisson's ratio (ν) can be determined by using equation given by Jaeger et al. (2007).

1.3.6 Swelling and absorption tests

The compacted bentonite mixed with the saturated brine at various brine content ranging from 5, 10, 15, 20, 25, 30, 35, 40, 45 to 50%. The results are used to determine the swelling and absorption properties of bentonite.

1.3.7 Discussions and Conclusions

Discussions are made on the reliability and adequacies of the approaches used here. Future research needs have been identified. All research activities, methods, and results are documented and complied in the thesis. The research or findings is published in the conference proceedings or journals.

1.3.8 Thesis writing

All research activities, methods, and results are documented and complied in the thesis. This study can be applied to design mine backfill which soil strength parameter of direct shear and uniaxial compressive strength tests. Swelling test can be studying the physical property of bentonite as an affected in the long-term operation of a backfill in salt and potash mines. The findings are published in the conference proceedings or journals.

1.4 Scope and limitations of the study

The scope and limitations of this study include as follows:

1) The collected soil samples including:

- Construction grade bentonite (<0.4 mm) obtained from Thai Nippon Chemical Industry Co., LTD, Thailand.
- Crushed salt (4-6 mm) obtained from the Middle and Lower members of the Maha Sarakham formation, northeast of Thailand.
- gravels (4-6 and 635-9.53 mm) obtained from Nakhon Ratchasima province.
- sand (1-2 mm) obtained from Nakhon Rachasima province.

- Sludge (<0.074 mm) obtained from dewatering plant of Bang Khen Water Treatment Plant located in Bangkok Metropolis.
- 2) Saturated brine is prepared from pure halite.
 - 3) The results obtained from the ASTM standard mold and three-ring mold is compacted to verify the parameters of three-ring compaction and direct shear mold (Sonsakul and Fuenkajorn, 2013).
 - 4) The uniaxial compressive strength test is carried out on cylindrical specimens with 101.6 mm in diameter and 150 mm in length.
 - 5) The applied normal stresses in the direct shear testing has been varied from 0.2, 0.4, 0.6, 0.8 to 1 MPa.
 - 6) The testing is follow the relevant ASTM standard practice, as much as, practical.
 - 7) The brine content in swelling and absorption tests have been varied from 5, 10, 15, 20, 25, 30, 35, 40, 45 to 50% by weight mixed with pure bentonite.
 - 8) The research findings are published in conference paper or journal.

1.5 Thesis contents

Chapter I describes the background of problems and significance of the study. The research objectives, methodology, scope and limitations are identified. **Chapter II** summarizes the research of the literature reviews. **Chapter III** describes the sample and mixture preparations. **Chapter IV** describes geotechnical and mechanical testing. **Chapter V** describes the results of swelling and absorption tests and **Chapter VI** discusses and concludes the research results, and provides recommendations for future research studies.

CHAPTER II

LITERATURE REVIEWS

2.1 Introduction

Relevant topics and previous research results are reviewed to improve an understanding of the compaction test, direct shear test, uniaxial compressive strength test, swelling test and experimental researches on backfill materials. The results of the literature review are presented below.

2.2 Compaction test of backfill materials in salt and potash opening

Compacted clayey soils are used as hydraulic barriers in earth structures, such as core of earth fill dams, landfill liners, and etc. These soils have some defects from technical points of view.

Sonsakul and Fuenkajorn (2013) develop the three-ring compaction and direct shear mold to determine the optimum water content, maximum dry density and shear strength of compacted soil sample with particle size up to 10 mm. They are designed to be used as a compaction and direct shear mold without removing the soil sample, and hence eliminating the sample disturbance. They presented the test results that the shear strength, maximum dry density and optimum water content of the bentonite samples obtained from the three-ring mold and the ASTM standard mold are virtually identical. The three-ring mold (Figure 2.1) consists of top, middle and bottom rings the inside diameter is 10.16 cm, outer diameter is 10.46 cm and combined height is 15.19

cm. The three rings are secured on the base plate using steel bolts and two steel clamps. The top and bottom rims of the rings have no locking edge. The steel clamps are used to prevent the rings from displacing during compaction. Compacted by dynamic compaction with a release of 10 pounds weight steel hammer in mold of twenty-seven times per layer in six layers. The three-ring shear mold (Figure 2.2) is the main components for the shear test frame. There are the lateral load system for pushing the middle ring, and the vertical load system for applying a constant normal load on the compacted soil sample. The applied loads are obtained from two 20-ton hydraulic load cells connected to hydraulic hand pumps. Pressure gages are used to measure the loads. The shear and normal displacements are monitored by high precision dial gages.

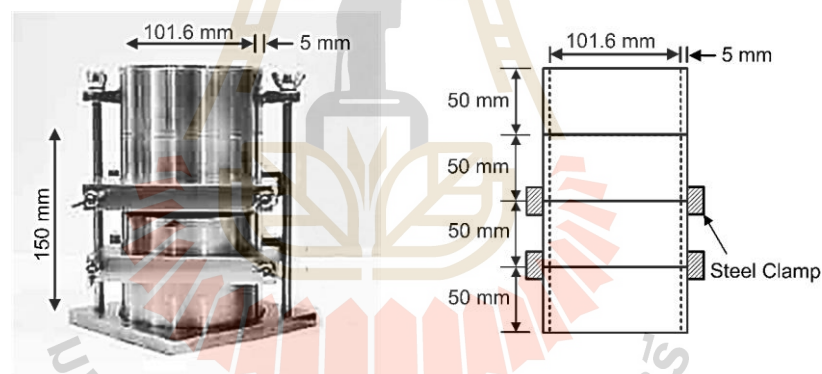


Figure 2.1 Three-ring mold (Sonsakul and Fuenkajorn, 2013).

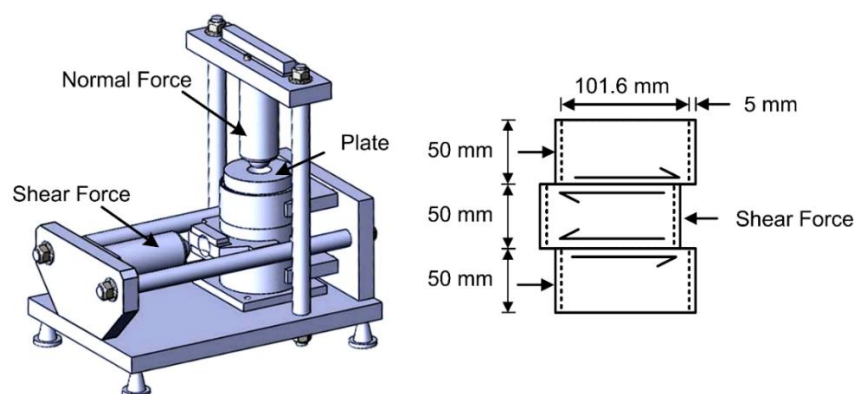


Figure 2.2 Three-ring shear mold apparatus (Sonsakul and Fuenkajorn, 2013).

Ito (2006) investigates compaction properties of granular bentonites for buffer materials for use in high-level nuclear waste repositories. This study performed the compaction tests of 21 kinds of granular bentonites. Results indicate that the degree of saturation at the maximum dry density and the optimum water content are 70-80% regardless of the kind of granular bentonite used. Compaction properties of granular bentonites from bentonite ore are influenced strongly by the kind of bentonite ore used as a raw material rather than the grain size range. Granular bentonite with a lower plastic limit has higher maximum dry density and lower optimum water content. This fact implies that microscopic interaction between aggregate of montmorillonite in the bentonite and water supplied for adjusting the water content of sample plays an important role in the compaction process of granular bentonite and this study proposes simplified evaluation methods for selecting suitable granular bentonite for construction of bentonite-based buffer materials by in-situ compaction methods.

Hansen and Mellegard (2002) study the dynamic compacted crushed salt specimens with a diameter of 100 mm and lengths up to 200 mm were derived from the full-scale compaction demonstration and from a laboratory scale dynamic compaction study. Starting material was wetted to moisture contents of nominally 1.6 % by weight. Figure 2.3 plots volumetric strain as a function of time on the primary axis and brine flow as a function of time on the secondary axis. Permeability testing of the dynamically compacted crushed salt provided further evidence that the permeability decreases as the fraction density of the salt increases.

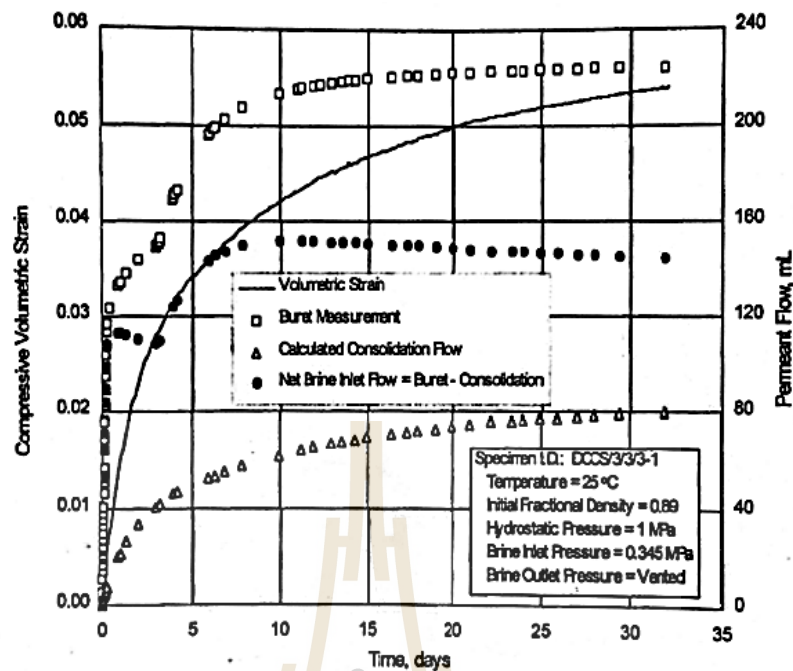


Figure 2.3 Volumetric strain and brine flow as function of time (Hansen and Mellegard, 2002).

Ran and Daemen (1995) present results of laboratory compaction testing to determine the influence of particle size, size gradation and moisture content on compaction of crushed rock salt. Included is a theoretical analysis of the optimum size gradation. The objective is to evaluate the relative densities that can be achieved with tamping techniques. Initial results indicate that compaction increases with maximum particle size and compaction energy, and varies significantly with particle size gradation and water content until the optimum water content is reached (5%), and decreases with further water content increases (Figure 2.4).

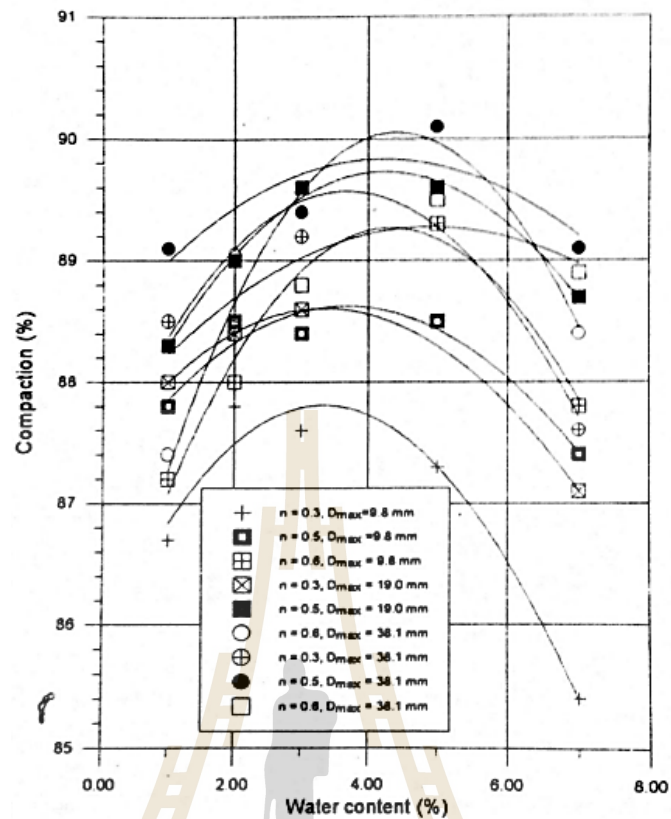


Figure 2.4 Compaction as a function of water content and particle size gradation (Ran and Deamen, 1995).

This conclusion agrees with and augments previous results. Shear consolidation creep test results were added to a database of similar results for the purpose of estimating parameter in a constitutive model that represents the behavior of crushed salt (Callahan and Hansen, 2002). Current testing was performed at higher initial fractional densities (0.9) and stresses (1 to 5 MPa) than were used in previous programs to give better coverage of the range of conditions likely to be experienced by salt seal element at the WIPP. The constitutive model predicted that stress states exist where the radial strain rate would initially be positive (consolidation) and then reverse direction and become negative as the specimen density increases. This phenomenon was clearly observed in multiple tests.

2.3 Direct shear tests of backfill materials in salt and potash opening

The shear strength of soils is an important aspect in many foundation engineering problems such as the bearing capacity of shallow foundations and piles, the stability of the slopes of dams and embankments, and lateral earth pressure on retaining walls (Das, 2008). Understanding the impact of different particle size ratio on soil behavior helps the application and interpretation of laboratory test result. Many investigations have considered the characteristics of various particles size combinations. As these materials often contain particles of large size, the direct shear box size become an issue.

Zhang et al. (2016) study shear strength of GMZ07 bentonite and its mixture with sand. The tests were carried out on compacted specimens of GMZ07 bentonite and GMZ07 bentonite-sand mixture with distilled water or salt solutions at different concentrations of 0, 0.2, 0.5, 1.0 and 2.0 mol/L. Specimens were prepared by mixing the dry powdered GMZ07 bentonite or the bentonite-sand mixture with distilled water or with NaCl solutions and the initial water content of 10% for the specimen preparation was adopted. Specimens with 5 cm diameter and 1.5 cm thickness were statically compacted at a velocity of about 0.2mm/min. Test materials are a sodium bentonite called GMZ07 bentonite and a quartz sand called Fujian standard sand. Bentonite/Sand ratio of the bentonite-sand mixture in mass is 1:1, i.e., the sand rate in the mixture is 50%. It can be seen that the grain size distribution of GMZ07 bentonite is b0.074 mm. In contrast, the particle size of Fujian standard sand is N0.074 mm. The shear resistances of GMZ07 bentonite and its sand mixture have an obvious increase with increasing the salt solution concentration (Figure 2.5).

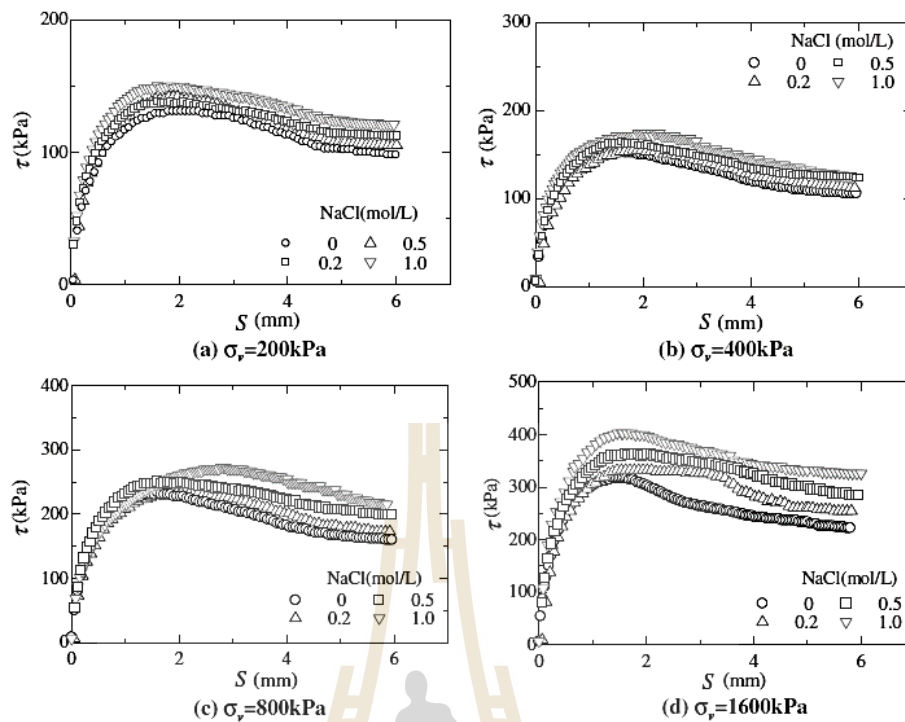


Figure 2.5 Shear stress as a function of displacement for GMZ07 bentonite saturated by NaCl solutions under different vertical stresses (Zhang et al., 2016).

For pure GMZ07 bentonite, the friction angle increases fairly with the salt solution concentration, but cohesion has negligible change. The increase in the shear resistances of GMZ07 bentonite and its sand mixture with the salt solution concentration is due to the change in the microstructure. The decrease in void ratio and the increase in the surface roughness and/or the specific surface area of particles and/or aggregates increase the interaction between particles and/or aggregates and thus increase the shear resistance.

Li et al. (2013) study the effects of particle shape on shear strength of clay-gravel mixture the samples is prepared by mixing kaolin and gravel-sized particles ($2.0 \text{ mm} < d < 15 \text{ mm}$) of different shapes at various volumetric proportions (40, 70 and 100%). Three types of gravel are used, i.e., glass beads, river cobbles and crushed

granite fragments. The applied normal stresses are 150 kPa and the shearing rate is 0.006 mm/min. They found that increasing gravel content certainly increases both peak and constant volume friction angle the result demonstrates that overall roughness of shear surface at constant volume state is negatively related to gravel particle smoothness (convexity) and positively related to area, occupied by gravel particles, of shear surface. Peak friction angle is associated with volumetric dilation. The dilation is found to have positive relationship with gravel content and difficulties for gravel particles to overtop each other when they come to contact.

Sonsakul et al. (2013) assess the performance of three-ring compaction and direct shear testing device (Figure 2.6). The three-ring compaction and direct shear mold has been developed to obtain the optimum water content, dry density and shear strength of compacted soil samples. The device can shear the soil samples with grain size up to 10 mm. It can be used as a compaction mold and direct shear mold without removing the soil sample, and hence eliminating the sample disturbance. Commercial grade bentonite is tested to verify that the three-ring mold can provide the results comparable to those obtained from the ASTM standard testing devices. Three types of soil, including clayey sand, poorly-graded sand and well-graded sand, are tested to assess the performance of the device. Their results are compared with those obtained from the ASTM standard test device. The results indicate that the shear strength, maximum dry density and optimum water content of the bentonite obtained from the three-ring mold and the ASTM standard mold are virtually identical. The three-ring mold yields the higher maximum dry density than those obtained from the standard mold. The shear strengths obtained from the three-ring mod are also higher than those from the standard shear test device. This is primarily because the three-ring mold can

accommodate the soil particles up to 10 mm for the shear test, and hence resulting in higher shear strengths that are closer to the actual behavior of the soil under in-situ conditions.

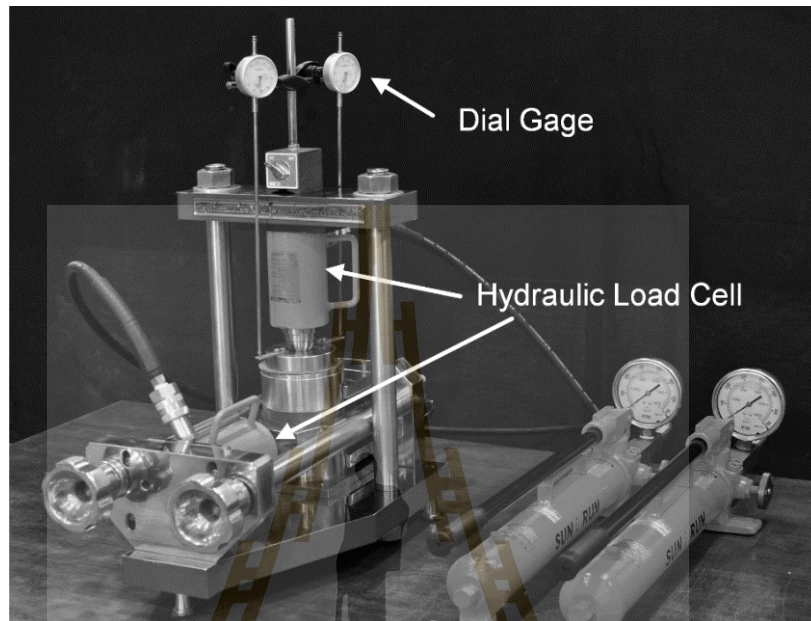


Figure 2.6 Three-ring compaction and direct shear testing device (Sonsakul et al., 2013).

Das (2008) states that the direct shear method is the oldest and simplest form of shear test arrangement. A diagram of the direct shear test apparatus is shown in Figure 2.7 the test equipment consists of a metal shear box in which the soil specimens may be square or circular. The size of the specimens generally used is about 3 to 4 in² across and 1 in high. The box is split horizontally into halves. Normal force on the specimen is applied from the top of shear box. The normal stress on the specimens can be as 150 psi. Shear force is applied by moving one half of the box relative to the other to cause failure in the soil specimen. Depending on equipment, the shear test can be either stress-controlled or strain-controlled. In stress-controlled tests, the shear force is

applied in equal increments until the specimen fails. The failure takes place along the plane of split of shear box. After the application of each incremental load, the shear displacement of the top half of the box is measured by a horizontal dial gauge. The change in the height of the specimen (and thus the volume change of the specimen) during the test can be obtained from the reading of the dial gauge that measures the vertical movement of the upper loading plate. In strain-controlled tests, a constant rate of shear displacement is applied to one half of the box by a motor that act through gears. The constant rate of shear displacement is measured by a horizontal dial gauge. The resisting shear force of the soil corresponding to any shear displacement can be measured by a horizontal proving ring or load cell. The volume change of the specimen during the test is obtained in a manner similar to the stress-controlled test.

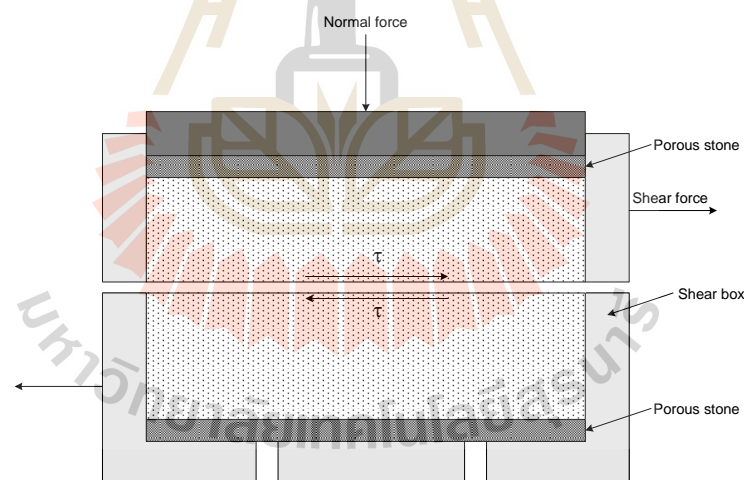


Figure 2.7 Diagram of direct shear test arrangement (Das, 2008).

Nakao and Fityus (2008) study direct shear testing of a marginal material using a large shear box this comparison between the results of three series of shear box tests on a typical ripped rock material. Tests performed used 300mm and 60mm shear box, soil sample prepared to sub-19mm and sub-4.75mm size, and range of shearing rates. The shearing results show that the large box results indicate higher shear strength values

than the small box (Figure 2.8). They found that the small shear box tests are no substitute for large shear box tests, and that downsizing the grading and the size of the sample tested will cause the effective friction angle to be under-estimated by as much as 4degrees.

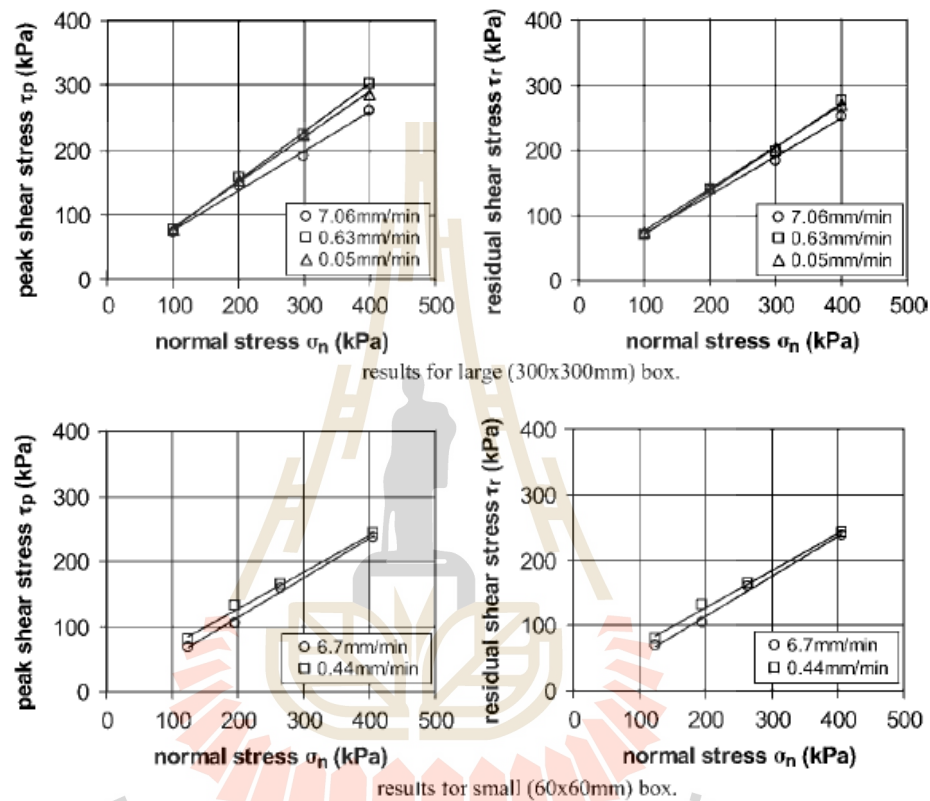


Figure 2.8 Comparison of results for different shearing rates in large and small boxes (Nakao and Fityus, 2008).

Cerato and Lutenegger (2006) present the direct shear tests of five sands with different properties were tested in three square shear boxes of varying sizes, each at three densities is dense, medium and loose. Creasing relative density in each of the three boxes. The tests indicate that for well-graded, angular sands, friction angle decreases as box size increases and that the influence of box size is dependent on relative density. Modeled the decreasing friction angle with increasing footing size found in model and prototype scale foundation tests very well. It is thought that

constraining the shear zone propagation in both the small footing tests and the small direct shear box tests are related and may help to explain the scale effects seen in footing tests on granular material.

Mohr (1900) present the theory for rupture in materials that contented that material fails because of a critical combination of normal stress and shearing stress and not from either maximum normal or shear stress alone. Thus, the functional relationship between normal stress and shear stress on a failure plane can be expressed in the following form:

$$\tau_f = c + \sigma_n \tan \phi \quad (2.1)$$

The equation is so called Mohr-Coulomb failure criterion as shown in Figure 2.9.

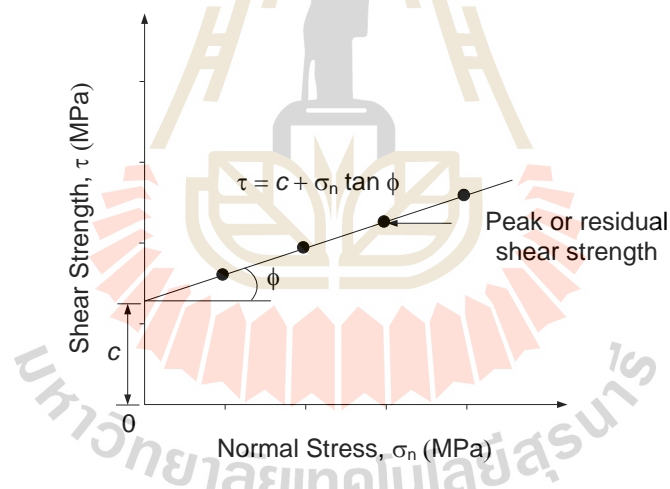


Figure 2.9 Mohr-Coulomb criterion as a function of shear strengths and normal stresses (Mohr, 1900).

2.4 Uniaxial compressive strength tests

Kumar and Dutta (2014) study the characteristics of lime-bentonite specimens, lime-bentonite-phosphogypsum and limephosphogypsum-bentonite specimens mixed with varying percentages of sisal fibers were studied. The content of lime and phosphogypsum was varied from 2 to 10% and 0.5 to 10% by dry weight of bentonite,

respectively. Unconfined compression strength tests were conducted on test specimens. The content of sisal fibers was varied from 0.5 to 2% by dry weight of bentonite. The unconfined compressive strength of the bentonite increased with the addition of 8% lime. Beyond 8%, the unconfined compressive strength decreased. The unconfined compressive strength of the bentonite + 8% lime increased up to 8% phosphogypsum. Beyond 8%, the unconfined compressive strength decreased.

Cho et al. (2002) review some literatures related to investigating the unconfined compressive strength and Young's modulus of elasticity of compacted sand-bentonite mixtures (Figure 2.10). They found that the unconfined compressive strength and Young's modulus decreased as the sand content increased. They also noted that the logarithm of compressive strength and Young's modulus increased linearly with the increase in dry density.

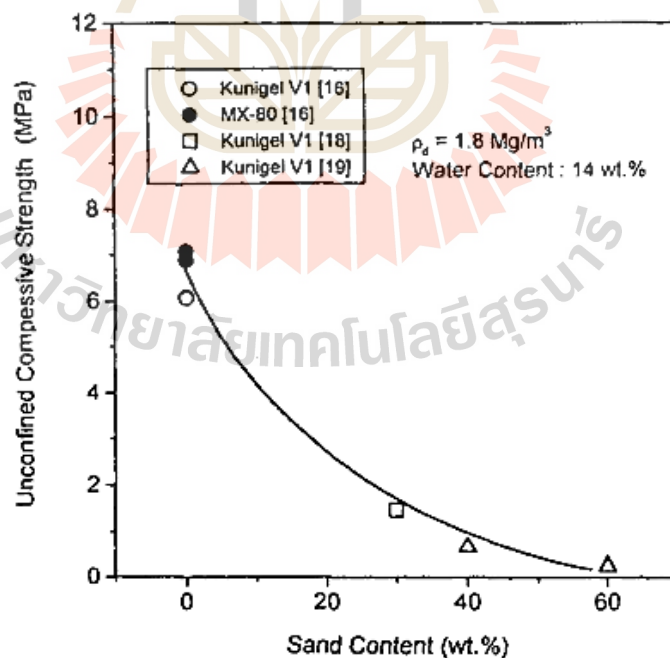


Figure 2.10 Effect of sand content on the unconfined compression strength of the bentonite-sand mixture (Cho et al., 2002).

2.5 Swelling test

During the long-term operation of a deep geological repository, infiltration of groundwater with different chemical compositions can affect the buffer/backfill properties of compacted bentonite (Zhu et al. 2013). Due to its low hydraulic conductivity, good swelling capacity and sorption properties etc., compacted bentonite has been considered as buffer/backfill material for construction of engineering barrier in deep geological repository for disposal of high-level radioactive nuclear waste (HLW). During the construction and long-term operation of a geological repository, compacted bentonite can work as an effective barrier, protecting the canister and restricting the transfer of radionuclide released from the waste packages after possible failure of canister (Wersin et al., 2007).

Weimin et al. (2014) study the effects of salinity of infiltrating solutions on the swelling strain, compressibility, and hydraulic conductivity of compacted GMZ01 Bentonite were investigated. After swelling under vertical load using either distilled water or NaCl solutions with concentrations of 0.1, 0.5 M, and 1 M, laboratory oedometer tests were conducted on the compacted GMZ01 Bentonite. Based on the oedometer test results, hydraulic conductivity was determined using the Casagrande's method. Results show that the swelling strain of highly compacted GMZ01 Bentonite decreases as the concentration of NaCl solution increases.

Cui et al. (2012) study the compacted mixture of bentonite and sand for use as a buffer/backfill material. laboratory tests on the swelling pressure and swelling deformation of GMZ bentonite-sand mixtures consisting of different sand contents of 0, 10, 20, 30, 40 and 50%. The results indicate that swelling occurs in three distinct phases: inter-void swelling, primary swelling and secondary swelling, where both

swelling pressure and swelling strain follow a sigmoid relationship with time. With constant initial water content, the maximum swelling pressure presents an exponential increase with increased initial dry density, and the maximum swelling strain increases linearly. As the sand content ratio increases, the maximum swelling pressure decreases exponentially while the maximum swelling strain follows a quadratic decrease.

Wang et al. (2012) study the swelling behavior of bentonite/claystone mixture were investigated by carrying out a series of experiments including determination of the swelling pressure of compacted samples by constant-volume method. All the tests in this study were performed on samples of compacted bentonite/claystone mixture with a bentonite content of 70% in dry mass. Bentonite and claystone powders with the initial water contents of 11.8% and 2.64% respectively. Results show that upon wetting the swelling pressure increases with decreasing suction; however, there are no obvious effects of synthetic water chemistry and hydration procedure on the swelling behavior in both short and long terms. For the same initial dry density, the swelling pressure decreases with increasing pre-swell strain; whereas there is a well-defined logarithmic relation between the swelling pressure and final dry density of the sample regardless of the initial dry densities and the experimental methods. It was also found that swelling pressure depends on the loading-wetting conditions as a consequence of the different microstructure changes occurred in different conditions.

Mitchell (1993) indicate that the clay particles carry negative charges at their surfaces due to the isomorphous substitution in the crystal lattice. Exchangeable cations in the clay media are attracted to these negative charges. In a clay–water electrolyte system, the adsorbed cations near the surface of the clay particles produce a much higher concentration as compared with the ion concentration in solution away from the

surfaces. Because of the difference in ion concentration in solution near the surfaces and away from the surfaces of the clay particles, the cations near the surfaces of the particles try to diffuse away to equalize the concentration throughout. Their tendency to do so, however, is opposed by the negative electric field originating in the particle surfaces. The tendency of the ions to diffuse away and the opposing electrostatic attraction lead to ion distribution adjacent to a clay particle in suspension. The charged clay surface and the distributed charge in the adjacent phase are together termed the diffuse double layer.

2.6 Experimental researches on backfill materials

Khamrat and Fuenkajorn (2018) predict the mechanical properties of crushed salt backfill emplaced in boreholes and shafts. Consolidation tests are performed on crushed salt for the periods of 3 to 180 days. The mechanical properties of the specimens are determined as a function of the applied mean strain energy densities during consolidation. The time-dependent closure of borehole and shaft is calculated in terms of the released mean strain energy density. The results suggest that the crushed salt becomes denser, stiffer, stronger and less compressible with time and applied stress. They report that under 15 MPa consolidation stresses the strength and elastic modulus increase up to 28.4 MPa and 9.46 GPa after being consolidated for 97 days. The prediction of the crushed salt properties after emplacement in shaft and borehole presented here may be conservative because the axial load imposed by the backfill gravity is excluded from the calculation. Depending on the emplacement depth the weight of the crushed salt backfill can contribute to the mean strain energy applied to the crushed salt.

Sinnathamby et al. (2014) present the shear behavior and the shear resistance of different bentonite based clay backfill materials and their interfaces of Finnish KBS-3V type nuclear waste repository, under varying hydraulic conditions. Three different backfill interfaces were tested under varying groundwater salinity and interface water content conditions. The tested bentonite-based granular backfill materials showed a decrease in internal shear parameters with increasing water content. Physical observations showed that the bentonite granules (GB) were relatively stable even at water contents as high as 50% compared with the bentonite pellets (QSEP). The effect of salt concentration on the FCB–FCB interface was studied and the results showed that the interface shear parameters increased as a result of the formation of a rough surface with increasing salt interface water salinity.

Lennart et al. (2003) study the influence of soil structure heterogeneities on the behavior of backfill materials based on mixtures of bentonite and crushed rock. Compaction of a mixture of bentonite and crushed rock or sand has been proposed for backfill or buffer materials for the concept of nuclear waste disposal in many countries. At present a mixture of 30% bentonite and 70% crushed rock is used for backfilling tunnels in two full-scale tests. In advance of those tests, mixtures of 0-50% bentonite and different ballast materials have been investigated in the laboratory regarding hydraulic conductivity, swelling pressure and other geotechnical properties. The results show that the influence of heterogeneities in the soil structure of backfill materials made of mixtures of crushed rock and bentonite powder on the hydro mechanical properties is very strong. At poor mixing or low bentonite content, the bentonite will be unevenly distributed in the pores between the ballast particles. With the present mixing technique and the materials used for the tests referred to in this article, it seems the limit where

the backfill will be inhomogeneous is between 30% and 50% bentonite content. 30:70 and low salt content seems though to be a good combination since the measured swelling pressure is higher and the measured hydraulic conductivity only slightly higher than the theoretical values for an ideally homogeneous material.

Bauer and Zhao (1993) study the shear strength tests for coarse granular backfill and reinforced soils. Coarse granular soils have been widely used as backfill material for embankments, trenches, and earth-retaining structures due to their high strength, good drainage, and compaction properties. This section summarizes the results of six direct shear tests on two granular soils. For small initial displacements, the shear force increased linearly. A distinct peak value was observed for the sand. This behavior is common for dense to very dense granular backfill in shear. The peak value occurred at 6 mm of shear displacement at low normal stress and at 9 mm at the high applied normal stress. The sand experienced a rapid decrease in strength beyond the peak value. The residual shear strength was on the order of 20 to 30% lower than the peak strength. The shearing behavior of the crushed limestone aggregate is similar to that of coarse sand unlike coarse sand, the crushed stone aggregate experienced a gradually decrease in strength after the peak value was reached. The reinforced soils exhibited higher shear resistance than the corresponding natural soils. Soil dilatancy is a key factor in mobilizing tensile strains in geogrids. Granular soils with larger particles tend to dilate more than soils having smaller particles at the same normal stress.

Ouyang and Daemen (1992) study the sealing performance of American Colloid C/S granular bentonite and crushed Apache Leap tuff. Bentonite weight percent and crushed tuff gradation are the major variables studied. The sealing performance assessments include high injection pressure flow tests, polyaxial flow tests, high

temperature flow tests, and piping tests. The results indicate that a composition would have at least 25% bentonite by weight mixed with well-graded crushed rock. Hydraulic properties of the mixture plugs may be highly anisotropic if significant particle segregation occurs during sample installation and compaction. Temperature has no significant effect on the sealing performance within the test range from room temperature to 60 °C. Piping damage to the sealing performance is small if the maximum hydraulic gradient does not exceed 120 and 280 for samples with a bentonite contents of 25 and 35%, respectively.

Butcher et al. (1991) concludes that a 70% by weight salt and 30 % by weight bentonite mixture is preferable to pure crushed salt as backfill for disposal rooms in the Waste Isolation Pilot Plant. The performance of two backfill materials is examined with regard to various selection criteria related to compliance with transuranic radioactive waste standard 40 CFR 191, Subpart B, such as the need for low liquid permeability after closure, chemical stability, strength, ease of emplacement, and sorption potential for brine and radionuclides. Both salt and salt/bentonite are expected to consolidate to a final state of permeability $\leq 10^{-18} \text{ m}^2$, which is adequate for satisfying government regulations for nuclear repositories. The real advantage of the salt/bentonite backfill depends, therefore, on bentonite's potential for absorbing brine and radionuclides. Estimates of the impact of these properties on backfill performance are presented.

Case and Kelsall (1987) study the potential of crushed for required sealing access shafts and drifts for long periods. Crushed salt backfill is being investigated as a potential backfill and seal material through laboratory testing to determine how fundamental properties such as permeability, porosity and creep rate are reduced by

pressure and time through consolidation. Tests with one- or two-month durations were conducted on samples with maximum particle sizes of 1, 10, and 20 mm, with initial porosities ranging from 26 to 36%, moisture contents of zero and 2%, and initial permeability from 10^3 to 10^5 m². The tests were performed at ambient temperature and confining pressures ranging from 0.34 to 17 MPa. The most significant observation from the tests was the influence of moisture on changes in permeability, porosity and volumetric creep strain rate. The final permeability and porosity of one moist sample were reduced after one month to about 10^{-5} m² and 5%, respectively, compared to about 10^{-2} m² and 14 to 19% for the dry samples. In addition, the consolidation rate for the moist sample was more rapid at comparable porosities. In all of the tests, the volumetric creep strain rate ranged from 10^{-8} to 10^{-6} strain/sec, and did not achieve steady state values after 1 to 2 months of load application.

Fuenkajorn and Daemen (1987) study the mechanical relationship between cement, bentonite and surrounding rock. The study deals with the mechanical interaction between multiple plugs and surrounding rock and identification of potential failure. Pipe tests have been performed to determine the swelling pressures of 60 mm diameter bentonite plugs and of 64 mm diameter cement plugs. The axial and radial swelling pressures of a bentonite plug specimen are 7.5 and 2.6 MPa after adsorbing water for 5 days. The maximum radial expansive stresses of the cement plugs cured for 25 days are 4.7 and 2.7 MPa for system 1 and system 3 cements. Results from the experiment indicate that in order to obtain sufficient mechanical stability of bentonite seal, the sealing should be done below groundwater level. If cement material is used to seal in hard rock, the mechanical stability will be higher than sealing in soft rock.

CHAPTER III

SAMPLE PREPARATION

3.1 Introduction

This chapter describes the sample preparation to obtain the optimum brine content, dry density, shear strength and compressive strength of compacted mixtures.

3.2 Granular material preparation

3.2.1 Bentonite

Bentonite used in this study is from Thai Nippon Chemical Industry Co., LTD, Thailand (Figure 3.1). The grain size distribution curve is shown in Figure 3.2.

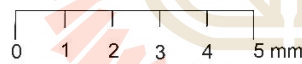


Figure 3.1 Bentonite from Thai Nippon Chemical Industry Co., LTD, Thailand.

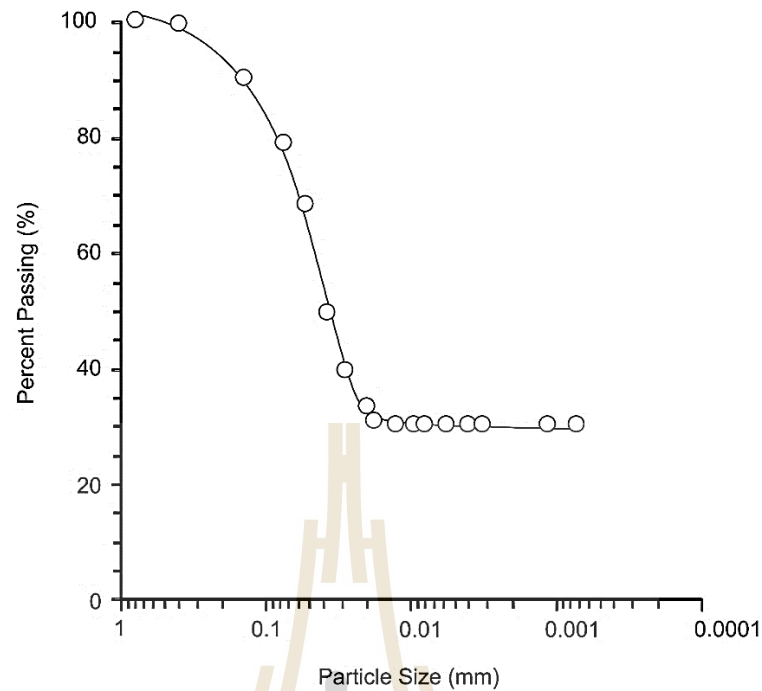
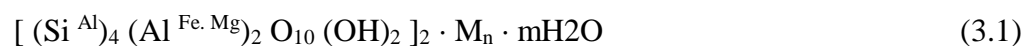


Figure 3.2 Particle size distribution of bentonite.

Bentonite is the name for the ore whose major constituent is the mineral, sodium montmorillonite has a high-water absorption capacity causing it to expand and swell. Bentonite is a clay mineral belonging to a class of phyllosilicates called smectites. Montmorillonites are three-layer minerals consisting of a central octahedral alumina (Al_2O_3) layer and two tetrahedral silica (SiO_2) layers (Figure 3.3). The silicon ion and the aluminum ion often undergo isomorphous substitutions by lower valence metals, such as magnesium and iron. In turn, these substitutions lead to a charge imbalance, compensated by exchangeable cations, in particular, calcium (Ca^{2+}), magnesium (Mg^{2+}) and sodium (Na^+) ions, together with water molecules bonded together by ion-dipole forces. These ions, with no more place inside the reticular structure, migrate to the external silica layers and are the main cause of hydration in the crystal lattice. Therefore, each platelet can be assumed to have the following general formulation:



where the first member in brackets refers to isomorphous constitutions in the tetrahedral layers, the second member refers to isomorphous constitutions in the octahedral layer; and M and mH₂O symbols refer to exchangeable cations and interposition water, respectively.

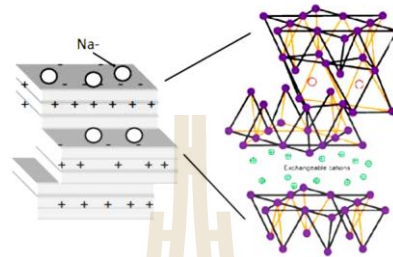


Figure 3.3 Crystalline structure of sodium montmorillonite with interlamellar water layer.

The bentonite is highly uniform and consistent in engineering properties. It is prepared for the compaction, direct shear and uniaxial compressive strength tests. Its mineral compositions, maximum dry density, optimum water content, shear strengths and compressive strength are determined. Tables 3.1 and 3.2 show the chemical compositions and engineering properties of the bentonite. The chemical compositions are determined by X-Ray Fluorescence (XRF).

Table 3.1 Chemical compositions of tested bentonite and sludge.

Compositions	Concentration (% weight)	
	Bentonite	Sludge (Wetchasat, 2013)
SiO ₂	48.272	52.37
Al ₂ O ₃	12.776	23.47
Fe ₂ O ₃	27.403	6.33
Na ₂ O	1.232	0.22
MgO	1.869	0.96
CaO	N/D	0.79
K ₂ O	1.806	1.55

Table 3.1 Chemical compositions of tested bentonite and sludge (Cont.).

Compositions	Concentration (% weight)	
	Bentonite	Sludge (Wetchasat, 2013)
TiO ₂	4.622	0.79
P ₂ O ₅	1.404	0.34
SO ₃	0.091	0.55
MnO	0.263	0.22
CuO	0.018	0.01
Rb ₂ O	N/D	0.01
SrO	N/D	0.01
Y ₂ O ₃	N/D	<0.01
ZrO ₂	N/D	0.03
Nb ₂ O ₅	N/D	<0.01
BaO	N/D	0.01
Cr ₂ O ₃	0.018	0.02
Cl	0.087	0.07
Co ₃ O ₄	0.071	N/D
Nio	0.022	N/D
CeO ₂	0.047	N/D
Total	100	100

Note: N/D = Not detectable

Table 3.2 Atterberg's limits and specific gravity of bentonite and sludge (Wetchasat, 2013).

Atterberg Limits	Bentonite (% weight)		Sludge (% weight)	
	SUT ¹	US ²	SUT ¹	KU ³
Liquid limit	357	478	55	69
Plastic limit	44	28	22	42
Plasticity index	313	449	23	28
Specific gravity	2.50	-	2.56	-

Note: ¹SUT = Suranaree University of Technology Laboratory,

²after Castelbaum and Shackelford (2009)

³after Kanchanamai (2003)

3.2.2 Crushed salt

Crushed salt is prepared from the Middle Salt members of the Maha Sarakham formation, northeast of Thailand. The crushed salt is passed through sieve size 6 mm and retained on sieve size 4 mm. Salt fragments are crushed by hammer mill to obtain grain sizes ranging from 4 to 6 mm. The grain size distribution curve is shown in Figure 3.4.

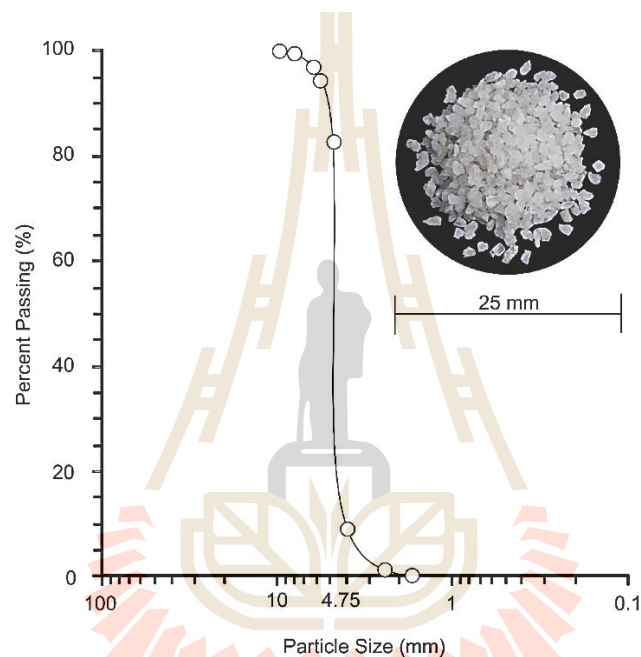


Figure 3.4 Particle size distribution of crushed salt particle with sizes from 4-6 mm.

3.2.3 Gravel

Gravel is collected from Khok Kruat sub-district, Nakhon Ratchasima Province, which is divided into 2 size ranges: 4-6 mm (FG) and 6.35-9.53 mm (CG). Figure 3.5 shows the particle size distribution of the gravels.

3.2.4 Sand

Sand is collected from Khok Kruat sub-district, Nakhon Ratchasima Province. The sand is passed through sieve size 2 mm and retained on sieve size 1 mm. Figure 3.6 shows particle size distribution of the sand.

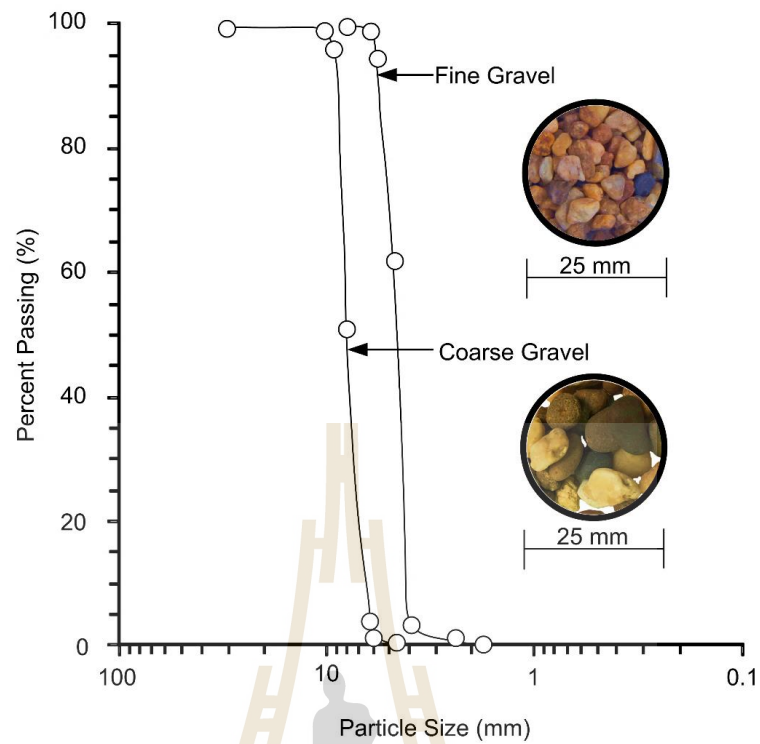


Figure 3.5 Particle size distribution of gravels with sizes of 6.35-9.53 and 4-6 mm.

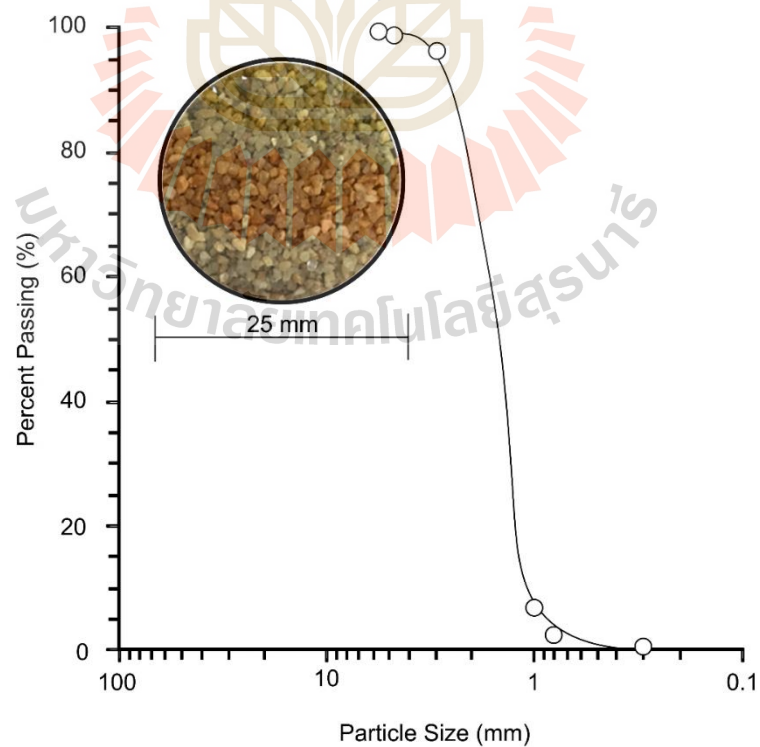


Figure 3.6 Particle size distribution of sand with particle sizes of 1-2 mm.

3.2.5 Granular classifications

The sphericity and roughness of the granular materials are determined from individual particles using an optical microscope (Olympus BX51M). Based on the widely used classification systems given by Power (1982), the sand is classified as rounded to sub rounded with high sphericity, crushed salt is angular with high sphericity, fine gravel is rounded with high sphericity and coarse gravel is classified as well rounded to rounded with high sphericity (Figures 3.7, through). The average of the roughness and sphericity for each material are shown in Table 3.3.



Figure 3.7 Examples of sand particles.

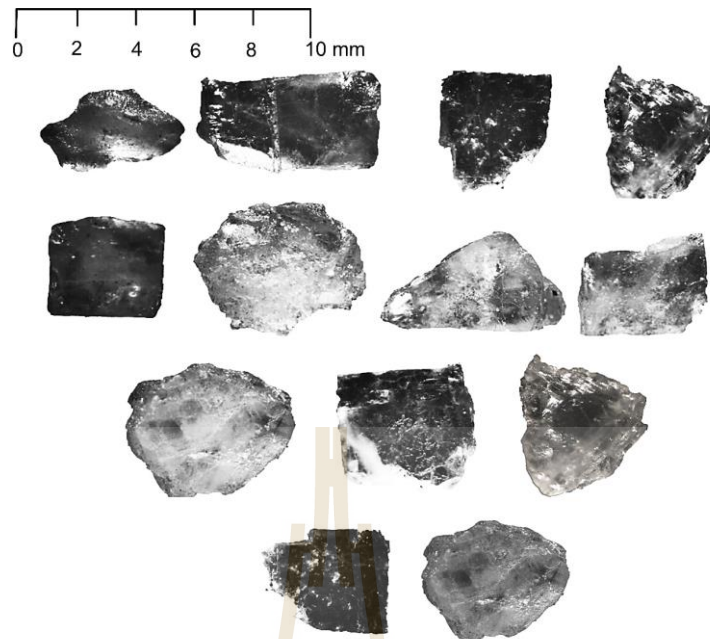


Figure 3.8 Examples of crushed salt particles.



Figure 3.9 Examples of fine gravel (a) and coarse gravel (b) particles.

Tale 3.3 Particle shape classification of granular materials based on Power (1982).

Materials	Particle size range (mm)	Roundness	Classification	Sphericity	Classification
Sand	1-2	3.5	Sub-rounded	4.5	Spherical
Crushed salt	4-6	1.5	Angular	4.5	Spherical
Fine gravel	4-6	4.5	Rounded	4.5	Spherical
Coarse gravel	6.35-9.53	5.5	Well-rounded	4.5	Spherical

3.2.6 Saturated brine

Saturated brine is prepared by mixing pure salt (NaCl) with distilled water in plastic tank. It is stirred continuously for 30 minutes. The proportion of salt to water is about 39.1% by weight. The SG of the saturated brine in this study is 1.211 at 21° C. The specific gravity of saturated brine can be calculated by:

$$SG_{\text{Brine}} = \rho_{\text{Brine}} / \rho_{\text{water}} \quad (3.1)$$

Where

SG_{Brine} is specific gravity of saturated brine

ρ_{Brine} is density of saturated brine (measured with a hydrometer (kg/m³))

ρ_{water} is density of water equal 1,000 kg/m³

3.2.7 Sludge

Sludge samples used in this research have been donated by Metropolitan Waterworks Authority, Bang Khen, Thailand. They are collected from the sludge dewatering plant of Bang Khen Water Treatment Plant located in Bangkok Metropolis

(Figures 3.10). The grain size distribution curve is shown in Figure 3.11. The Atterberg's limits are index properties of the sludge shown in Table 3.2.



Figure 3.10 Sludge samples from Metropolitan Waterworks Authority.

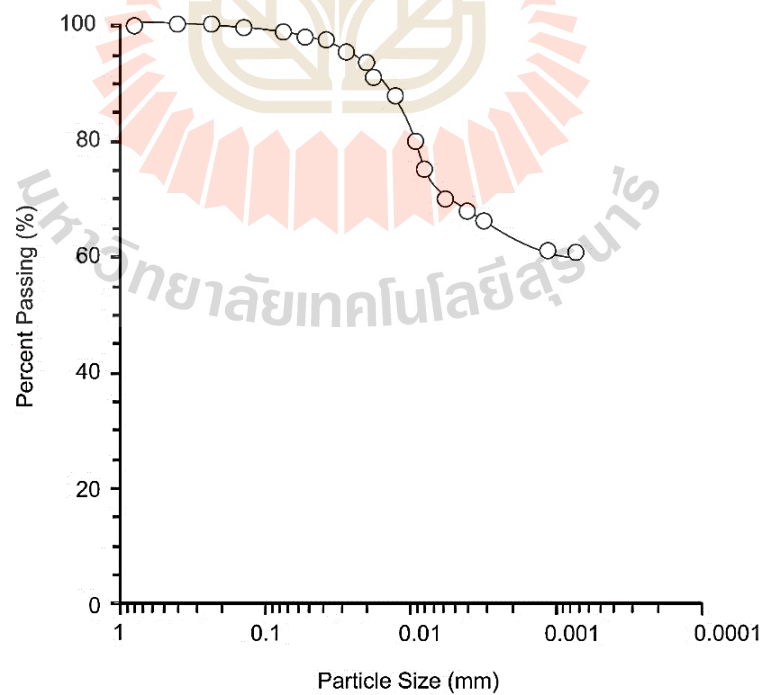
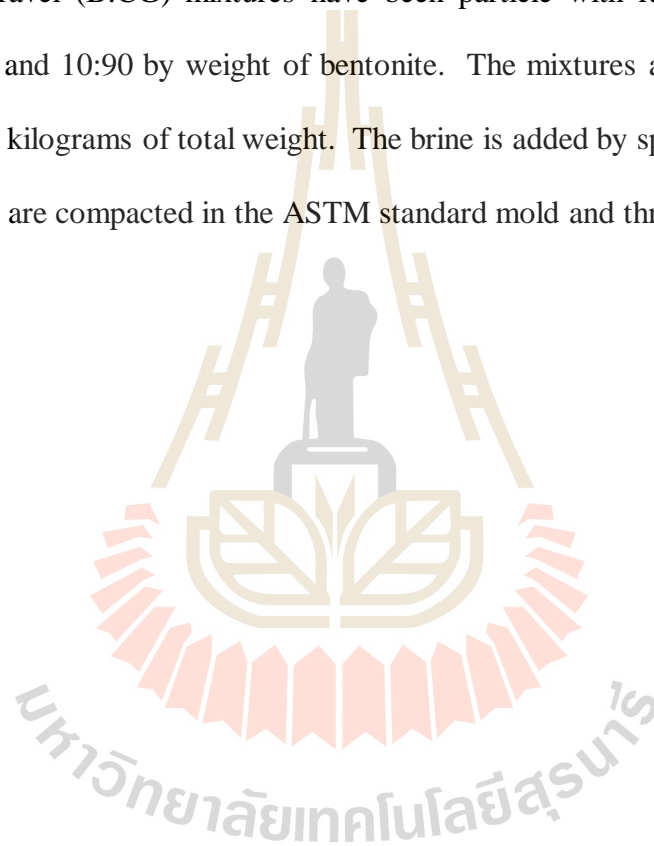


Figure 3.11 Particle size distribution of sludge.

3.3 Mixing preparations

The crushed salt and fine gravel with grain size of 4-6 mm diameters are prepared for the compaction and shear tests by using the three-ring mold and the ASTM standard test mold. The bentonite-and-sludge (B:SL), bentonite-and-sand (B:SA), bentonite-and-crushed salt (B:CS), bentonite-and-fine gravel (B:FG) and bentonite-and-coarse gravel (B:CG) mixtures have been particle with ratios of 90:10, 70:30, 50:50, 30:70 and 10:90 by weight of bentonite. The mixtures are prepared in plastic tray by 2,700 kilograms of total weight. The brine is added by spaying on the mixture. The mixtures are compacted in the ASTM standard mold and three-ring mold.



CHAPTER IV

GEOTECHNICAL AND MECHANICAL TESTING

4.1 Introduction

The chapter describes the methods and results of the compaction, direct shear and compression testing. The tests are performed on all mixtures described in the previous chapter. Comparison of the results obtained here with those obtained elsewhere is given, where applicable.

4.2 Test methods

The tests are divided into 3 parts: 1) compaction test to determine the optimum brine content and maximum dry density 2) direct shear test to determine the shearing resistance of the compacted materials, and 3) compression test to determine the compressive strength and elastic parameters of the compacted samples.

4.2.1 Compaction test

The mixtures are compacted in the three-ring mold (Sonsakul and Fuenkajorn, 2013) and ASTM mold in accordance with ASTM D1557 (Standard Test Methods for Laboratory Compaction Characteristics of Soil Using Modified Effort). They are mixed with the saturated brine varying from 0 to 30%. The test mold is 10.16 cm in diameter and 15 cm in height. The compacted materials are dynamic compaction with a release of weight steel hammer 10 pounds in mold of 27 times per layer in six layers of three-ring mold and 25 times per layer in five layers of ASTM standard mold.

Total energy of compaction is 2,700 kN·m/m³. The energy of compaction for the three-ring mold can be calculated by (Proctor, 1933):

$$n = (J \times V) / (W \times L \times t) \quad (4.1)$$

where J is compaction energy per unit volume, W is weight of hammer, L is height of drop of hammer, t is number of layers, n is number of blows per layer, V is Volume of mold. The dry densities are plotted as a function of brine contents to determine the maximum dry density and optimum brine content. The brine content is calculated by (Fuenkajorn and Daemen, 1988).

$$W_B = \frac{[100 + S_B] \times [W_1 - W_2 - (W_1 / 100)(W_2 - W_{can})]}{100(W_2 - W_{can}) - S_B(W_1 - W_2)} \times 100 \quad (4.2)$$

where W_B is brine content (%), W_1 is initial bentonite content (%), W_{can} is weight container (g), W_1 is weight wet soil and container (g), W_2 is weight dry soil and container (g), and S_B is solubility of salt in dissolved water (weight crushed salt / weight water) $\times 100\%$.

4.2.2 Direct shear test

The direct shear test is performed to determine the maximum shear strength of the mixtures by using both the three-ring (Sonsakul and Fuenkajorn, 2013) and the ASTM standard (ASTM D 3080-11) direct shear devices. The applied normal stresses in the direct shear test are varied from 0.2, 0.4, 0.6 to 0.8 MPa for both test devices. Shear force is applied by a horizontal hydraulic pump. A vertical movement gage is installed on top of the samples to measure the vertical displacement. The peak shear strength is used to calculate the cohesion and friction angle of the materials. The specimens are sheared under the predefined constant normal stress by using a direct

shear apparatus. The shear force and the corresponding vertical displacements are continuously recorded for every 0.05 mm until a total shear displacement of 6 mm is reached. The peak shear strength is used to calculate the cohesion and friction angle:

$$\tau = c + \sigma_n \tan \phi \quad (4.3)$$

where τ is shear stress, c is cohesion, σ_n is normal stress and ϕ is friction angle.

4.2.3 Compression test

The compressive strength and elastic parameters of the compacted mixtures under their optimum brine content can be determined by pushing the specimen out of the mold. The specimen is trimmed to obtain flat end surfaces and is placed in the uniaxial compression load frame (Figure 4.1). Neoprene sheets are used to minimize the friction at the interfaces between the loading platen and the sample surface. The axial and lateral displacements are monitored.

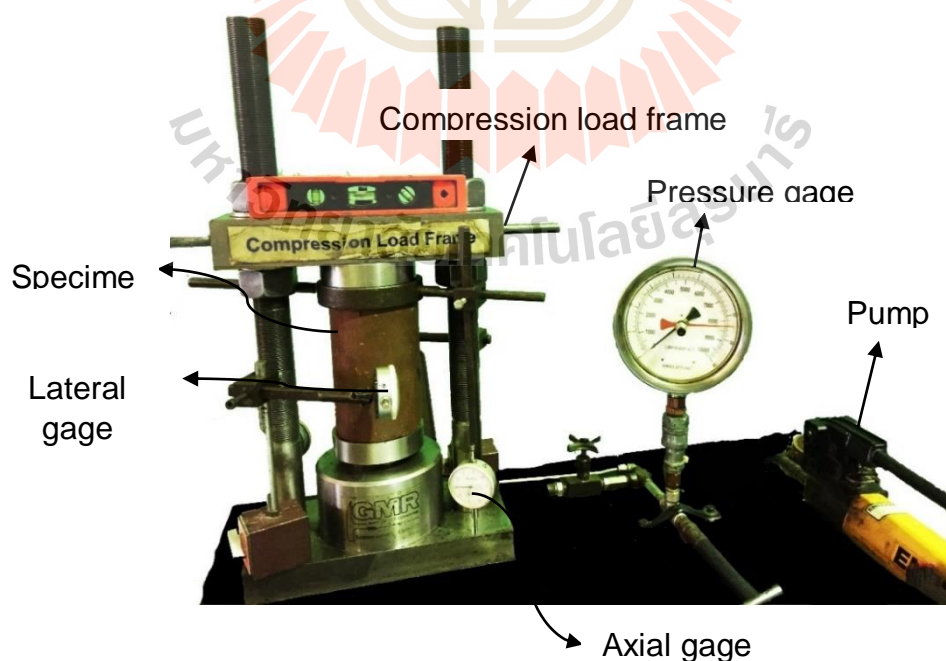


Figure 4.1 Uniaxial compression test equipment.

The compressive strengths are determined by axially loading under constant rate of 0.5-1 MPa/second until failure. The elastic modulus (E) and Poisson's ratio (ν) are determined from the tangent of the stress-strain curves at 50% of the failure stress. The compressive strength, elastic modulus and Poisson's ratio are determined in accordance with the ASTM (D2938-95) standard practice.

4.3 Test results

4.3.1 Compaction results

The results of compaction test at various brine contents are presented to determine the maximum dry density and optimum brine content in Figure 4.2. The results show that the coarser particles (gravels) show higher dry densities and lower optimum brine contents than the finer particles (sludge). The bentonite content decreases with increasing dry density and decreases with decreasing the optimum brine content. The increase of bentonite contents tends to increase the optimum brine content, probably due to the physical properties of bentonite (high absorption and swelling capacity). Increasing bentonite content also decreases the dry densities. This is probably because the specific gravity of bentonite is less than those of the granular materials. The optimum brine content is from 9.7% to 19.7% with the corresponding maximum dry densities from 1.82 to 2.03 g/cc. Results of the maximum dry densities and optimum brine content are shown in Figure 4.3. The compaction test results are summarized in Table 4.1. They agree reasonably well with the test results obtained by Soltani-Jigheh and Jafari (2012) and Kaya and Durakan (2004). Figures 4.4 and 4.5 plot the dry density as a function of brine content for both methods. The results of the compaction test obtained from the three-ring and ASTM standard test molds show that

the maximum dry density decreases with decreasing of granular content, while optimum brine content increases with decreasing of granular content (Figure 4.6). The results show that the maximum dry densities and the optimum brine contents of the samples obtained for both methods are virtually identical. This is suggested that the three-ring mold can provide the results that are comparable to those of the ASTM standard test mold. The results are consistent with the test results obtained by Sonsakul and Fuenkajorn (2013). The results of compaction test for the both methods are summarized in Table 4.2

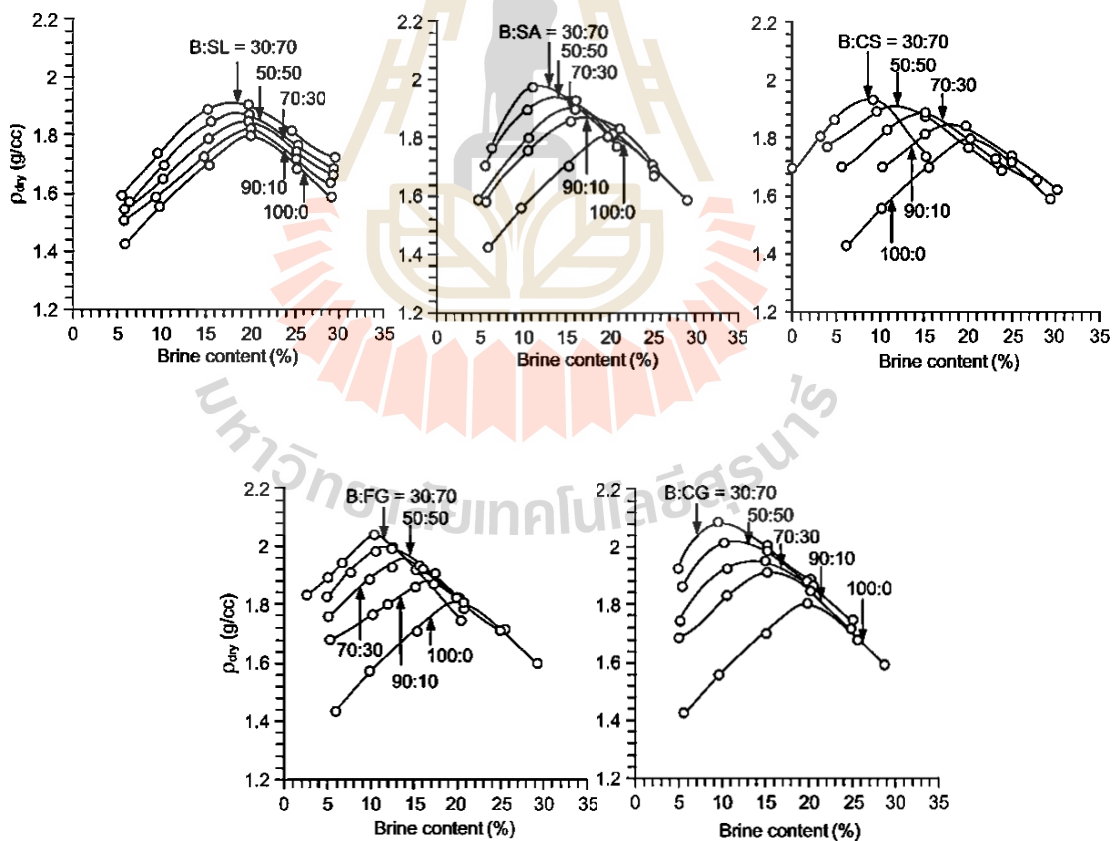


Figure 4.2 Maximum dry densities as a function of brine contents.

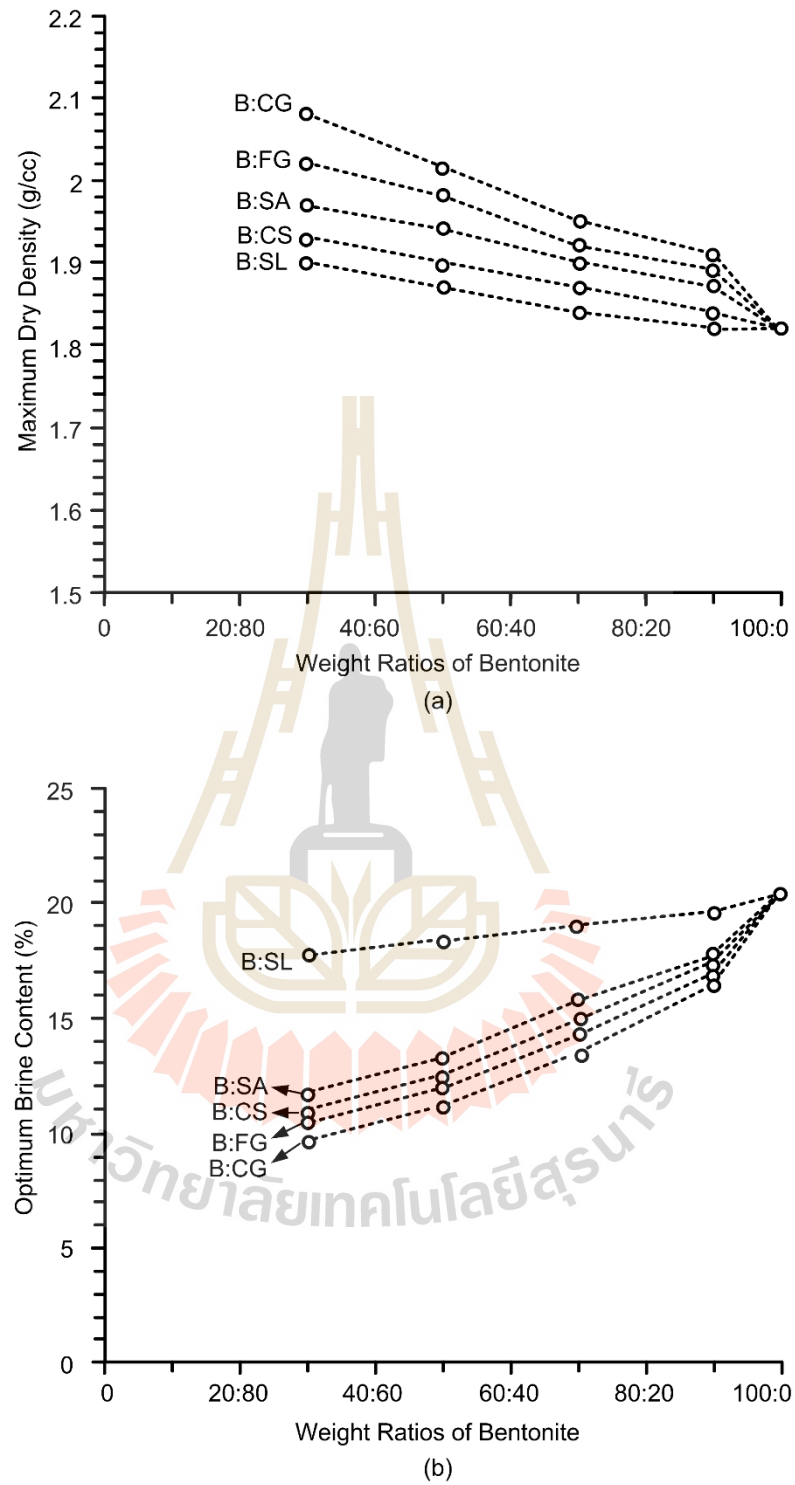


Figure. 4.3 Maximum dry densities (a) and optimum brine contents (b) as a function of bentonite-to-granular weight ratios.

Table 4.1 Compaction test results.

Materials	Ratios of bentonite-to-aggregates	Optimum brine content (%)	Maximum dry density (g/cc)
Bentonite:Sludge	30:70	17.80	1.90
	50:50	18.40	1.87
	70:30	19.10	1.84
	90:10	19.70	1.82
Bentonite:Sand	30:70	11.80	1.97
	50:50	13.30	1.94
	70:30	15.80	1.90
	90:10	17.80	1.87
Bentonite:Crushed salt	30:70	10.30	1.93
	50:50	10.80	1.90
	70:30	15.80	1.84
	90:10	17.80	1.82
Bentonite:Fine gravel	30:70	10.10	2.02
	50:50	11.20	1.98
	70:30	12.00	1.92
	90:10	16.00	1.89
Bentonite:Coarse gravel	30:70	9.70	2.03
	50:50	11.20	1.99
	70:30	13.50	1.93
	90:10	16.50	1.92

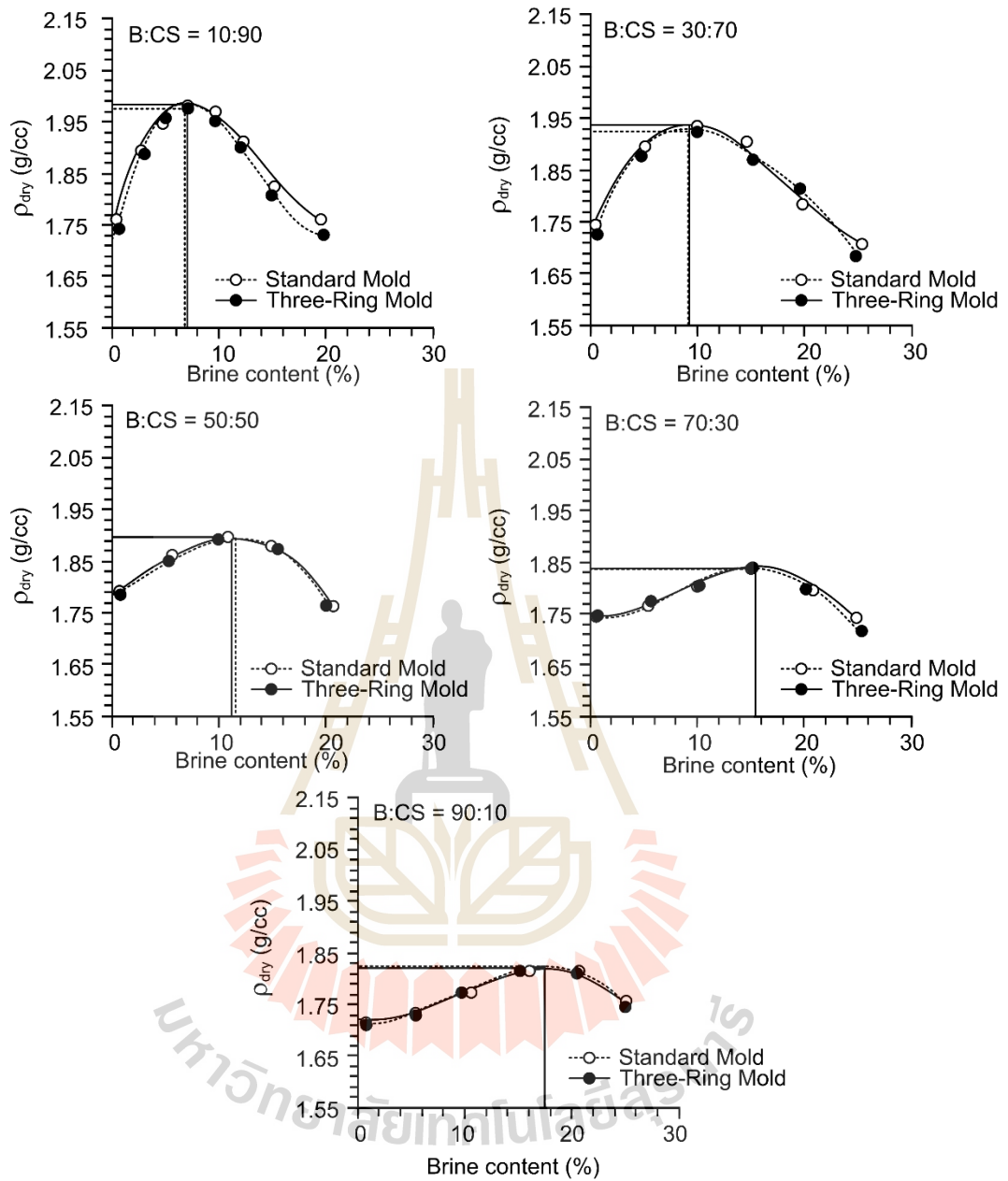


Figure 4.4 Dry density as a function of brine content of bentonite-to-crushed salt obtain from the three-ring mold and the ASTM standard mold.

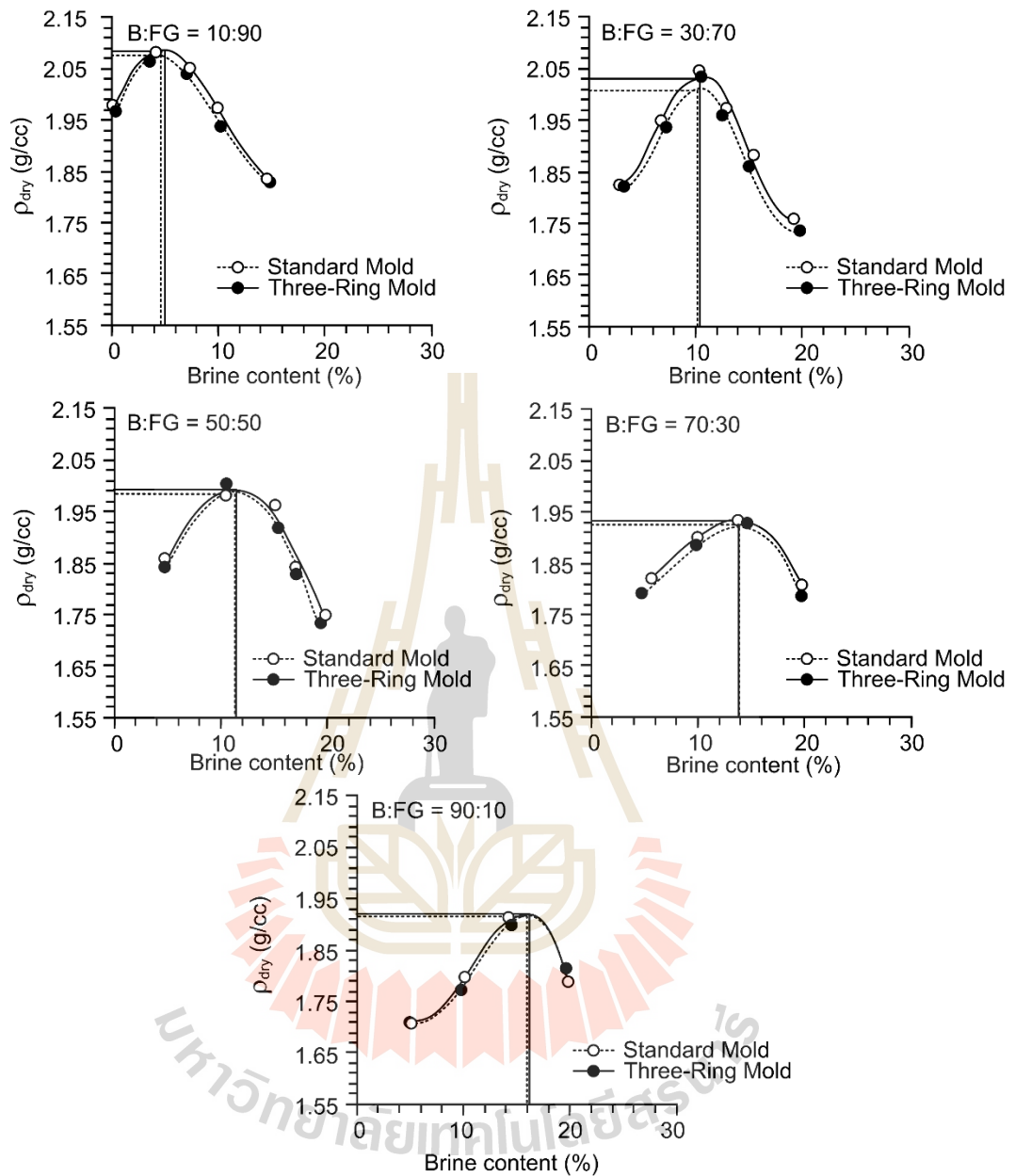


Figure 4.5 Dry density as a function of brine content of bentonite-to-fine gravel obtain from the three-ring mold and the ASTM standard mold.

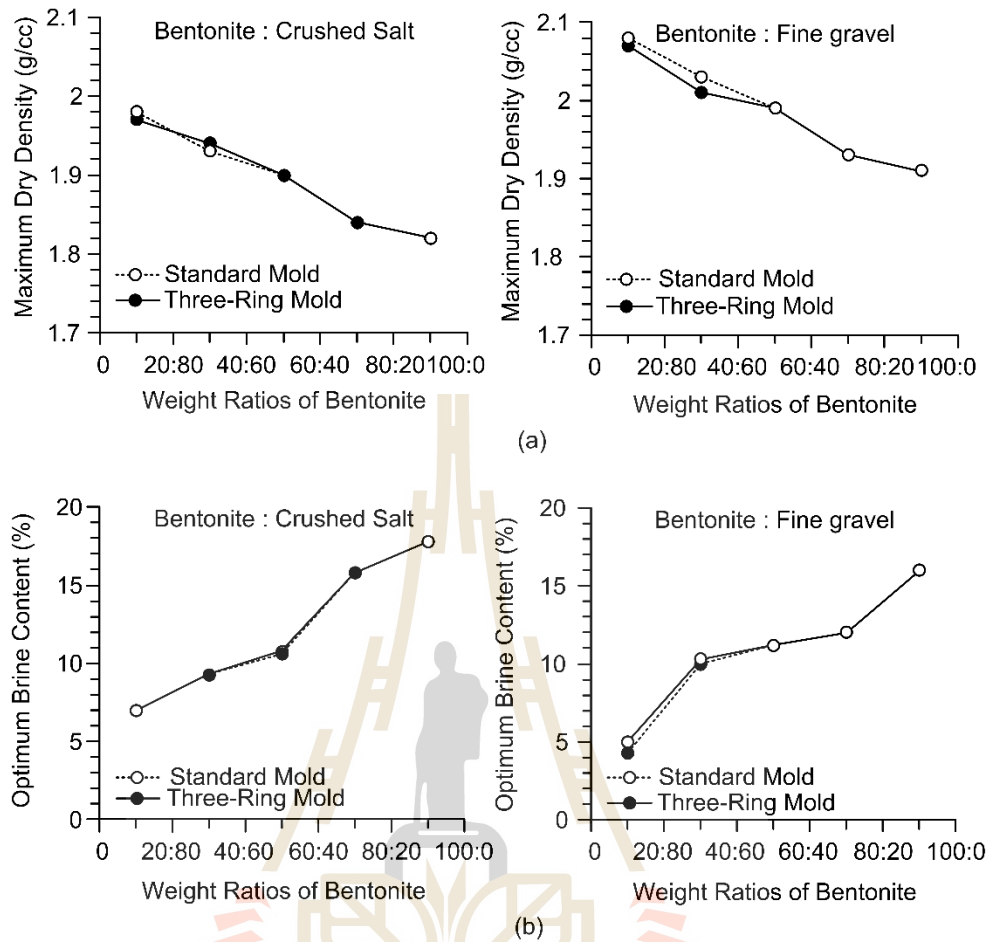


Figure 4.6 Maximum dry density as a function of weight ratios of bentonite obtain from the three-ring mold and the ASTM standard mold (a) and optimum brine content as a function of weight ratios of bentonite obtain from the three-ring mold and the ASTM standard mold (b).

Table 4.2 Compaction test results of three-ring and ASTM standard molds.

Materials	Ratios of bentonite-to-aggregates	Optimum brine content (%)		Maximum dry density (g/cc)	
		Three-ring mold	ASTM Standard mold	Three-ring mold	ASTM Standard mold
Bentonite: Crushed salt	10:90	7.00	7.00	1.97	1.98
	30:70	10.30	10.30	1.93	1.94
	50:50	10.80	10.60	1.90	1.90
	70:30	15.80	15.80	1.84	1.84
	90:10	17.80	17.80	1.82	1.82
Bentonite: Fine gravel	10:90	4.30	5.00	2.07	2.08
	30:70	10.10	10.30	2.01	2.03
	50:50	11.20	11.20	1.99	1.99
	70:30	12.00	12.00	1.93	1.93
	90:10	16.00	16.00	1.92	1.92

4.3.2 Direct shear results

Figures 4.7 to 4.11. plot the shear stress as a function of shear displacement for all materials. The results indicate that the shear stresses increase with increasing contents of granular materials, particularly under high normal stresses (Figure 4.12). The shear strengths are from 0.22 to 0.84 MPa (finer to coarser particles). Increasing granular content with larger particle sizes affect the shear strength, due to the particle slippage. Figure 4.13 shows the results of cohesion and friction angle obtained from the direct shear testing. The results show that the cohesion of coarser mixing particles (e.g. gravels and crushed salt) is lower than those of the fine particles (e.g. sludge). The friction angle of coarser particle is however higher than that of the finer particles. This is due to the inter-locking between grains for coarse materials. The friction angles and cohesions range from 19° to 37° and 0.14 MPa to 0.26 MPa, respectively. The results above agree with the results obtained by Li (2013). The results of direct shear testing for both methods can determine the shear strength, cohesion and friction angle. The shear stress as a function of shear displacement are shown in Figures 4.14 and 4.15. The higher shear stress is obtained for higher contents of granular materials (Figures 4.16 and 4.17), which results in a higher cohesion and friction angle (Table 4.4).

The three-ring direct shear device gives higher friction angle and cohesion than those obtained from the ASTM standard direct shear device (Figure 4.18) particularly, under higher contents of granular material. This is because the larger three-ring mold can accumulate more granular material with particle size of 4-6 mm than the smaller ASTM standard mold. The results suggest that the shear box size can affect to the shear

strength of the testing material with large particle sizes. This is explained by the experimental observations by Alias et al. (2014) and Nakao and Fityus (2008).

The normal displacement as a function of horizontal displacement for all materials are shown in Figures 4.19 to 4.23. The results indicate that the dilation increase with increasing granular contents because the dilation is restrained within the shear zone. An increase of the coarser particles leads to increase the dilation angles. The roughness of the shear surface at constant volume state is negatively related to particle smoothness and positively related to the area of the shear surface occupied by particles with particular shapes (Li et al, 2013). The dilation angle as a function of normal stresses are shown in Figure 4.24. The dilation rates (d_n/d_s) are plotted as a function of weight ratios of bentonite in Figure 4.25, which agree well with the results that observed by Afzali-Nejad et al. (2017) and Li and Aydin (2010).

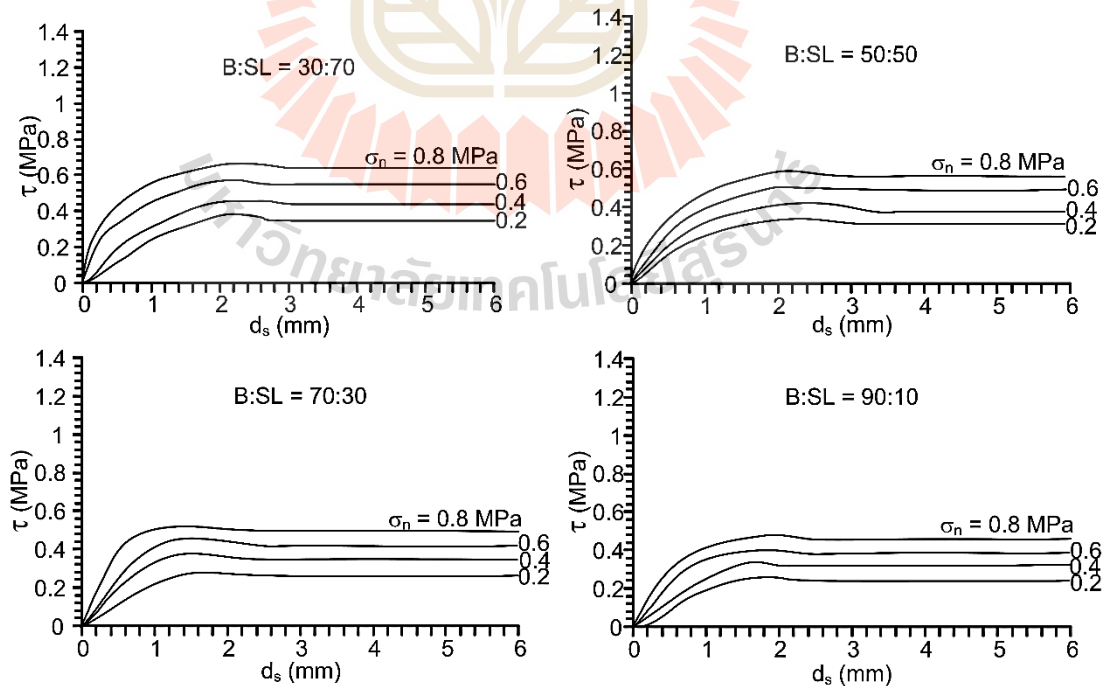


Figure 4.7 Shear strength as a function of displacement of bentonite-to-sludge.

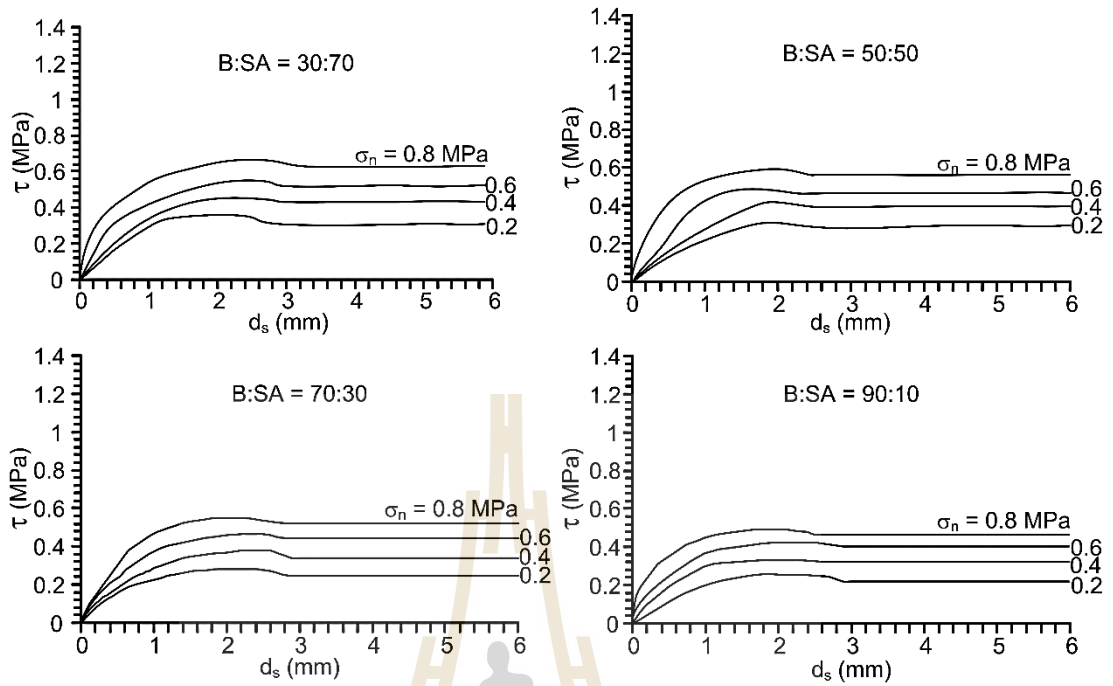


Figure 4.8 Shear strength as a function of displacement of bentonite-to-sand.

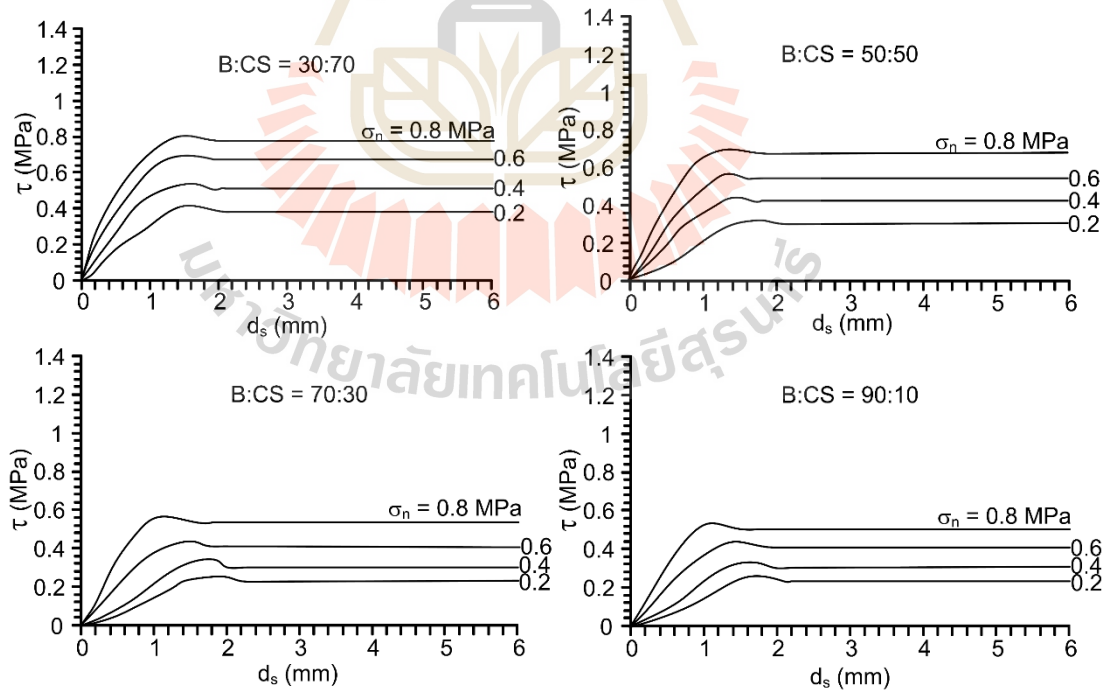


Figure 4.9 Shear strength as a function of displacement of bentonite-to-crushed salt.

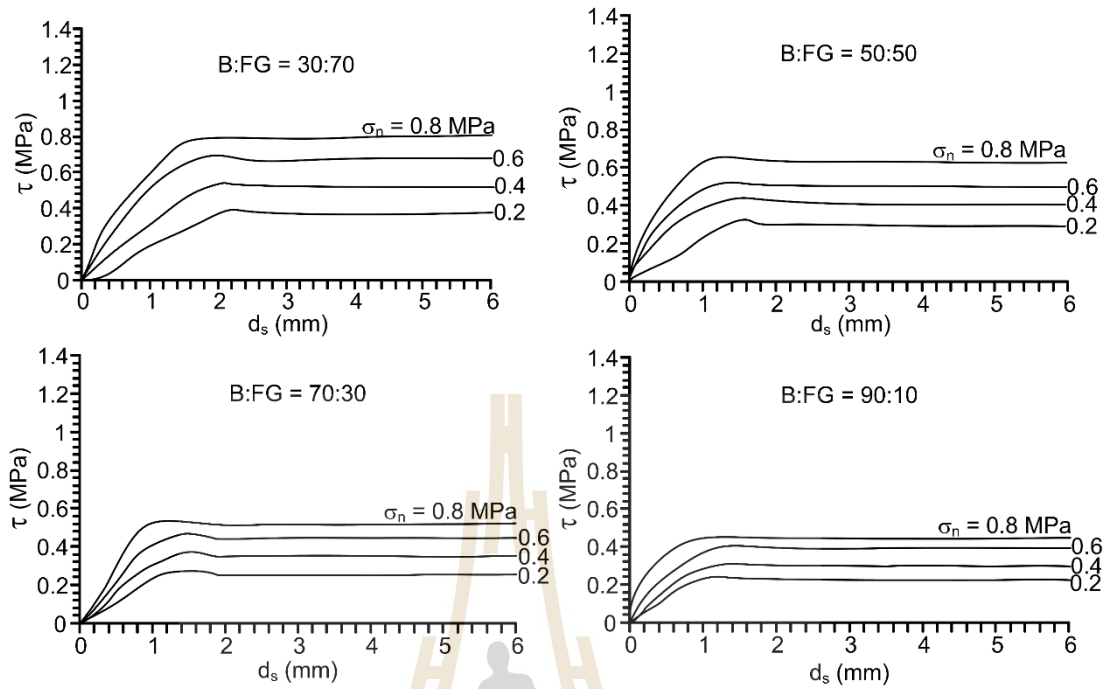


Figure 4.10 Shear strength as a function of displacement of bentonite-to-fine gravel.

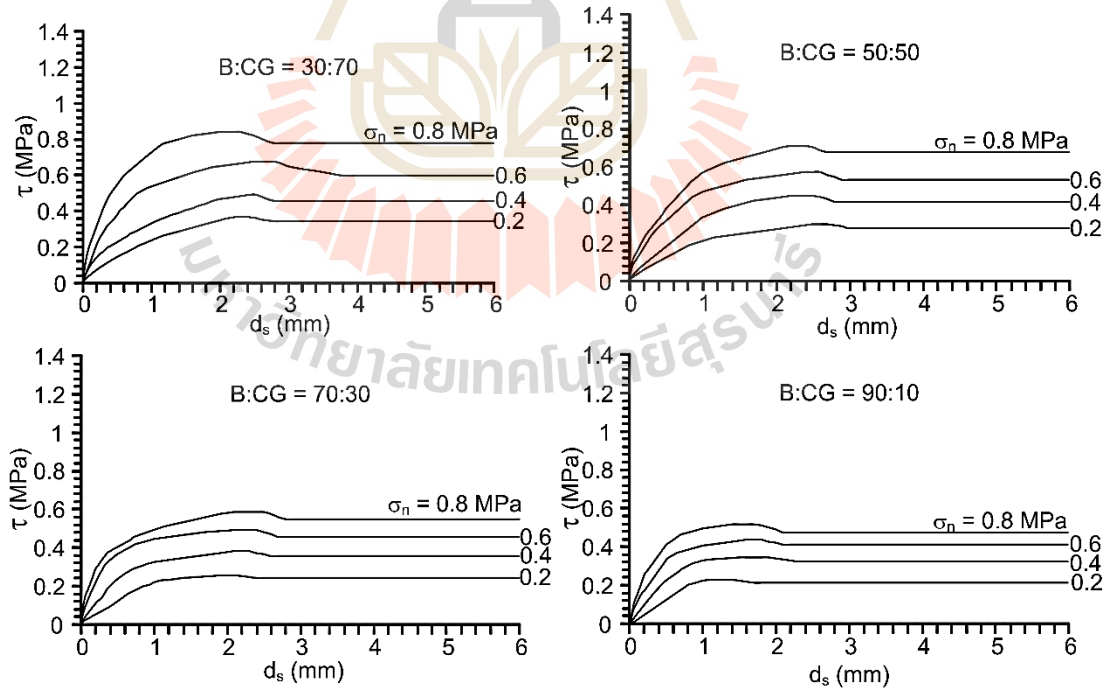


Figure 4.11 Shear strength as a function of displacement of bentonite-to-coarse gravel.

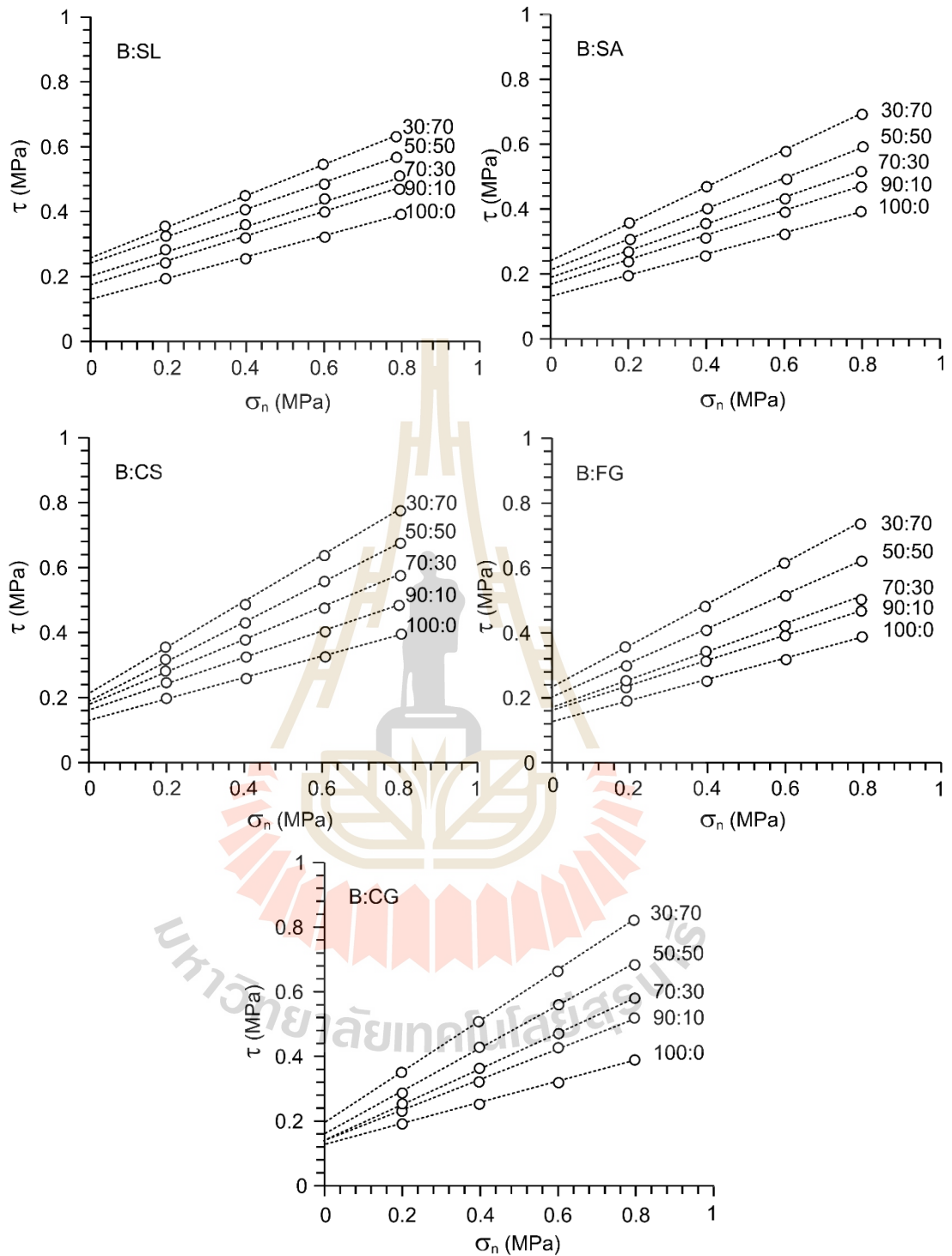


Figure 4.12 Shear strength as a function of normal stress of granular materials.

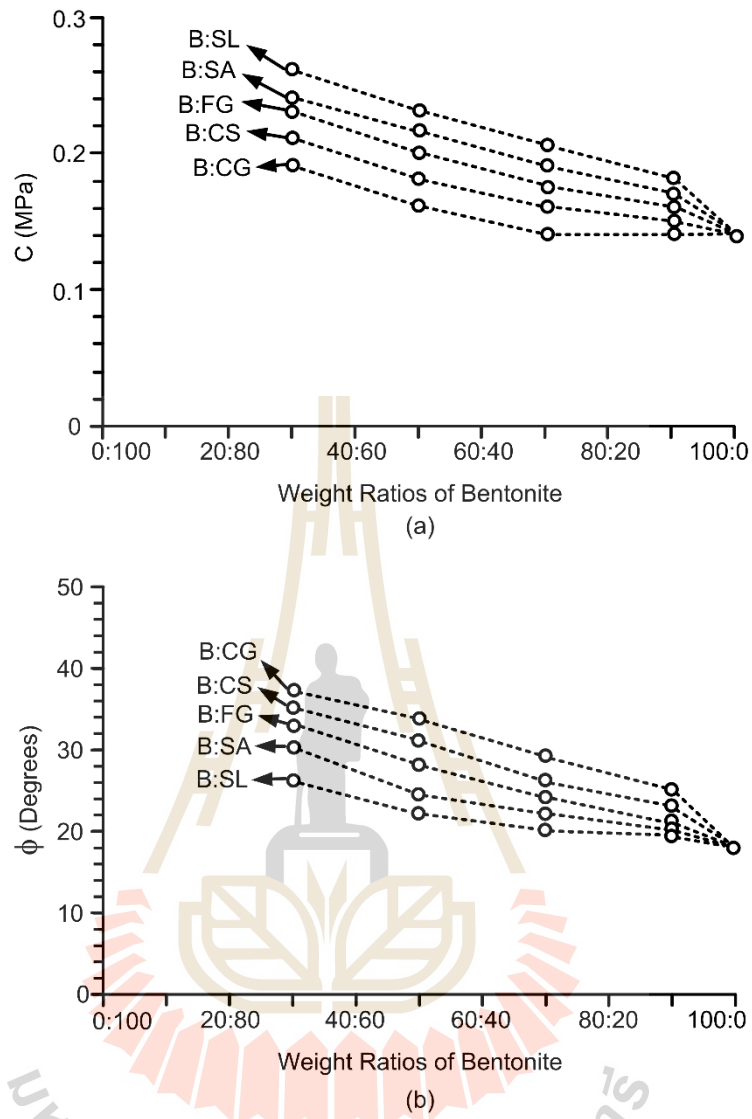


Figure 4.13 Cohesions (a) and friction angles (b) as a function of bentonite-to-granular weight ratios.

Table 4.3 Direct shear results.

Materials	Ratios of bentonite-to-aggregates	Cohesion (MPa)	Friction angles (Degrees)	R ²
Bentonite:Sludge	30:70	0.26	26	0.999
	50:50	0.23	22	0.999
	70:30	0.21	20	0.999
	90:10	0.18	19	0.997
Bentonite:Sand	30:70	0.24	30	0.998
	50:50	0.22	25	0.999
	70:30	0.19	22	0.996
	90:10	0.17	20	0.993
Bentonite:Crushed salt	30:70	0.21	35	0.996
	50:50	0.18	31	0.997
	70:30	0.16	26	0.996
	90:10	0.15	23	0.999
Bentonite:Fine gravel	30:70	0.23	33	0.999
	50:50	0.20	28	0.998
	70:30	0.18	24	0.995
	90:10	0.16	21	0.990
Bentonite:Coarse gravel	30:70	0.19	37	0.995
	50:50	0.16	34	0.996
	70:30	0.14	29	0.999
	90:10	0.14	25	0.996

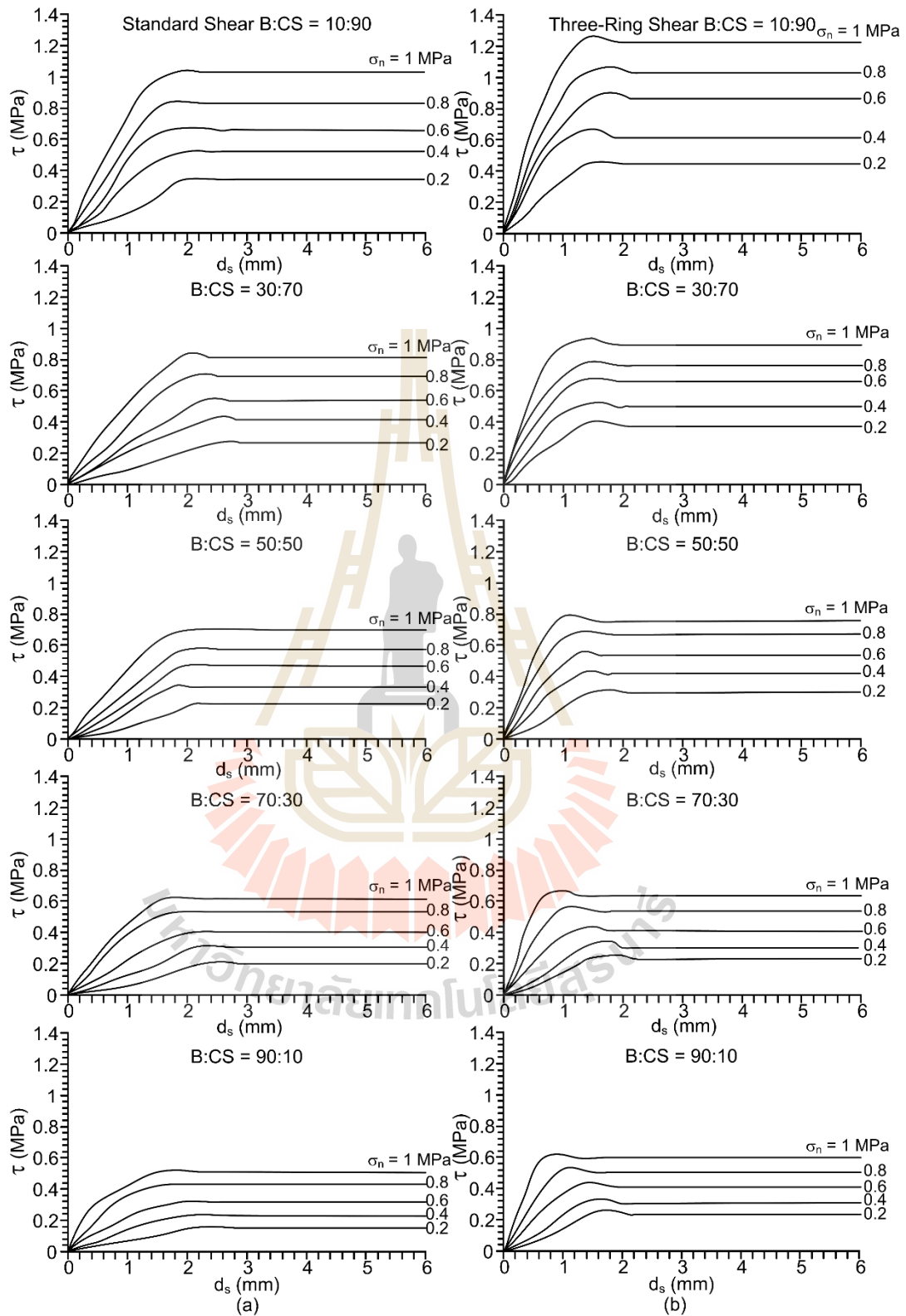


Figure 4.14 Shear strength as a function of displacement of bentonite-to-crushed salt for ASTM direct shear (a) and three-ring direct shear (b) apparatus.

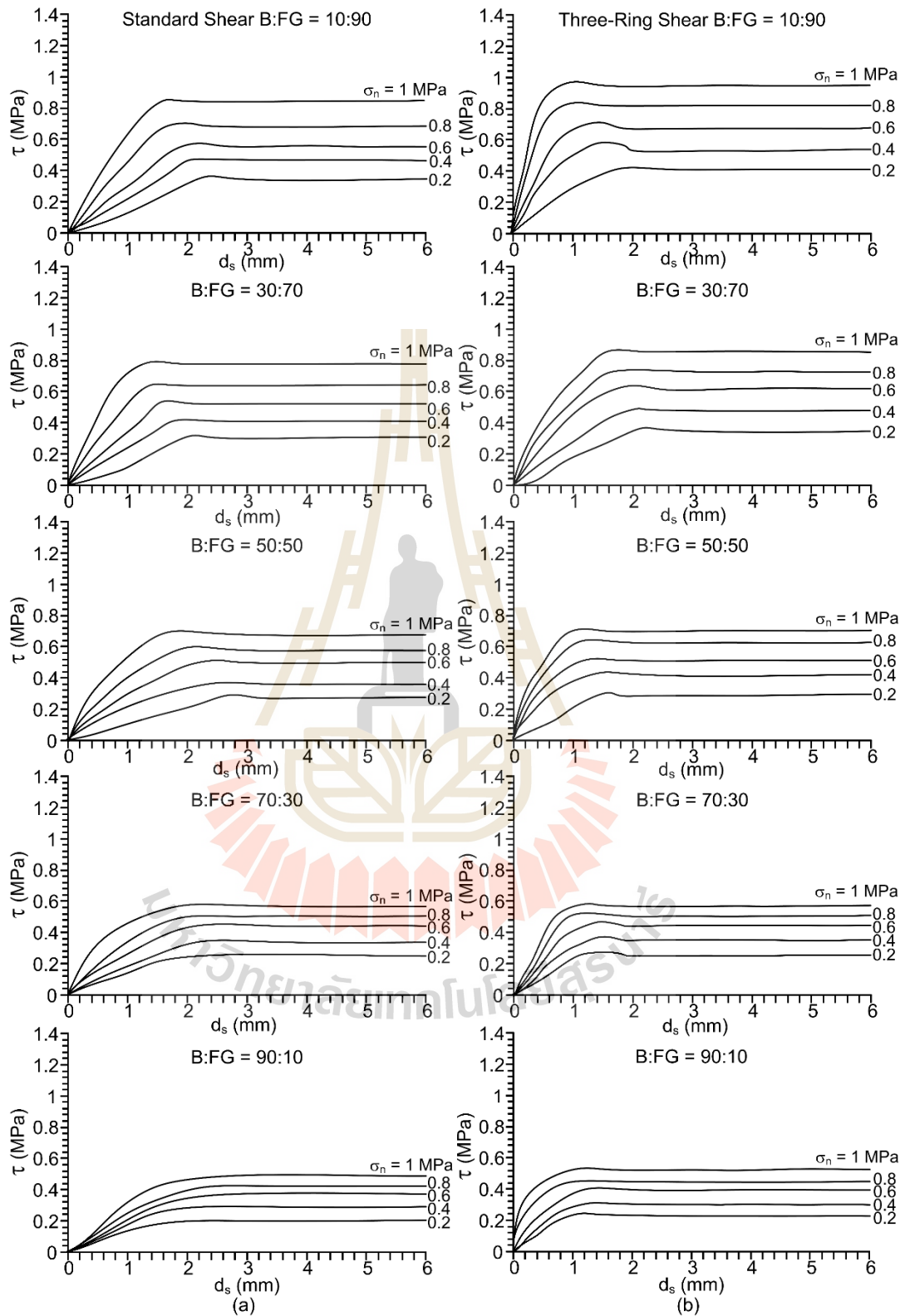


Figure 4.15 Shear strength as a function of displacement of bentonite-to-fine gravel for ASTM direct shear (a) and three-ring direct shear (b) apparatus.

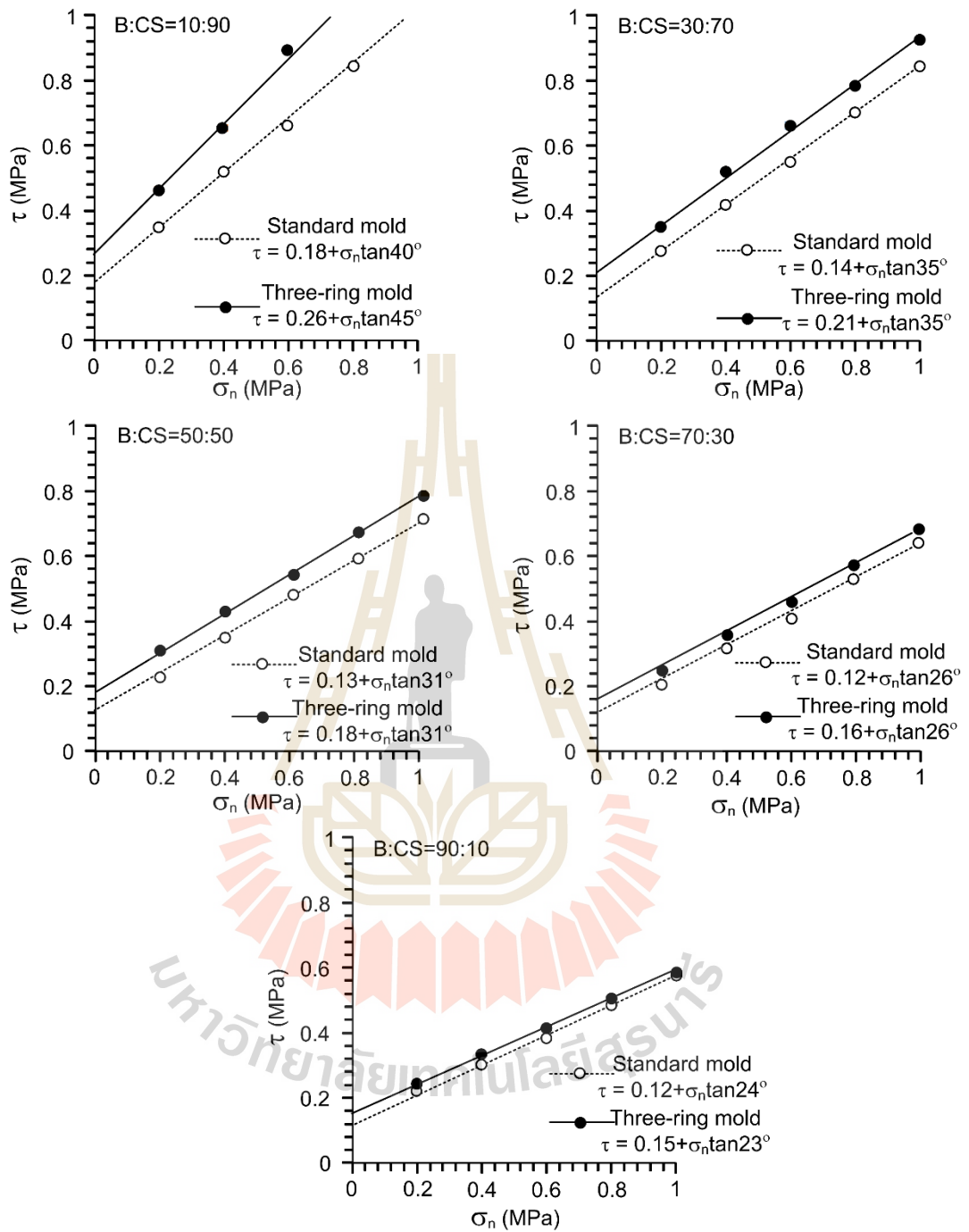


Figure 4.16 Shear strength as a function of normal stress obtain from the three-ring mold and the ASTM standard mold of bentonite-to-crushed salt.

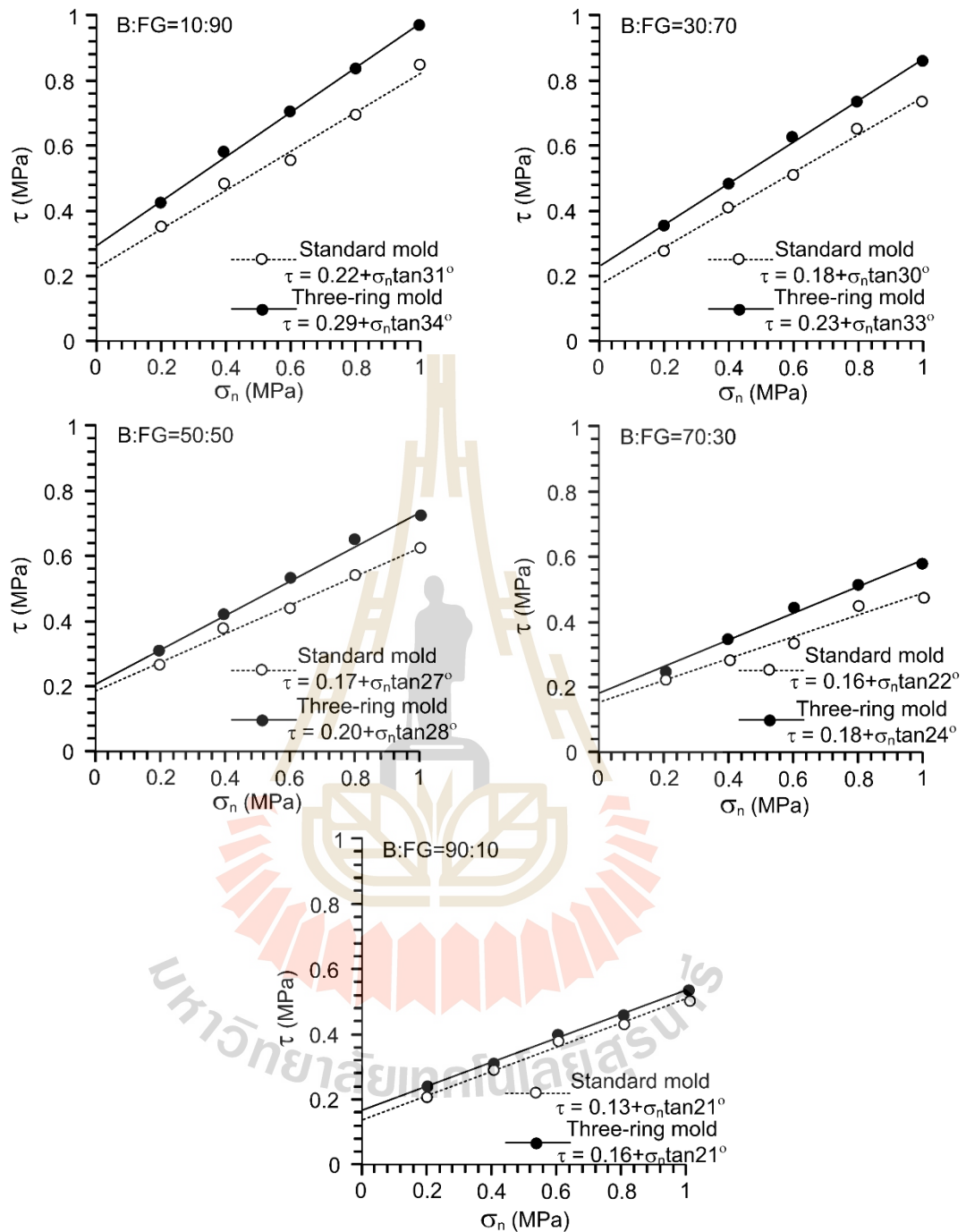


Figure 4.17 Shear strength as a function of normal stress obtain from the three-ring mold and the ASTM standard mold of bentonite-to-fine gravel.

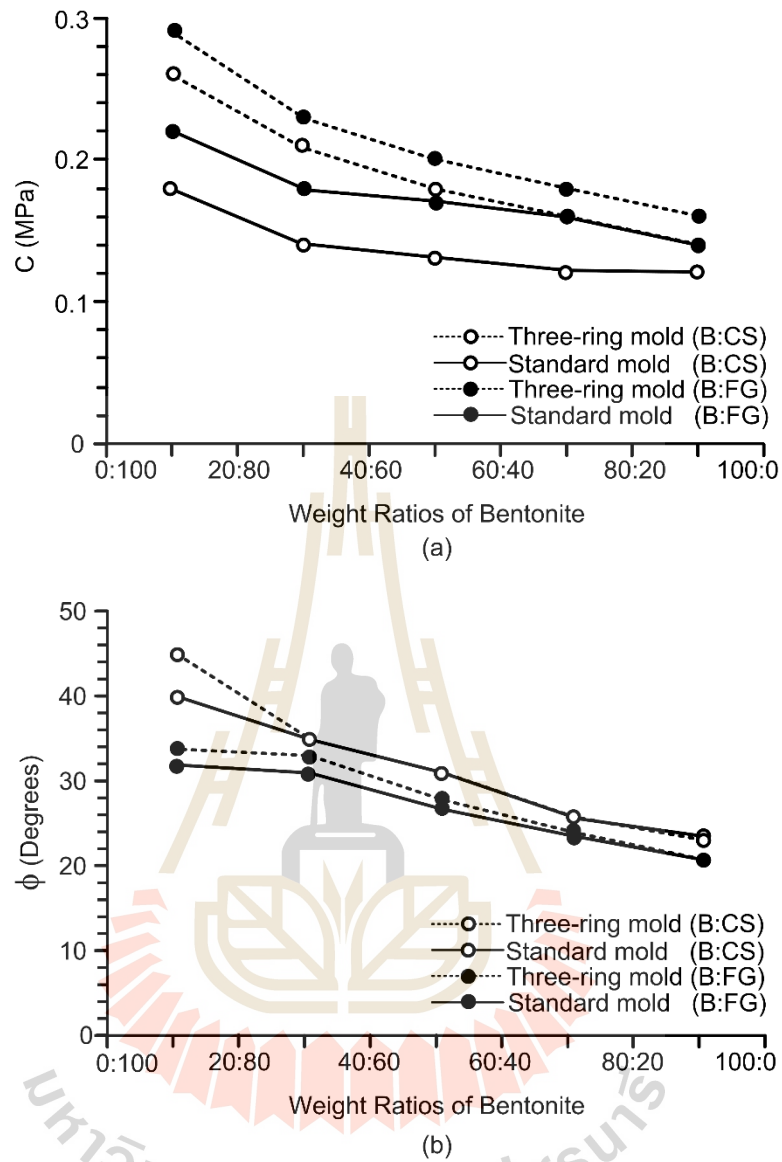


Figure 4.18 Cohesion(a) and friction angle (b) as a function of weight ratios of bentonite obtain from the three-ring mold and the ASTM standard mold.

Table 4.4 Direct shear test comparison result.

Materials	Ratios of bentonite-to-aggregates	Cohesion (MPa)		Friction angle (Degrees)	
		Three-ring mold	ASTM Standard mold	Three-ring mold	ASTM Standard mold
Bentonite:Crushed salt	10:90	0.26	0.18	45.00	40.00
	30:70	0.21	0.14	35.00	35.00
	50:50	0.18	0.13	31.00	31.00
	70:30	0.16	0.12	26.00	26.00
	90:10	0.15	0.12	23.00	24.00
Bentonite:Fine gravel	10:90	0.29	0.22	34.00	31.00
	30:70	0.23	0.18	33.00	30.00
	50:50	0.20	0.17	28.00	27.00
	70:30	0.18	0.16	24.00	22.00
	90:10	0.16	0.13	21.00	21.00

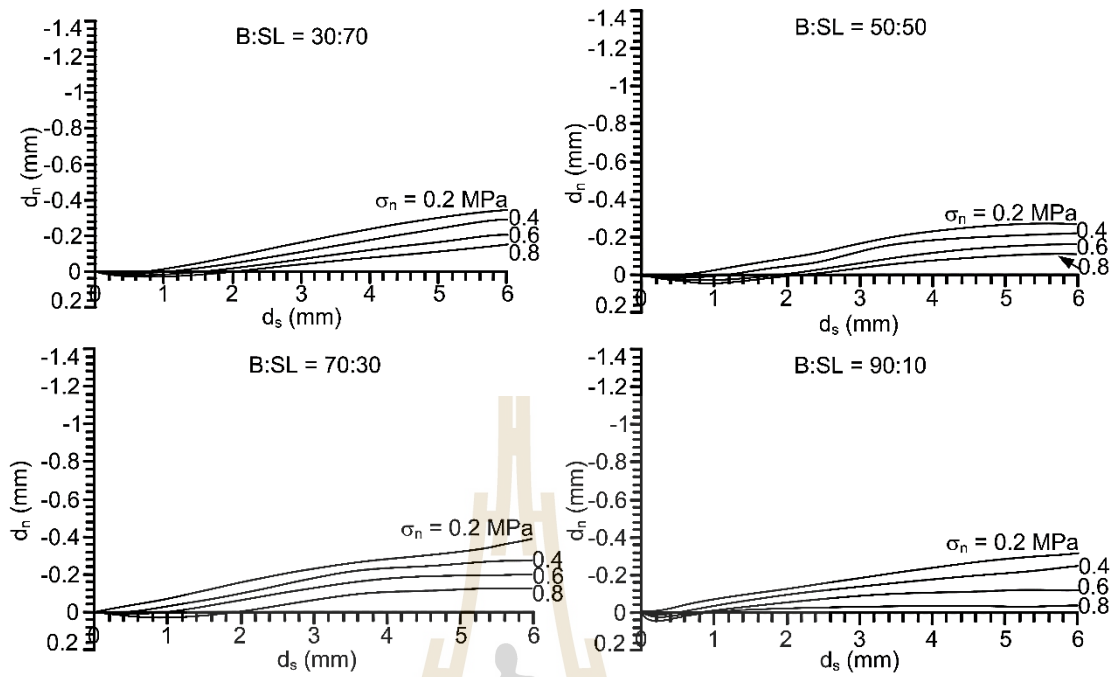


Figure 4.19 Normal displacement as a function of displacement of bentonite-to-sludge.

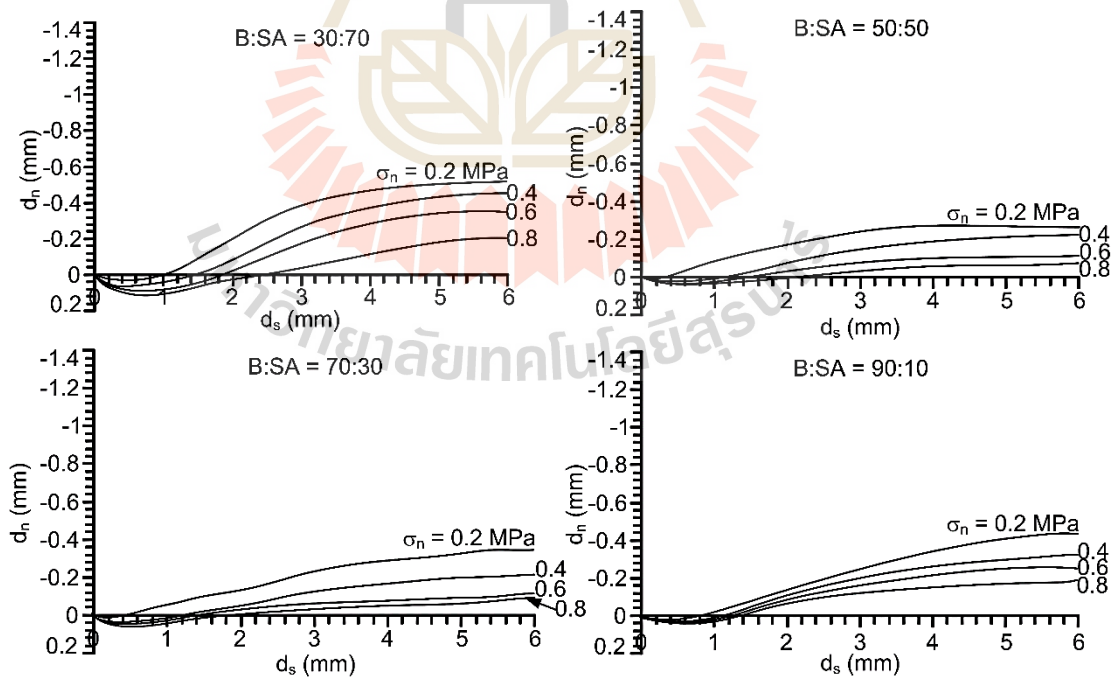


Figure 4. 20 Normal displacement as a function of displacement of bentonite-to-sand.

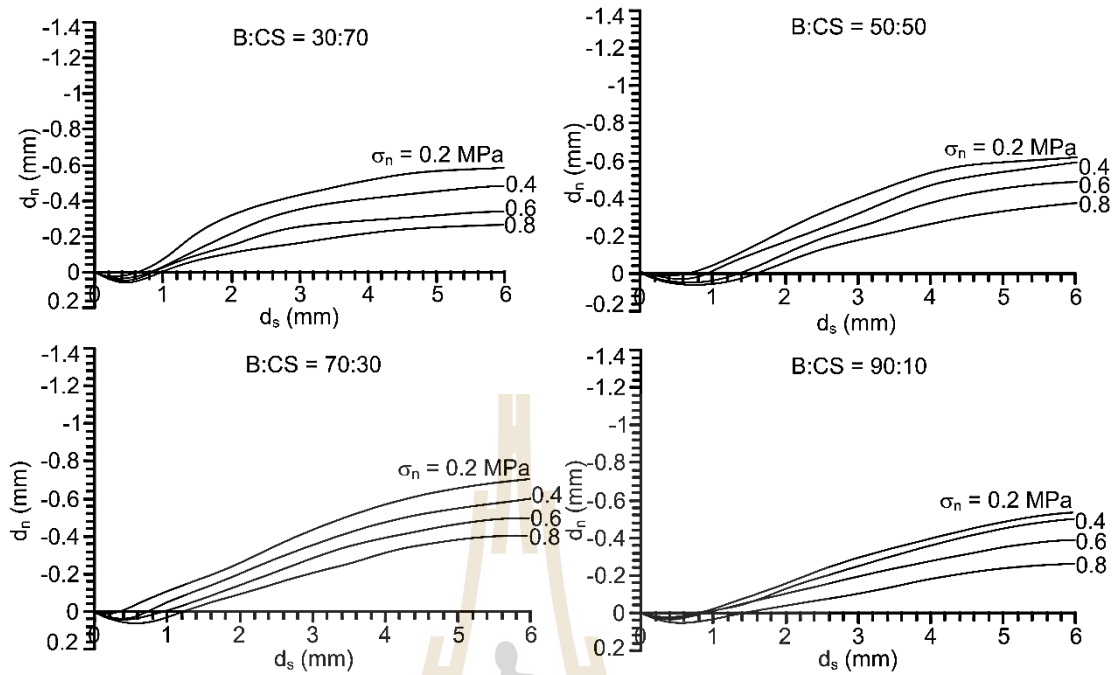


Figure 4.21 Normal displacement as a function of displacement of bentonite-to-crushed salt.

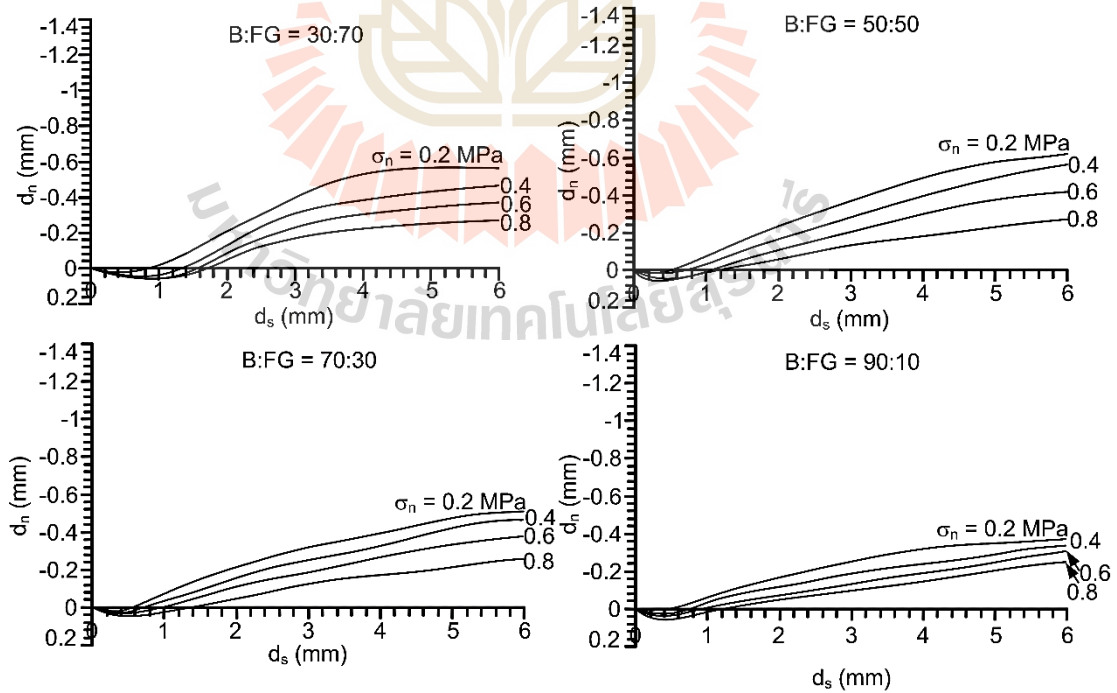


Figure 4.22 Normal displacement as a function of displacement of bentonite-to-fine gravel.

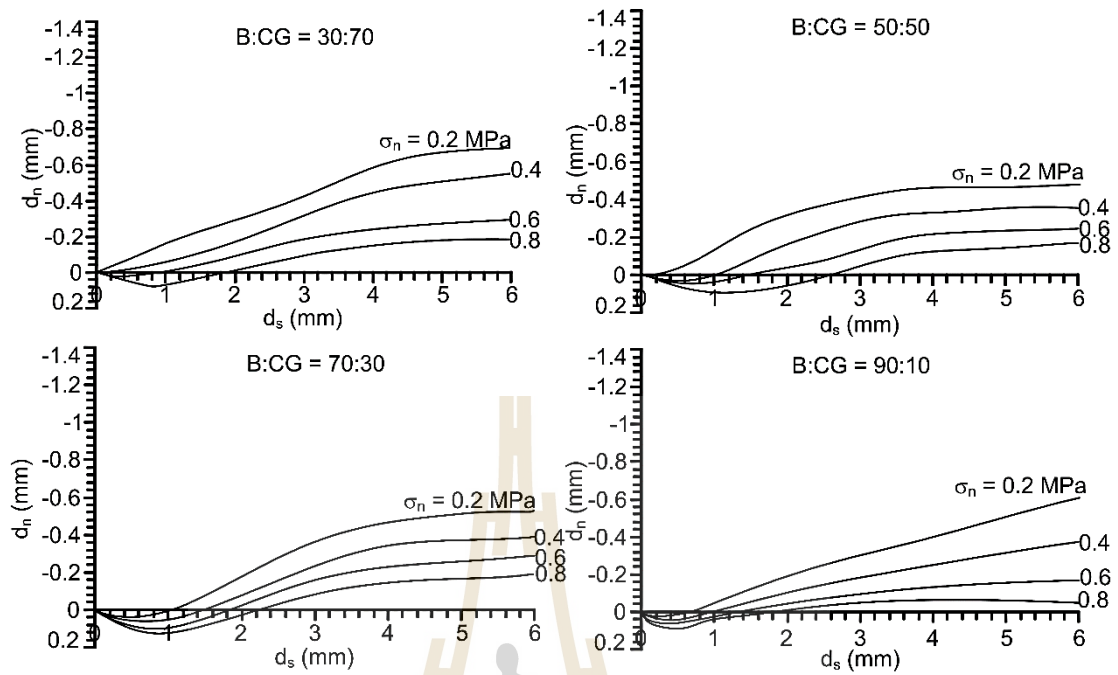


Figure 4.23 Normal displacement as a function of displacement of bentonite-to-coarse gravel.

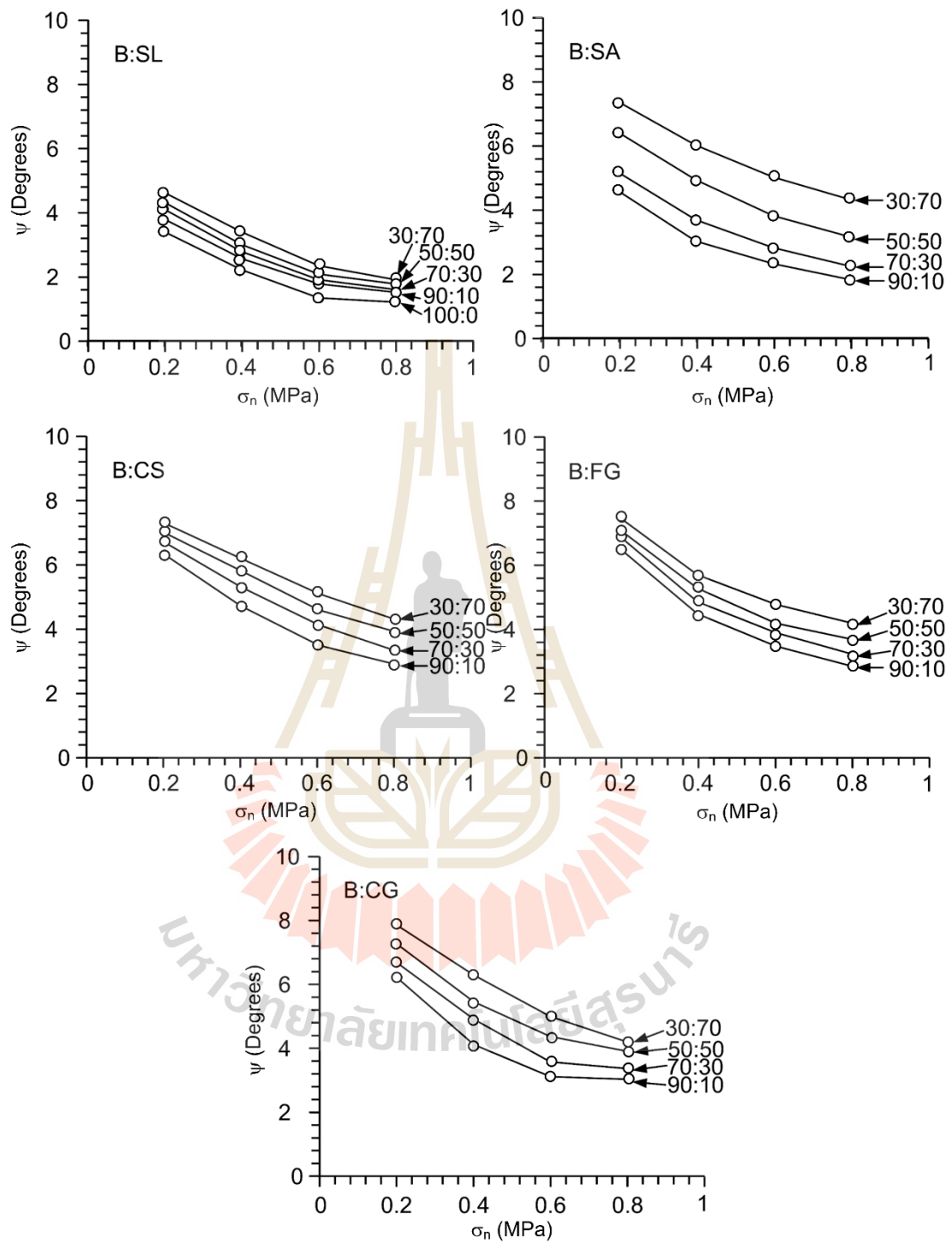


Figure 4.24 Dilation angles as a function of normal stress of granular materials.

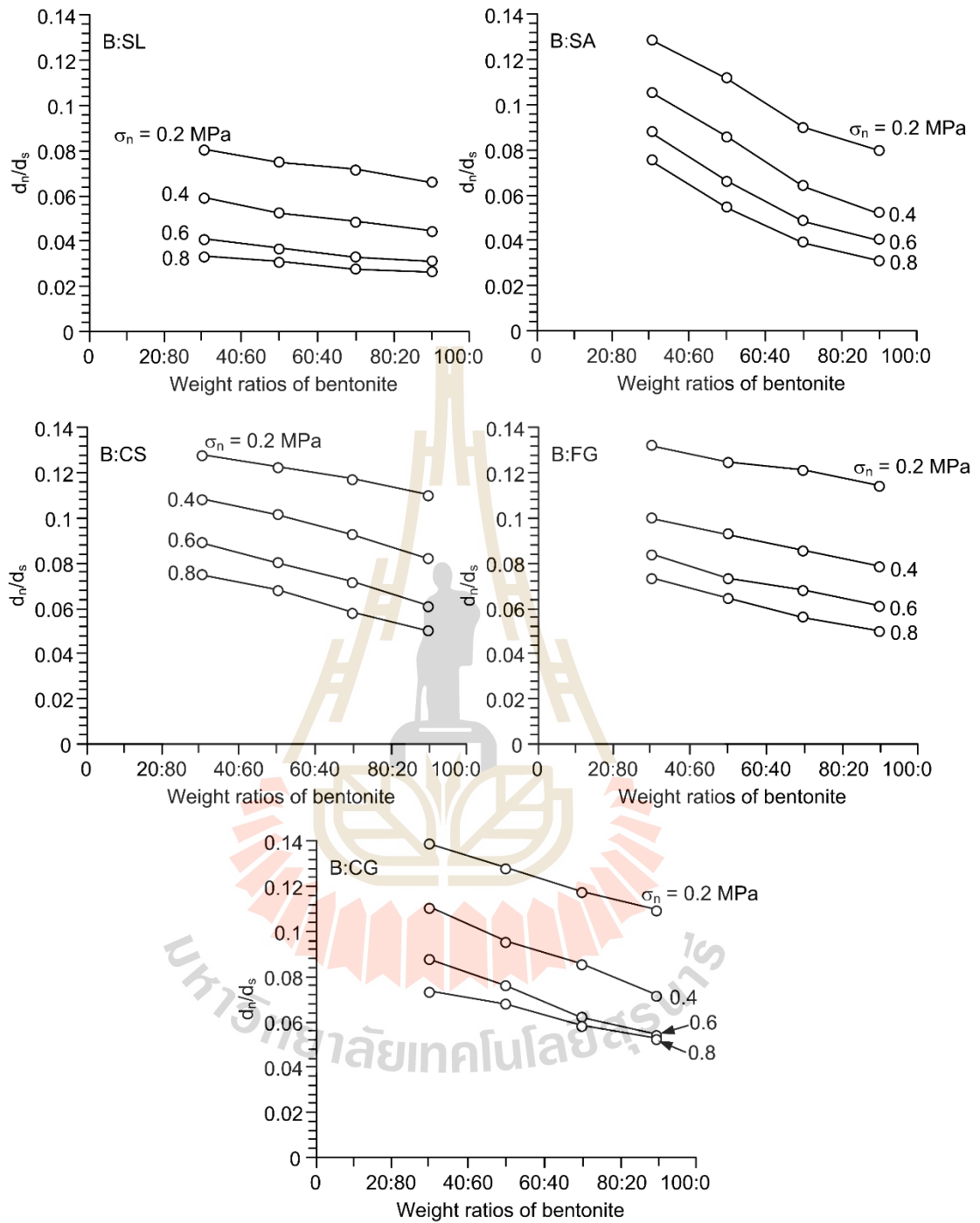


Figure 4.25 Dilation rate as a function of weight ratios of bentonite.

4.3.3 Compression results

Figure 4.26 shows post-test specimens of granular materials after compression testing these fractures tend to be shear plane. Figure 4.27 plots stress-strain curves, Figure 4.28 plots compressive strength and Figure 4.29 plots elastic parameters of all mixtures as a function of bentonite-granular weight ratio. The mixtures with higher bentonite content give greater compressive strengths and elastic moduli than those with the lower bentonite content. The Poisson's ratio, however tends to decrease with the bentonite weight ratios increase. This is probably because the increase of bentonite content can densify the mixtures, and hence increases their strength and stiffness. The mixtures with finer granular particles (e.g. sludge and sand) tend to show higher strengths and elastic moduli than those with coarser particles (e.g. gravels). The Poisson's ratios of the coarser particles are greater than those of the finer particles. The test results are consistent with Ghazi (2015), Kumar et al. (2006) and Cho et al. (2002). The results are summarized in Table 4.5.



Figure 4.26 Post-test specimens of granular materials after compression testing.

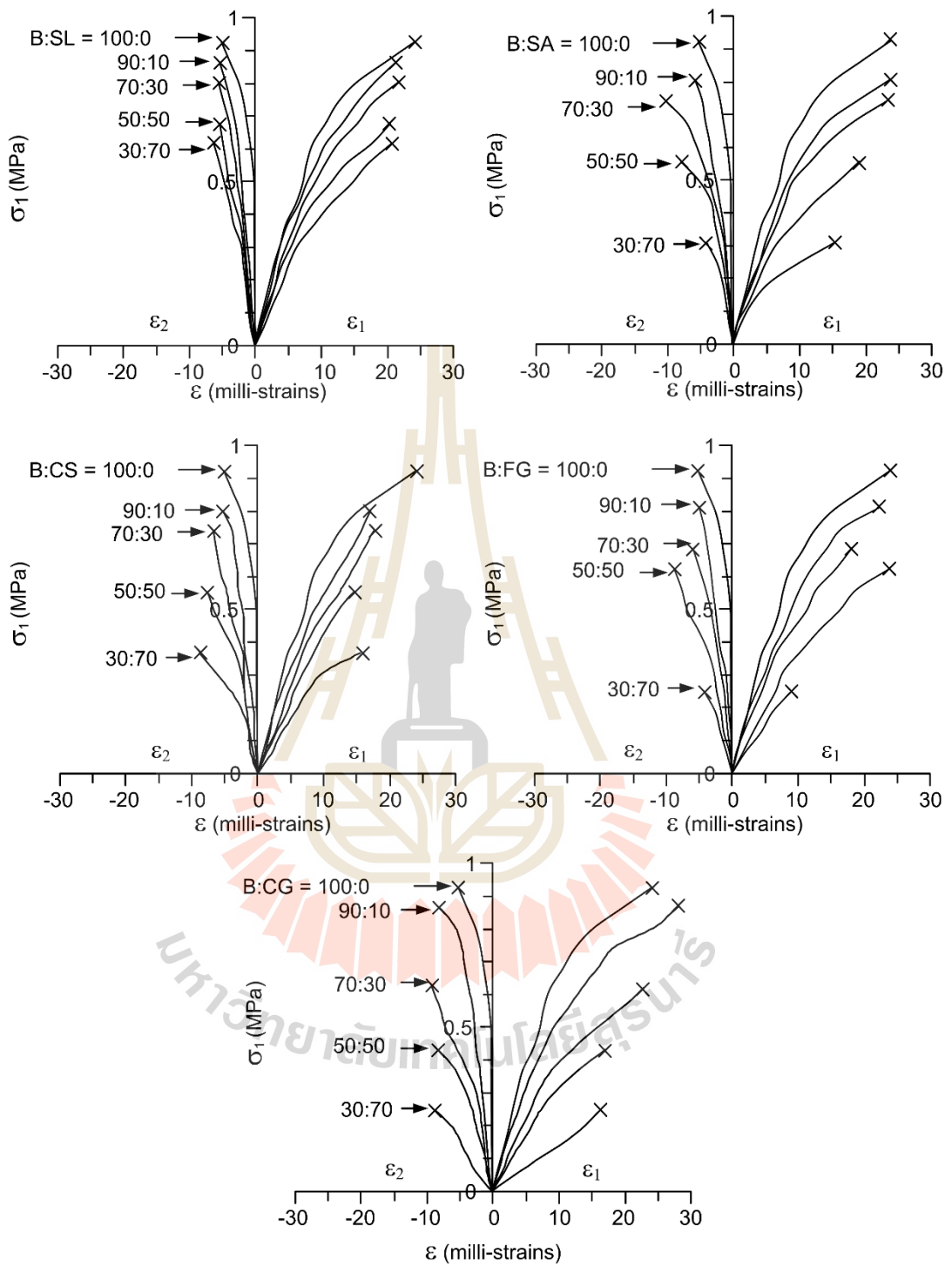


Figure 4.27 Stress-strains curves.

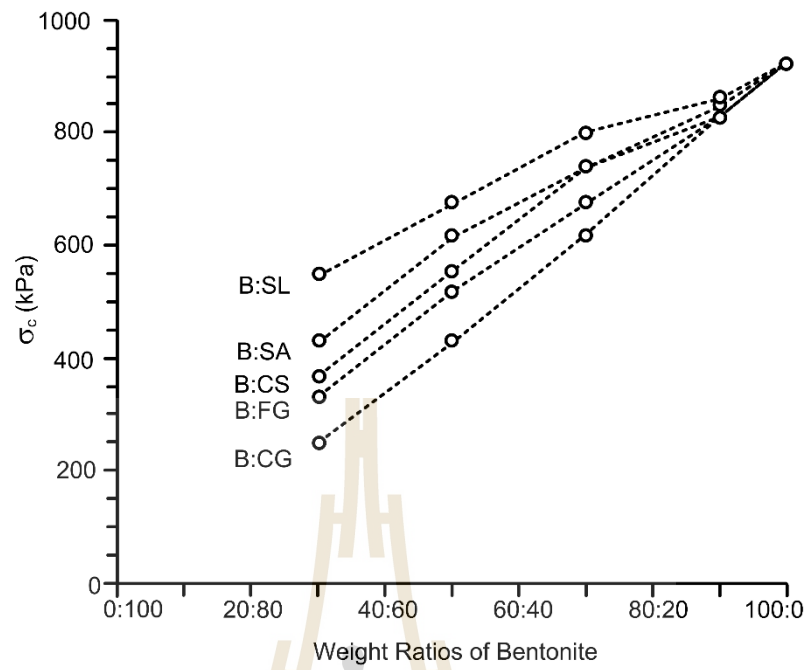


Figure 4.28 Compressive strengths as a function of bentonite-to-granular weight ratios.

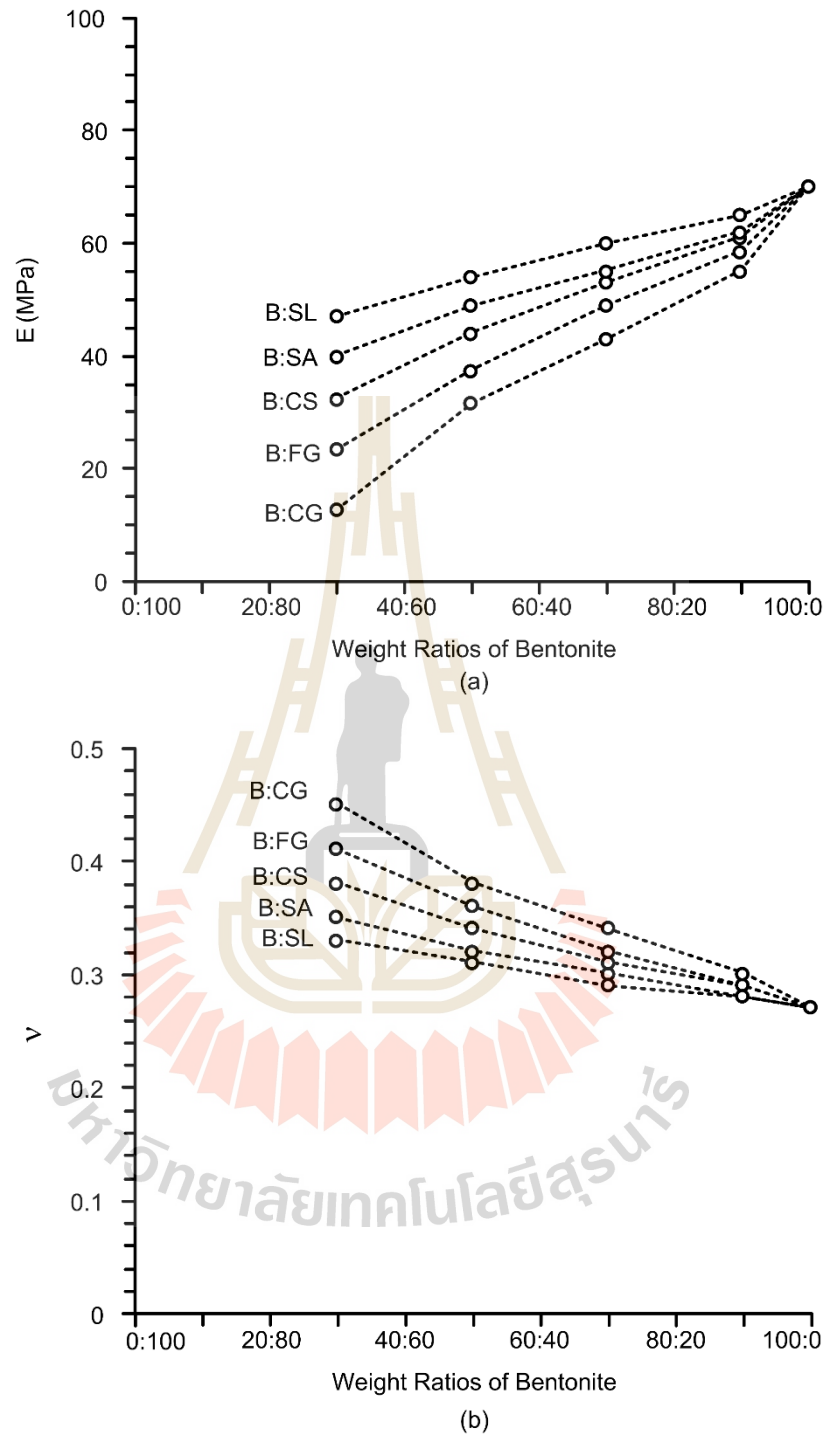


Figure 4.29 Elastic moduli (a) and Poisson's ratio (b) as a function of bentonite-to-granular weight ratios.

Table 4.5 Compression test results.

Materials	Ratios of bentonite-to-aggregates	Compressive strength (kPa)	Elastic moduli (MPa)	Poisson's ratios
Bentonite:Sludge	30:70	550	47.0	0.33
	50:50	678	54.0	0.31
	70:30	802	60.0	0.29
	90:10	863	65.0	0.28
Bentonite:Sand	30:70	430	40.0	0.35
	50:50	617	49.0	0.32
	70:30	740	55.0	0.30
	90:10	850	62.0	0.28
Bentonite:Crushed salt	30:70	370	32.5	0.38
	50:50	555	44.0	0.34
	70:30	740	53.0	0.31
	90:10	830	61.0	0.29
Bentonite:Fine gravel	30:70	333	23.5	0.41
	50:50	520	37.5	0.36
	70:30	678	49.0	0.32
	90:10	830	58.5	0.29
Bentonite:Coarse gravel	30:70	250	12.8	0.45
	50:50	430	31.7	0.38
	70:30	620	43.0	0.34
	90:10	830	55.0	0.30

CHAPTER V

SWELLING AND BRINE ABSORPTION TESTING

5.1 Introduction

The objective of this chapter is to determine the physical properties of bentonite by swelling and absorption testing. This chapter describes the test methods and results. Compaction test is also performed to obtain specimens for the swelling and absorption tests. A total of 10 samples are prepared from pure bentonite at various brine contents.

5.2 Test method

The bentonite samples are mixed with saturated brine varying from 5, 10, 15, 20, 25, 30, 35, 40, 45 to 50% by weight. Each sample is compacted using the ASTM standard mold before swelling and brine absorption testing. The initial properties of the samples are summarized in Table 5.1 and Figure 5.1. After compaction the sample is trimmed and installed into the 50 ml glass cylinder. The saturated brine is added at the top of the sample. Swelling test is conducted following the procedure described in the ASTM (D5890-11) standard practice. The measurements of swelling are recorded for 15 days. The swelling capacity is calculated by:

$$D = (\Delta V/V) \times 100 \quad (5.1)$$

where D is swelling capacity (%), ΔV is the change of the volume and V is initial volume.

After the swelling testing, the saturated specimens are dried in the oven at

100°C. This is to determine the effectiveness of brine absorption of bentonite specimens at various brine contents, which is represented by the change of moisture. The brine absorption capacity is calculated by Equation (4.2) in Chapter 4, where W_i is initial bentonite content at various brine contents.

Table 5.1 Bentonite properties after compaction.

Initial brine content (%)	Wet density (g/cc)	Dry density (g/cc)
5	1.47	1.39
10	1.75	1.58
15	1.99	1.72
20	2.18	1.81
25	2.12	1.68
30	2.08	1.59
35	1.98	1.46
40	1.91	1.36
45	1.82	1.25
50	1.82	1.22

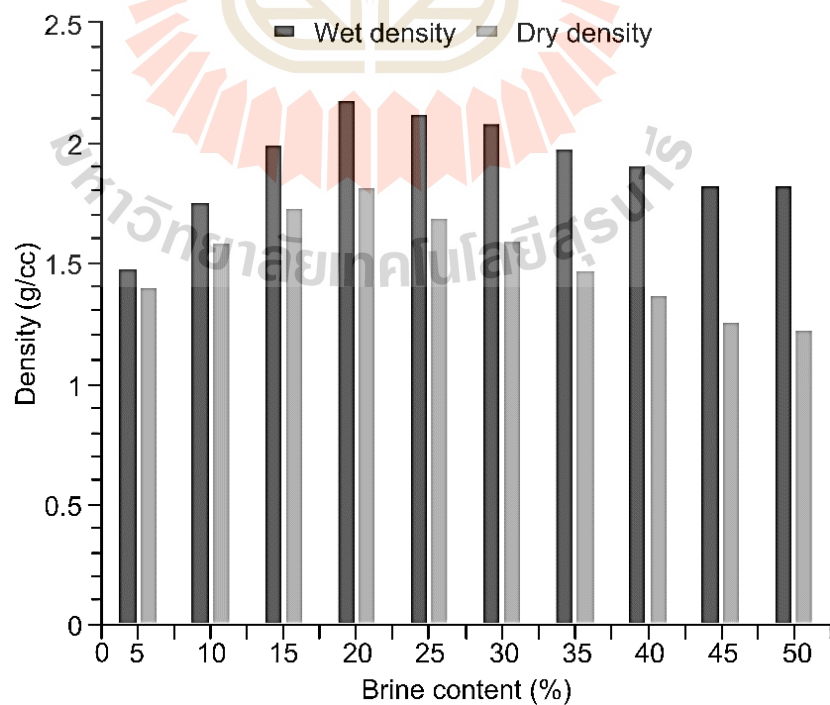


Figure 5.1. Density of bentonite as a function of brine content.

5.3 Test results

Table 5.2. shows bentonite specimens at various brine contents before testing. The brine is added on the specimen for 15 days under ambient temperature. The swelling capacity decreases with increasing brine content, as shown in Table 5.3. The swelling tends to increase as logarithmic functions with time at an early stage of the test, and then tends to be constant. The increase of swelling is plotted as a function of time for different initial brine contents (5% to 50%) in Figure 5.2. The results show that a lower initial brine content yields higher rates of absorption and swelling. The test results agree with those of Karnland et al. (2006). Bentonite can swell considerably due to brine penetrating the inter-layer molecular spaces and the absorption of hydrated cations and water molecules, resulting in strong repulsive forces and inter-layer expansion in the presence of electrolyte solutions (Mitchell,1993). However, the measurement of swelling capacity can be affected by several factors, including inconsistency in the add brine procedure, failure to spread the bentonite evenly, and friction between the bentonite and the glass cylinder (Shackelford et al., 2000). The results of swelling test are summarized in Table 5.4.

The results of brine absorption after 15 days are shown in Figure 5.3. The results show that the bentonite compacted under lower initial brine content yields higher absorption capacity. This may be because under low initial brine content the specimens have higher air-filled gaps, and hence brine added on the top of the sample can flow and fill in the gap easier than bentonite that compacted under high initial brine content. These results agree with Dueck et al. (2008) who state that the bentonite compacted under lower the initial water content shows the higher rates of absorption and swelling. The smaller the size of the gap, the higher the rate of absorption and swelling. Air

movement increases the rates of both the absorption and the swelling. The results of brine absorption capacity test are summarized in Table 5.5.

The results of swelling and absorption testing are useful for selection of initial backfill parameters in salt and potash mine opening. The high absorption capacity of bentonite also makes it plastic and resistant to fracturing or cracking. The ability of bentonite swelling can be used to seal the gap of compaction in backfilling materials, to make the backfill material more effective and higher compressive strength. Absorption property helps protection of groundwater into the underground excavations and absorbed the pollutants. Swelling and absorption capacities are good properties. The compacted bentonite has also been considered as buffer/backfill material in deep geological repository for disposal of waste.

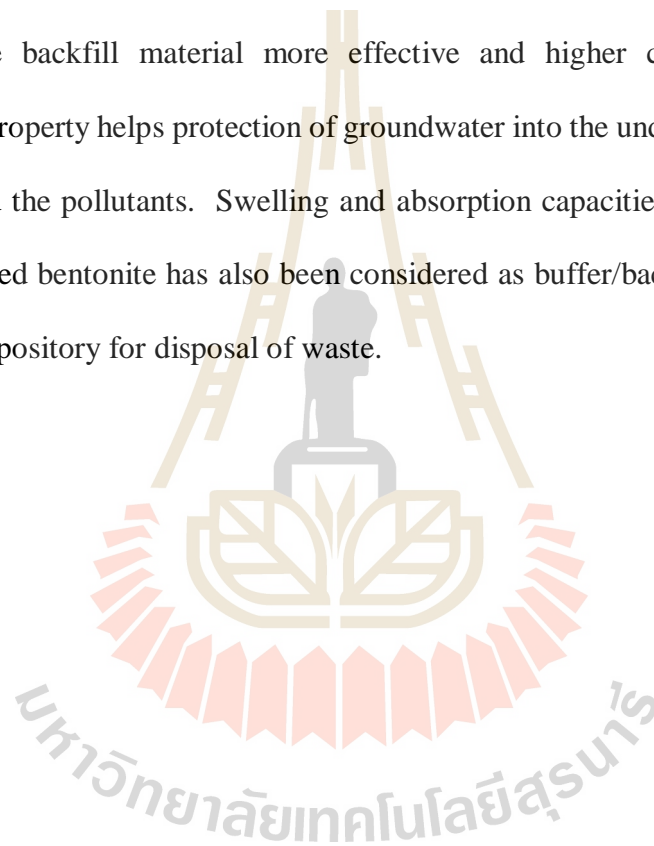


Table 5.2 Pictures of specimens before swelling.

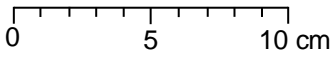
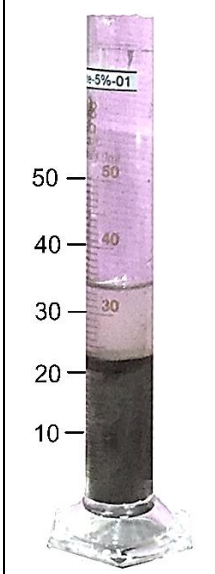
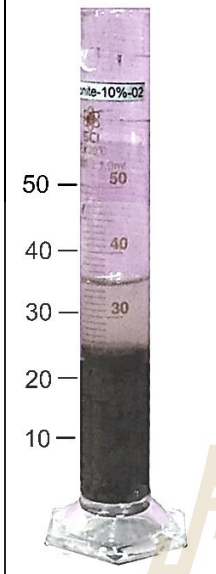
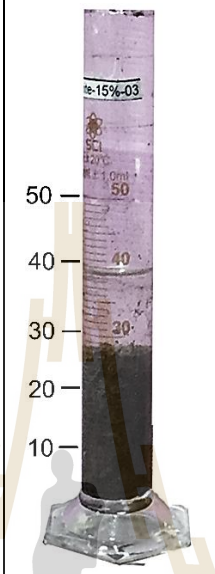
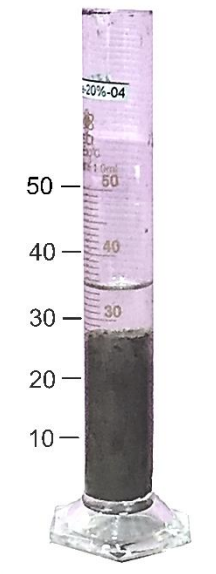
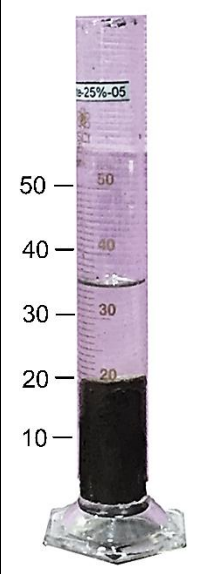
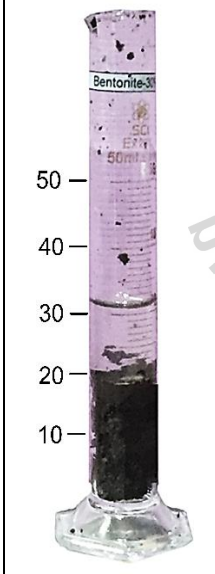
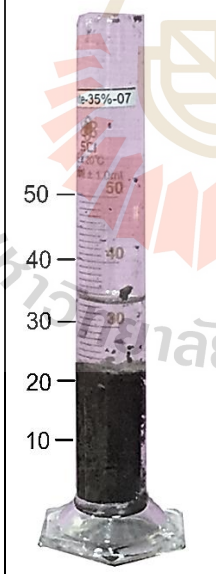
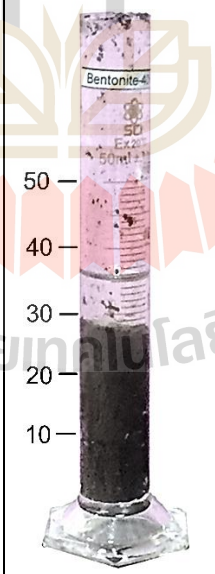

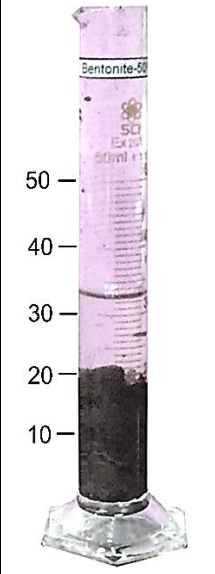
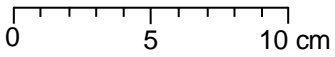
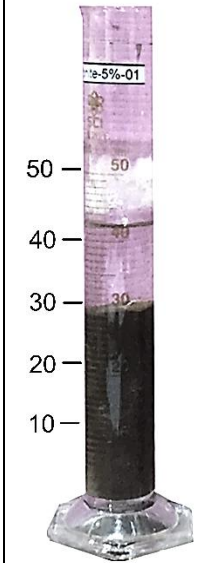
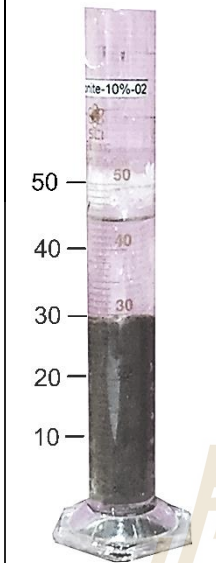
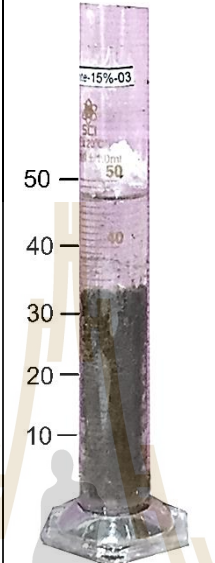
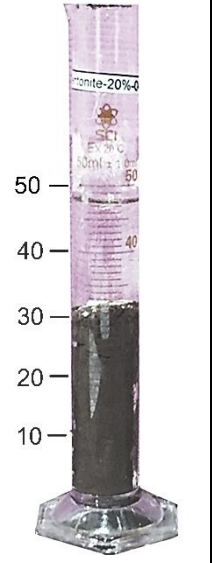
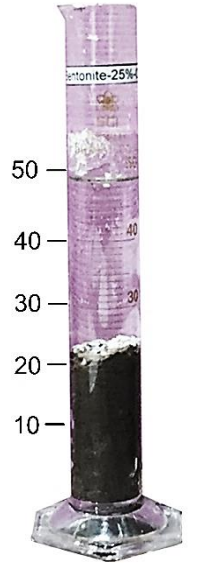
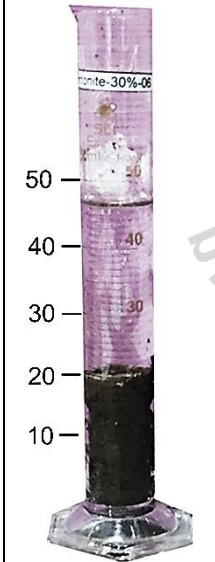
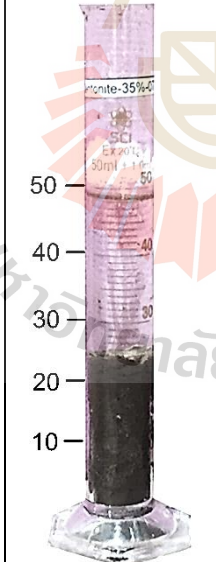
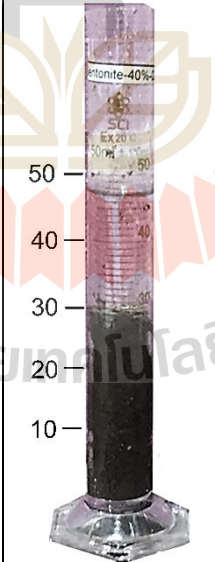
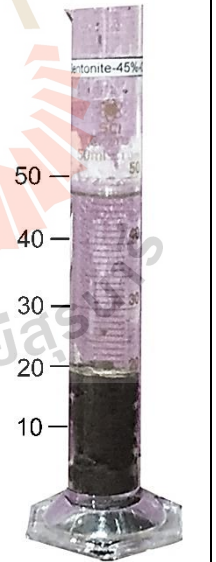
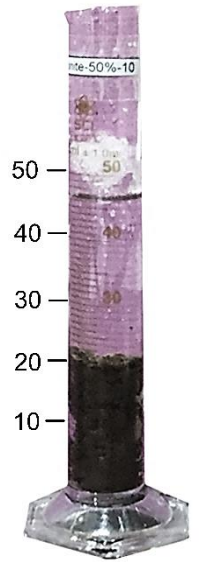
Initial brine content = 5%	10%	15%	20%	25%
				
				
30%	35%	40%	45%	50%
				

Table 5.3 Pictures of specimens after swelling.

Initial brine content = 5%	10%	15%	20%	25%
				
				
30%	35%	40%	45%	50%
				

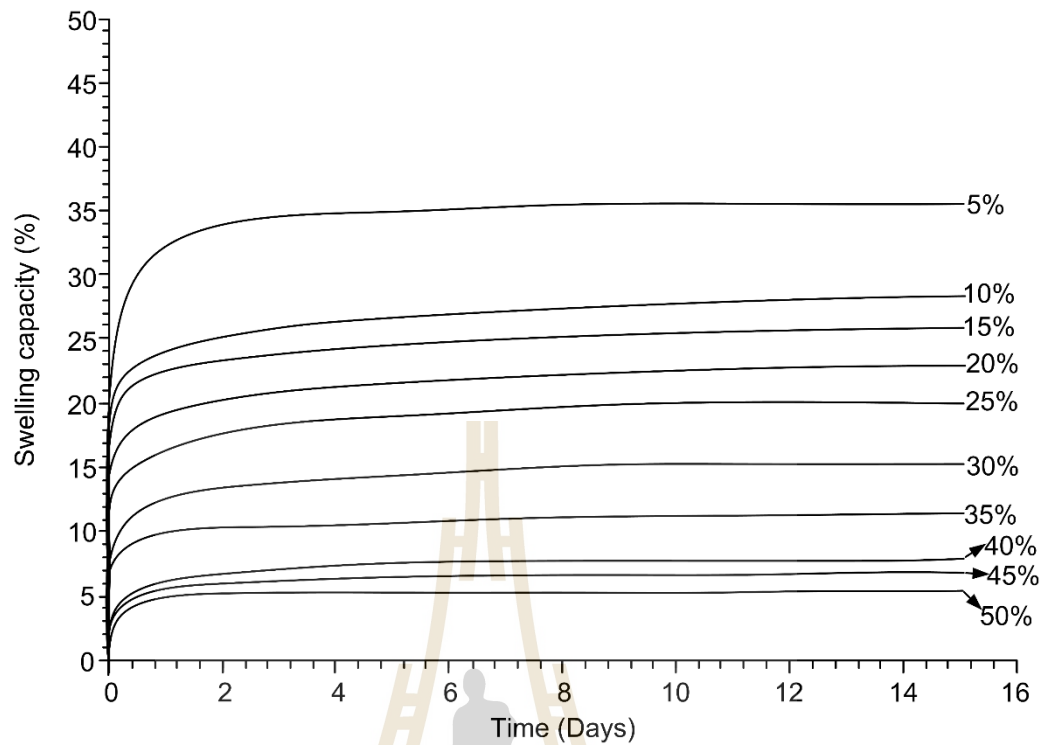


Figure 5.2 Swelling capacity of bentonite as a function of times for various brine contents from 5 to 50%.

Table 5.4 Results of swelling capacity of bentonite.

Initial brine content (%)	Volume _{int} (ml)	Volume ₁ (ml)	Swelling capacity (%)
5	20.0	30.5	35.6
10	22.5	31.0	27.4
15	27.0	35.5	23.9
20	27.0	33.0	22.2
25	20.0	24.0	20.0
30	19.5	22.5	15.4
35	22.5	25.0	11.1
40	28.0	30.0	8.1
45	20.0	21.5	7.0
50	19.0	20.0	5.3

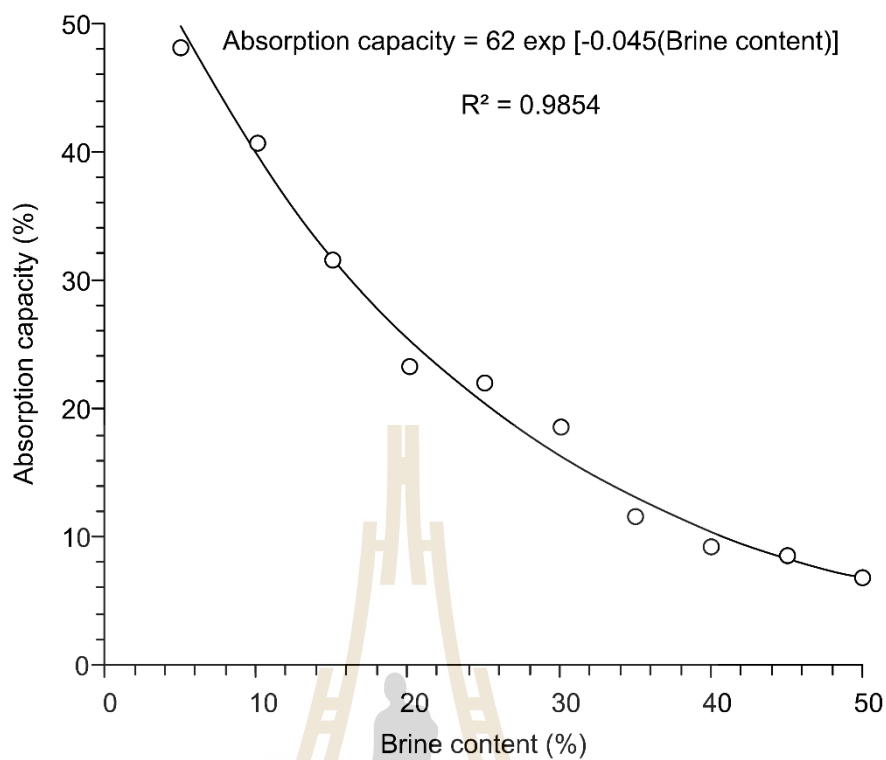


Figure 5.3. Absorption capacity of bentonite as a function of brine contents.

Table 5.5. Results of absorption capacity.

Initial brine content (%)	Absorption capacity (%)
5	48.3
10	40.9
15	31.7
20	23.4
25	22.1
30	18.7
35	11.5
40	9.4
45	8.5
50	6.9

CHAPTER VI

DISCUSSIONS, CONCLUSIONS AND RECOMMENDATIONS FOR FUTURE STUDIES

6.1 Discussions

The bentonite used in this study is mixed with sludge, sand, crushed salt, fine and coarse gravels. The experimental results shown in Figure 4.3 indicate that the mixing materials affect the compaction properties of the mixtures. Bentonite content can decrease the optimum brine content because it has high absorption capacity. Increasing bentonite content also increases the dry densities. This is probably because the specific gravity of bentonite is less than those of the granular materials. This agrees reasonably well with the test results obtained by Soltani-Jigheh and Jafari (2012) and Kaya and Durakan (2004). The maximum dry densities and the optimum brine contents of the samples obtained for both ASTM standard device and three-ring mold are virtually identical. This suggests that the three-ring mold can provide the results that are comparable to those of the ASTM standard test mold. The results from the three-ring mold are consistent with those obtained by Sonsakul and Fuenkajorn (2013).

The increase of granular content, particularly, with larger particle sizes can increase the shear strength and friction angles of the mixtures. This is probably due to the inter-locking between grains of materials. The granular content can decrease the cohesion of specimen because the amount of bentonite is insufficient to adhere the

granular materials, and hence their surfaces can slip easily. This agrees with the test results obtained by Li (2013). For bentonite-gravel mixtures, the three-ring direct shear device gives higher friction angle and cohesion than those obtained from the ASTM standard direct shear device (Figure 4.18) particularly, under higher contents of granular materials. Increasing shear box size can increase the shear strength of the testing materials with larger particle sizes. The results agree with those obtained by Sonsakul et al. (2013). The dilations from Figures 4.19 to 4.23 show that, for each type of mixture, the maximum dilation increases with granular content. The movement of gravel particles into voids may lead to contraction but when particle interlocking occurs, it will lead to dilation.

The swelling that represents the swelling volume in brine per unit weight of bentonite, is the simplest parameter to indicate swelling ability of bentonite. The initial brine content seems to be the most important factor for swelling and absorption. The effect of low initial brine content affects high swelling (Figure 5.4). This may be because under low initial brine content the specimens have higher air-filled gaps, and hence brine added on the top of the sample can flow and fill in the gap easier than bentonite that compacted under high initial brine content. As a result, the higher the rate of swell and absorption. These results agree with Dueck et al. (2008).

6.2 Conclusions

The results of compaction test indicate that the coarser particles (gravels) show higher dry densities and lower optimum brine contents than the finer particles (sludge). The dry densities of the mixtures increase with decreasing bentonite content. The results of the compaction test obtained from the three-ring and ASTM standard test

molds show that the maximum dry densities and the optimum brine contents of the samples obtained for both methods are similar.

The results of direct shear test indicate that the shear stresses increase with increasing granular materials, particularly under high normal stresses (Figure 4.12). The shear strengths are from 0.22 to 0.84 MPa (finer to coarser particles). Increasing granular content with larger particle sizes increases the shear strength. The cohesion of coarser mixing particles (e.g. gravels and crushed salt) is lower than those of the fine particles (e.g. sludge). The friction angle of coarser particle is however higher than that of the finer particles. For the mixtures with coarse particles (crushed salt, gravels), the three-ring direct shear device gives higher shear stress, friction angle, and cohesion than those obtained from the ASTM standard direct shear device (Figure 4.18) particularly, under higher granular contents. The dilation increases with increasing granular contents.

The mixtures with higher bentonite contents give greater compressive strengths and elastic moduli than those with the lower bentonite content. The Poisson's ratio, however tends to decrease when the bentonite weight ratios increase. This is probably because the increase of bentonite content can densify the mixtures, and hence increases their strength and stiffness. The mixtures with finer granular particles (e.g. sludge and sand) tend to show higher strengths and elastic moduli than those with coarser particles (e.g. gravels). The Poisson's ratios of the coarser particles are greater than those of the finer particles.

The swelling tends to increase as logarithmic functions with time at an early stage of the swelling process, and then tends to be constant. The lower initial brine content yields higher rates of swelling. The test results agree with those of Karnland et

al. (2006). The brine absorption tests show that the bentonite compacted under lower initial brine content yields higher absorption capacity and tends to decrease as exponential functions with increasing initial brine content. This agrees with the results obtained by Dueck et al. (2008). The results of swelling and absorption testing are useful for selection of initial backfill parameters in salt and potash mine openings. The high absorption capacity of bentonite also makes it plastic and resistant to fracturing or cracking.

6.3 Recommendations for future studies

1. Effect of sample disturbance due to cutting and trimming should be further investigated particularly on low cohesive soils. Effect of the large particle sizes (>10 mm) for the ASTM standard mold testing should also be further examined.
2. Different compressive efforts (energy) should be used to obtain mixtures with different dry densities and brine content. The results are useful for the design of the initial installation parameters of the bentonite-to-granular backfill.
3. Flow test should be performed to determine the permeability of the mixtures after compaction.
4. Consolidation test on the compacted mixtures is also desirable to determine their long-term deformations.

REFERENCES

- Afzali-Nejad, A., Lashkari, A., and Shourijeh, P.T. (2017). Influence of particle shape on the shear strength and dilation of sand-woven geotextile interfaces. **Geotextiles and Geomembranes**. 45(1): 54-66.
- Alias, R., Kasa, A., and Taha, M.R. (2014). Particle size effect on shear strength of granular materials in direct shear test. **International Journal of Civil, Environmental, Structural, Construction and Architectural Engineering**. 8(11): 1144-1147.
- ASTM D1557-12. (2012). Standard test methods for laboratory compaction characteristics of soil using modified effort (56,000 ft-lbf/ft³ (2,700 kN-m/m^{3Annual Book of ASTM Standards (Vol.04.08). Philadelphia: American Society for Testing and Materials.}
- ASTM D2938-95. (1995). Standard test method for unconfined compressive strength of intact rock core specimens. In **Annual Book of ASTM Standards** (Vol.04.08). Philadelphia: American Society for Testing and Materials.
- ASTM D3080-11. (2011). Standard test method for direct shear test of soils under consolidated drained conditions. In **Annual Book of ASTM Standards** (Vol.04.08). Philadelphia: American Society for Testing and Materials.
- ASTM D5890-11. (2011). Standard test method for swell index of clay mineral component of geosynthetic clay. In **Annual Book of ASTM Standards** (Vol.04.08). Philadelphia: American Society for Testing and Materials.

- Bagherzadeh, K.A. and Mirghasemi, A.A. (2009). Numerical and Experimental Direct Shear Tests for Coarse-Grained Soils. **Particuology**. 7(1): 83-91.
- Bauer, G.E. and Zhao, Y. (1993). Evaluation of shear strength and dilatancy behavior of reinforced soil from direct shear tests. **Special Technical Publication**. 1190: 138-157.
- Butcher, B.M., Novak, C.F., and Jercinovic, J. (1991). The advantages of a salt/bentonite backfill for waste isolation pilot plant disposal rooms. **Sandia National Laboratories**. Albuquerque, NM.
- Callahan, D. and Hansen, D. (2002). Crushed salt constitutive model. In **Proceedings of the Fifth Conference on the Behavior of Salt** (pp. 239-252). Balkema, Netherlands.
- Case, J.B. and Kelsall, P. (1987). Laboratory investigation of crushed salt consolidation. **International Journal of Rock Mechanics and Mining Science and Geomechanics Abstracts**. 25(5): 216-223.
- Castelbaum, D. and Shackelford, C.D. (2009). Hydraulic conductivity of bentonite slurry mixed sands. **Geotechnical and Geoenvironmental Engineering**. 135(12): 1941-1956.
- Cerato, A. and Lutenecker, A. (2006). Specimen size and scale effects of direct shear box tests of sands. **Geotechnical Testing Journal**. 29(6): 507-516.
- Cho, W.J., Lee, J.O., and Kang, C.H. (2002). A compilation and evaluation of thermal and mechanical properties of bentonite-based buffer materials for a high-level waste repository. **Journal-Korean Nuclear Society**. 34(1): 90-103.

- Cui, S.L., Zhang, H.Y., and Zhang, M. (2012). Swelling characteristics of compacted GMZ bentonite-sand mixtures as a buffer/backfill material in China. **Engineering Geology**. 141-142(3): 65-73.
- Das, B.M. (2008). **Introduction to Geotechnical Engineering**. Tomson, Ontario, Canada. pp. 110-115.
- Dueck, A., Börgesson, L., Goudarzi, R., Lönnqvist, M., and Åkesson, M. (2008). Humidity-induced water absorption and swelling of highly compacted bentonite in the project KBS-3H. **Physics and Chemistry of the Earth**. 33: 499-503.
- Fuenkajorn, K. and Daeman, J.J.K. (1988). Borehole closure in salt. **Technical Report Prepared for the U.S. Nuclear Regulatory Commission**. Report No. NUREG/CR-5243 RW. University of Arizona.
- Fuenkajorn, K. and Daemen, J.J.K. (1987). Mechanical interaction between rock and multi-component shaft or borehole plugs. In **Proceedings of the Twenty-eight U.S. Symposium Conference on Rock Mechanics** (pp. 165-172). University of Arizona, Tucson.
- Ghazi, A.F. (2015). Engineering characteristics of compacted sand-bentonite mixtures. **Master's Thesis**. Department of Engineering Science, Engineering, Edith Cowan University.
- Hansen, F.D. and Mellegard, K.D. (2002). Mechanical and permeability properties of crushed salt. In **Proceedings of the Fifth Conference on the Mechanical Behavior of Salt** (pp. 253-256). Bucharest, Romania.
- Ito, H. (2006). Compaction properties of granular bentonites. **Applied Clay Science**. 31(1-2): 47-55.

- Jaeger, J.C., Cook N.G.W., and Zimmerman R.W. (2007). **Fundamentals of Rock Mechanics**. Fourth edition, Blackwell Publishing, Australia. pp. 475.
- Kanchanamai, P. (2003). The utilization of sludge from bang khen water treatment plant in construction industry. **Master's Thesis**. Department of Environmental, Engineering, Kasetsart University.
- Karnland, O., Olsson, S., and Nilsson, U. (2006). Mineralogy and sealing properties of various bentonites and smectite-rich clay materials. **Technical Report for Swedish Nuclear Fuel and Waste Management Co.** Report No. SKB TR-06-30. Stockholm, Sweden.
- Kaya, A. and Durukan, S. (2004). Utilization of bentonite-embedded zeolite as clay liner. **Applied Clay Science**. 25(1): 83-91.
- Khamrat, S. and Fuenkajorn, K. (2018). Mechanical performance of consolidated crushed salt as backfill in boreholes and shafts. **Songklanakarinn Journal of Science and Technology**. 40(2): 431-439.
- Kumar, A., Walia, B.S., and Mohan, J. (2006). Compressive strength of fiber reinforced highly compressible clay. **Construction and Building Materials**. 20(10): 1063-1068.
- Kumar, S. and Dutta, R.K. (2014). Unconfined compressive strength of bentonite-lime-phosphogypsum mixture reinforced with sisal fibers. **Jordan Journal of Civil Engineering**. 8(3): 239-250.
- Lamandé, M., Schjønning, P., and Tøgersen, F.A. (2007). Mechanical behaviour of an undisturbed soil subjected to loadings: Effects of load and contact area. **Soil and Tillage Research**. 97(1): 91-106.

- Lennart, B., Lars-Erik, J., and David, G. (2003). Influence of soil structure heterogeneities on the behaviour of backfill materials based on mixtures of bentonite and crushed rock. **Applied Clay Science**. 23(1-4): 121-131.
- Li, Y. (2013). Effects of particle shape and size distribution on the shear strength behavior of composite soils. **Bulletin of Engineering Geology and the Environment**. 72(3-4): 371-381.
- Li, Y., Huang, R., Chan, L.S., and Chen, J. (2013). Effects of particle shape on shear strength of clay-gravel mixture. **Korean Society of Civil Engineers Journal**. 17(4): 712-717.
- Li, Y.R. and Aydin, A. (2010). Behavior of rounded granular materials in direct shear: Mechanisms and quantification of fluctuations. **Engineering Geology**. 115(1-2): 96-104.
- Liu, C.N., Ho, Y.H., and Huang, J.W. (2009). Large scale direct shear tests of soil/pet-yarn geogrid interfaces. **Geotextiles and Geomembranes**. 27: 19-30.
- Mitchell, J.K. (1993). **Fundamentals of Soil Behavior**. John Wiley and Sons, New York. pp.437.
- Mohr, O. (1900). Welche umstände bedingen die elastizitätsgrenze und den bruch eines materials. **Zeitschrift Des Vereins Deutscher Ingenieure**. 46(1524-1530): 1572-1577.
- Nakao, T. and Fityus, S. (2008). Direct shear testing of a marginal material using a large shear box. **Geotechnical Testing Journal**. 31(5): 393-403.

- Ouyang, S. and Daemen, J.J.K. (1992). Sealing performance of bentonite and bentonite/crushed rock borehole plugs. **Technical Report Prepared for the U.S Nuclear Regulatory Commission (NUREG)**. Report No. NUREG/CR-5685. Washington, DC.
- Powers M.C. (1982). Comparison charts for estimating roundness and sphericity. **AGI Data Sedimentary Petrology**. 23(2): 117-119.
- Proctor, R.R. (1933). Fundamental principles of soil compaction. **Engineering News-Record**. 111(13).
- Ran, C. and Daemen, J.J.K. (1995). The influence of crushed salt particle gradation on compaction. In **Proceedings of The Thirty-fifth U.S. Symposium on Rock Mechanics** (pp.761-766). Reno. NV. A.A. Balkema, Rotterdam.
- Shackelford, C.D., Benson, C.H., Katsumi, T., Edil, T.B., and Lin, L. (2000). Evaluating the hydraulic conductivity of GCLs permeated with non-standard liquids. **Geotextiles and Geomembranes**. 18(2-4): 133-162.
- Sinnathamby, G., Korkiala-Tanttu, L., and Fores, J.G. (2014). Interface shear behaviour of tunnel backfill materials in a deep-rock nuclear waste repository in Finland. **Soils and Foundations**. 54(4): 777-788.
- Soltani-Jigheh, H. and Jafari, K. (2012). Volume change and shear behavior of compacted clay-sand/gravel mixtures. **International Journal of Engineering and Applied Sciences**. 4: 52-66.
- Sonsakul, P. and Fuenkajorn, K. (2013). Development of three-ring compaction and direct shear test mold for soils with oversized particles. **Research and Development Journal of the Engineering Institute of Thailand under H.M. the King's Patronage**. 24(2): 1-7.

- Sonsakul, P., Walsri, C., and Fuenkajorn, K. (2013). Shear strength and permeability of compacted bentonite-crushed salt seals. In **Proceeding of the Fourth Thailand Symposium on Rock Mechanics** (pp. 99-109). Thailand.
- Wang, Q., Tang, A.M., and Cui, Y.J. (2012). Experimental study on the swelling behavior of bentonite/claystone mixture. **Engineering Geology**. 124: 59-66.
- Weimin, M.Y., Zhang, F., Chen, B., Chen, Y.G., Wang, Q., and Cui, Y.J. (2014). Effects of salt solutions on the hydro-mechanical behavior of compacted GMZ01 Bentonite. **Environmental Earth Sciences**. 72(7): 2621-2630.
- Wersin, P., Johnson, L.H., and McKinley, I.G. (2007). Performance of the bentonite barrier at temperatures beyond 100 °C: a critical review. **Physical Chemical Earth**. 32: 780-788.
- Wetchasat, K. (2013). Performance assessment of sludge-mixed cement grout in rock fractures. **Doctor's Thesis**. Department of Geotechnology, Engineering, Suranaree University of Technology.
- Zhang, L., Sun, D.A., and Jia, D. (2016). Shear strength of GMZ07 bentonite and its mixture with sand saturated with saline solution. **Applied Clay Science**. (132-133): 24-32.
- Zhu, C.M., Ye, W.M., Chen, Y.G., Chen, B., and Cui, Y.J. (2013). Influence of salt solutions on the swelling pressure and hydraulic conductivity of compacted GMZ01 bentonite. **Engineering Geology**. 166(10): 74-80.

BIOGRAPHY

Miss Korakoch Pongpeng was born on May 28, 1994 in Chaingrai, Thailand. She received her Bachelor's Degree in Engineering (Geotechnology) from Suranaree University of Technology in 2016. For her post-graduate, she continued to study with a Master's degree in the Geological Engineering Program, Institute of Engineering, Suranaree university of Technology. During graduation, 2016-2017, she was a part time worker in position of research assistant at the Geomechanics Research Unit, Institute of Engineering, Suranaree University of Technology.

